

New Process for Grain Refinement of Aluminum

Final Report
September 22, 2000

Contract No. DE-FC07-98ID13665

I. Executive Summary

A new method of grain refining aluminum involving in-situ formation of boride nuclei in molten aluminum just prior to casting has been developed in the subject DOE program over the last thirty months by a team consisting of JDC, Inc., Alcoa Technical Center, GRAS, Inc., Touchstone Labs, and GKS Engineering Services.

The manufacturing process to make boron trichloride for grain refining is much simpler than preparing conventional grain refiners, with attendant environmental, capital, and energy savings. The manufacture of boride grain refining nuclei using the fy-Gem process avoids clusters, salt, and oxide inclusions that cause quality problems in aluminum today.

In foundry alloys the fy-Gem process gives grain refining roughly equivalent to the best commercial grain refiners. The process has been demonstrated in commercial pilot equipment at the Reynolds Metals Research and Development Center in Chester, VA, and is ready for commercial demonstration.

At the present stage of development fy-Gem has not been able to consistently equal the grain refining performance of commercial grain refiners in wrought products. The process does work for all major aluminum alloys, except those containing significant levels of zirconium, and if incrementally improved, it would offer economic and quality advantages to the wrought aluminum industry.

Table of Contents

I.	Executive Summary	1
II.	Introduction	2
III.	Brief Overview of Grain Refining Technology	4
IV.	Supporting Theoretical Studies	7
	A. Water Model Studies	7
	B. Model of Boron Diffusion from Bubble	11
V.	Equipment and Procedures	15
	A. Melting Equipment	16
	B. fy-Gem Gas Delivery Systems	16
	C. Lance Unit	19
	D. CILGAR Unit	20
	F. Sampling Equipment	21
	G. Experimental Procedure	23
	H. Grain Size Analysis	24
VI.	Experimental Results and Discussion	26
	A. Use of Carbonaceous Gases	26
	B. <i>In-Situ</i> Refinement with Boron	26
	1. Initial Experiments	27
	2. Trials at Littlestown Hardware and Foundry	28
	3. Boron Trifluoride	30
	4. Boron Trichloride	31
VII.	Discussion of Results	50
	A. Effective Nuclei Form	50
	B. Composition of fy-Gem Nuclei Varies with Alloy	50
	C. Metal Treatment Unit Conditions Appropriate for fy-Gem	50
	D. Titanium Level Important in fy-Gem Process	51
	E. Rotor Geometry Important	51
	F. Concentration of Boron Introduced	53
	G. Boride Size	53
	H. Foundry Process	55
	I. Wrought Alloys	55
	J. The Composition Theory	55
	K. The Duplex Theory	57
	L. The Nuclei Formation Rate Theory	58
	M. Holding Time	58
	N. Gas Delivery System	59
IX.	Conclusions and Recommendations for Future Work	59
X.	References	
XI.	Appendices	
	A. Use of Carbon in fy-Gem Process	
	B. Test Procedures Used in This Study	
	1. TP-1 Grain Size Test	
	2. Alcoa 'Cold Finger' Test	
	3. LAIS samples	
	C. The role of Mixing During Degassing of Molten Aluminum	
	D. Reports on Plant Trials	
	1. Trials at Littlestown Hardware and Foundry	
	2. Trials at Alcoa Technical Center	
	3. Trials at Reynolds Metals Company	
	E. Environmental, Capital, and Labor Cost of Production of fy-Gem and Conventional Grain Refiners	
	F. Description of BCl ₃ Production furnace	
	G. Supporting Experimental Data	

- 1. Experimental Heat Logs**
- 2. Tables of Boride Size Measurements**
- 3. Reports of work at Touchstone Laboratories**
 - a. April 8, 1999 report**
 - b. June 11, 1999 report**
 - c. September, 28, 1999 report**

II. Introduction

At present nearly all aluminum cast in the world either from primary (approximately 4×10^{10} pounds) or secondary and internal scrap (5×10^{10} lbs.) are grain refined with heterogeneous nuclei which contain about 700,000 pounds of boron. The exception is a small but growing amount of aluminum grain refined with Ti-C and some minor amount of foundry alloys. Thus, on average aluminum contains about 8 ppm B in the form of insoluble TiB_2 nuclei approximately one micron in diameter, which nucleate a fine grain structure in aluminum. In fact, they cause a decrease in aluminum grain size, from a twinned columnar structure with linear grain dimensions of something over $2,500 \cdot \text{m}$, to equiaxial grains of less than $200 \cdot \text{m}$. Since grain size is a volume consideration this modest amount of grain refiner gives four orders of magnitude reduction in grain size. In systems with appropriate additions of “constitutional supercooling” growth restricting elements (e.g. ~ 150 ppm Ti), conditions in the aluminum alloy melt allow the heterogeneous nuclei to be more effective, and the job of grain refinement can be done with only 5 ppm boron addition.

Grain refining improves many of the metallurgical properties of aluminum alloys, such as mitigating cracking in castings, improving fatigue strength and crack propagation, ductility, and strength of the metal.

Although necessary for grain refining, the insoluble, foreign particles are otherwise undesirable in the aluminum, particularly in the form of particle agglomerates (“clusters”). The master alloys used now frequently contain potassium aluminum fluoride (KAlF) salt and aluminum oxide impurities which arise from the conventional manufacturing process of aluminum grain refiners. These give rise to local defects in aluminum (e.g. “leakers” in beverage cans and “pin holes” in thin foil), machine tool abrasion, and surface finish problems in aluminum.

The current grain refiners, which are present in the form of compounds in aluminum base master alloys, are produced by a complicated string of mining, beneficiation, and manufacturing processes resulting in a cost of grain refiner of almost \$130 per pound¹ of “contained boron”. The current cost of the aluminum cast primary alloy shapes is around \$1,500 per short ton. Therefore, the current cost of grain refiner is on the order of \$91 million per year in a product valued at about \$68 billion, or about 0.13% of the cost of making aluminum product.

Although reducing cost of the grain refiner and simplifying its manufacture is a driver for this program, an even more important goal is to improve aluminum metal quality and final product yield by eliminating boride clusters, KAlF, and aluminum oxide inclusions and making the nuclei more uniform in size.

This DOE project (DE-FC07-98ID13665) was conducted over a thirty-month period to bring to commercialization a novel method of continuous in-line generation of nuclei in-

¹ After taking credit for the aluminum in the master alloy at scrap metal prices.

situ in the molten aluminum during to casting. This process is described in US Patent No. 5,935,295, issued to J. Megy on August 10, 1999

The environmental, capital and labor costs associated with production of conventional grain refiners, as compared with a proposed fy-Gem process is described in appendix E, together with other safety and cost information. The fy-Gem process promises to provide grain refining in aluminum with simpler overall manufacturing requirements, with attendant cost, environmental, capital, and power savings, and produces nuclei of uniform size without clusters, KAlF or oxide impurities.

The process is carried out by introducing an argon/boron trichloride gas mixture into molten aluminum in the form of fine bubbles, whereupon the boron is dissolved into the aluminum and combines with titanium and other solute elements (V, Fe, Mn, etc.) to form heterogeneous nuclei, which effectively grain refine the aluminum during solidification. In practice the boron trichloride is introduced at the in-line metal treatment box where a gas dispersion device is commonly used for hydrogen, sodium, calcium, and oxide reduction from molten aluminum just prior to casting. The shape of the rotor head is important to creating the right size of nuclei and may need to be changed on some gas fluxing systems, but otherwise the use of the fy-Gem process is compatible with current practice.

The fy-Gem process is a safer way to store and add chlorine during gas fluxing. This is because boron trichloride has a significantly lower vapor pressure than chlorine, and forms an observable smoke when it contacts air at a concentration of more than one part per million. Data from scale up tests at the Alcoa Technical Center on 6061 alloy, and at the Reynolds Metals Test Center in 356 foundry alloys, show that over 99% of the boron and chlorine is absorbed into the aluminum.

As discussed in this report fy-Gem is ready for a commercial trial in foundry alloys where its effectiveness is equal to Al-Ti-B commercial master alloys. In its current state of development, the fy-Gem process usually gives grain refining inferior to present commercial refiners in wrought alloys. Since the fy-Gem process sometimes gives a grain refinement comparable to current practice, we believe that with further research, this new method of grain refinement could also be used successfully in wrought alloys. The greater relative effectiveness of fy-Gem in foundry alloys is probably the result of the higher levels of titanium (typically >0.10%), which are normally present.

We also present data to show that attempts to form effective Ti-C nuclei by injection of gaseous carbonaceous reactants were unsuccessful, presumably because of the very low solubility of carbon in molten aluminum.

The use of BF_3 as a gaseous injection reactant was also not promising. This appears to be due to the formation of a solid coating of fluoride salt (i.e., AlF_3 , MgF_2 , etc.) on the surface of the bubble. This solid layer interferes with the transfer of boron from the gas phase into the molten aluminum.

A theoretical model is presented which shows that the boron reaches high concentrations in the metal surrounding the bubbles, which contain the Ar/BCl₃ mixture. The model helps to visualize how bubble size and BCl₃ concentration in the gas play a dominant role in determining nuclei size and grain refining performance. It also explains why the nuclei that are formed have high levels of other elements besides titanium.

This work focused on producing small, uniform nuclei ($< c. 1 \cdot m$) that would be effective as grain refiners. As this study began, Greer and co-workers [1] presented a convincing argument, based on theoretical grounds, that larger particles ($c. 2 - 5 \cdot m$ in size), although present in relatively small numbers, are more effective as nuclei in traditional grain refiners. Their treatise was especially convincing, because it seemed to explain the well established fact that less than one percent of all particles in conventional master alloys are effective in forming solid aluminum grains. If fy-Gem operation parameters were able to give a more uniform size of boride particles, it was thought that the fy-Gem process may be able to give a more efficient use of boron, and cleaner cast products.

The fy-Gem process does produce a more uniform size of boride particles, but the results of our study show that particle size does not have a measurable effect on grain refining performance. Instead, the results of this study point to the overwhelming importance of the impeller head design, which is used to introduce the reactive gas mixture into the liquid metal. With further optimization of the fluxing process, the fy-Gem process may yet compete with conventional grain refining master alloys in wrought alloys.

III. Brief Overview of Grain Refining Technology

Until Cibula's work in 1949 [2] titanium in the form of titanium-aluminum (TiAl₃) particles in aluminum master alloys and concentrations of titanium above the Al-Ti peritectic composition ($\sim 0.15\%$ Ti) were used commercially to grain refine aluminum. Foreign inclusions of oxides and carbides contributed to grain refining, but in an uncontrolled manner.

In 1949 Cibula showed that small stable, heterogeneous (insoluble) nuclei of titanium carbide and titanium boride were effective in grain refining aluminum at very small sizes and concentrations, and gave relatively consistent results in a range of alloys, and at temperatures and conditions employed in aluminum cast houses.

In the late 1960's Kawecki discovered that it was possible to manufacture concentrated master alloys, such as Al-5%Ti-1%B, by the reaction of Ti- and B-containing salts with molten aluminum. These master alloys, which contain millions of TiB₂ heterogeneous nuclei in a single cubic centimeter, have since become the dominant grain refiner used for all alloys of aluminum. Recent improvements in the technology include:

- Continuous in-line addition at the point of discharge to the casting operation
- improving the cleanliness of the master alloy (reducing clusters, salt, and oxide inclusions), and
- optimizing grain growth conditions through better control of constitutional

super-cooling and alloy additions for purposes of optimized growth restriction [3,4,5]

Over the last several years, following the method of Sigworth [6] Al-Ti-C heterogeneous nuclei grain refiners have become important commercially, and enjoy a small, but growing use for grain refining aluminum.

The concept of producing *in-situ* Ti-C nuclei by gas injection of candidate carbon gases was studied in this program. A literature review on the development of Ti-C as a grain refiner is presented in Appendix A, together with some theoretical discussions, and experimental work on attempts to prepare Ti-C nuclei via gaseous injection of acetylene, freon, and propane gas. None of the carbon gases gave grain refinement, presumably because of the low solubility of carbon in aluminum. The chemical stability of Ti-C may also be an issue at low concentrations of titanium. (See Appendix A.)

The TiB_2 nuclei were much easier to prepare commercially, due to the higher solubility of boron in molten aluminum, c. 500 ppm @ 730 °C [7], and the high stability and low solubility in molten aluminum of the resulting boride nuclei.

A significant recent development in grain refining science is an improved understanding of the role “constitutional supercooling” plays in grain refinement [3,4,5]. Grain refinement of aluminum is comprised of two stages:

1. Initial formation of a small micro-grain of solid aluminum on a suitable nucleate particle. This is called the nucleation event.
2. Growth of the solid micro-grain into the surrounding liquid metal, as freezing progresses.

After the individual aluminum grains form, and they begin to grow into the liquid, they release their latent heat of fusion and thereby reduce the thermal undercooling at their surface. They also reject dissolved solute elements into the adjacent molten aluminum. The locally high concentration of dissolved solutes reduce the freezing point of the liquid metal, so the grain growth slows down, and may even stop for a while. This constitutional supercooling is controlled by diffusion of dissolved solutes in a boundary layer surrounding the solid micro-grain. Elemental diffusion is much slower than thermal diffusion of heat in metal, and so grain growth in alloys (containing dissolved solutes such as Si, Cu, and Fe) is much slower than in pure aluminum. As a consequence, the first grains to form grow so slowly, that other nuclei, located nearby, may also nucleate new solid grains. In other words, by adding relatively small amounts of a suitable solute element, a much finer grain size can be obtained.

It happens that dissolved titanium is much more effective than any other solute element, for restricting the rate of grain growth. An addition of only 100-300 ppm of titanium to relatively pure aluminum alloys significantly improves the ability of nuclei to grain refine, regardless of whether the nuclei are borides or carbides. A more complete description of “constitutional supercooling” is offered in Appendix A, as it profoundly affects the interpretation of the results of the experiments discussed below.

Another major issue in grain refinement is the role of nucleus size and composition in its effectiveness as a grain refiner. Throughout the work on this project we had assumed that nucleation of the freezing aluminum grains was dependent primarily on the surface of the nuclei, not its size. There is a significant body of technical information to support this viewpoint. Numerous studies [8] have established that there are favorable epitaxial relationships between solid aluminum and effective nuclei. For example, the (110) planes of TiAl_3 match well with the (112) planes of solid aluminum. The lattice discrepancy between the two planes is less than 2 percent. This means that the (110) planes of the titanium aluminide crystal seem almost like a piece of solid aluminum, and so a grain can nucleate very easily there.

The results of this study have shown that the fy-Gem process can produce boride nuclei of a more uniform size than is possible with conventional master alloy production. With fy-Gem it was also possible to make nuclei in the $0.5\mu\text{m}$ size range, which is about one half the size of particles found in conventional grain refiners.

From these observations, and the considerations on epitaxy discussed above, it is possible to conclude that the smaller *in situ* produced nuclei would allow us to use less boron for a given level of grain refinement. It should also permit more of the nuclei to pass through metal filters, and yield smaller “foreign inclusions” in the product for a significant quality improvement. We also thought that *in-situ* nuclei would be precipitated directly from, and be in equilibrium with, the molten aluminum. Consequently, their surfaces may well be more effective in nucleating than particles in commercial refiners.

As the study progressed, and more results became available, we gradually became aware that the fy-Gem process was usually not as effective as existing commercial TiBor® refiners. It was at this time that we became aware of the theoretical work of Greer and co-workers [1]. They made the case that smaller particles would not be as effective as larger particles. Besides being a convincing theoretical study, their model seemed to explain why the fy-Gem process (with smaller particles) was less effective. It suggested that our persistent attempts to make “small” effective nuclei, was a primary reason why we were not able to match the performance of commercial grain refiners in wrought alloys. We consequently began to vary the fy-Gem process to produce larger boride particles, and a considerable effort was made to measure the average boride size, and to relate that to the grain refining performance.

The results of our experiments do not support Greer’s conclusions. Although the ratio of grains formed to boride nuclei added becomes larger (i.e., more efficient use of nucleating particles)¹ as the size of the nuclei increased, there was no relationship between grain size in the cast sample and the boride size.

¹ This apparent increase in nucleating efficiency with larger boride particle size may be an artifact of the grain refining process, and not due to any inherent property of the particles. When fewer particles are added, and they are spaced further apart in the melt, they do not have so much competition from their neighbors, and the apparent nucleating ‘efficiency’ will increase. One would have to decrease the boron addition so that the same number particles (both large and small) were added, to have a valid scientific comparison.

This conclusion is valid for a fixed boron addition. Consider that if you cut the size of the borides in half, and add the same amount of boron, you will have eight times as many of the smaller particles! Thus, even if they are less efficient,¹ a smaller grain size may result.

An analysis of the data shows that the design of the rotary gas impeller is the single most important factor in optimizing the fy-Gem process. Six different head designs were used in this study. Studying the results obtained with each head points one clearly to the desired method of treatment in this new method of grain refinement. The best results were found when there is a high degree of local shear at the point where the gas first contacts the metal. Bubble size in the bulk of the molten aluminum is not important, presumably because the reaction takes place very quickly, before individual bubbles detach from the head and float up through the melt.

We also found that the composition of the fy-gem boride nuclei varies considerably, depending on the alloy being treated and the level of certain impurities therein (particularly vanadium, and manganese in can stock). These compositional effects may have an important effect, depending on the alloy to be refined. This topic will be addressed in more detail in the discussion section of this report, together with other factors influencing the performance of the new grain refining process.

As expected from the well-known ‘poisoning’ effect found with conventional grain refiners, the fy-Gem process is not suitable for alloys containing significant levels of zirconium.

IV. Supporting Theoretical Studies

During the course of this work, two theoretical studies were undertaken in an effort to fundamentally describe the fy-Gem process. The first focused on the role of mixing and how agitator geometries and rotation velocities affected the bubble sizes. The second study concentrated on how the bubble size affected boron distribution through the melt.

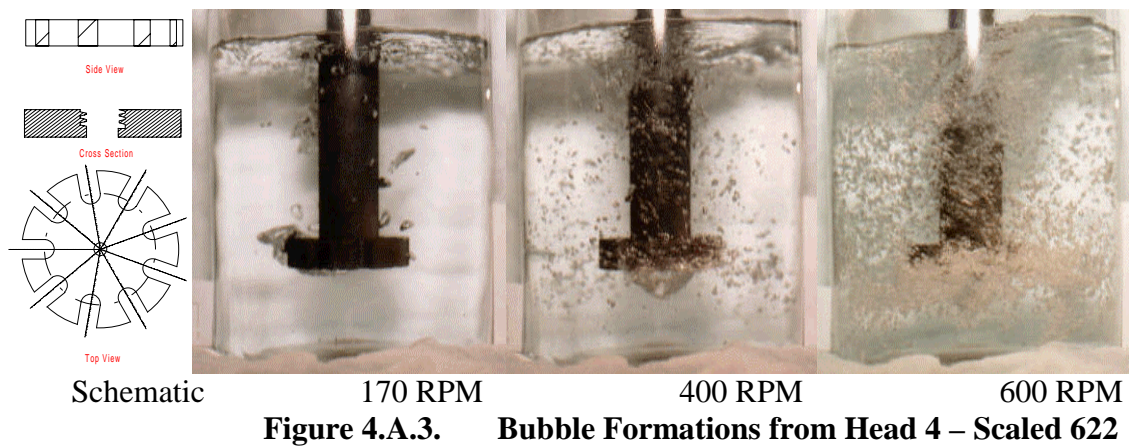
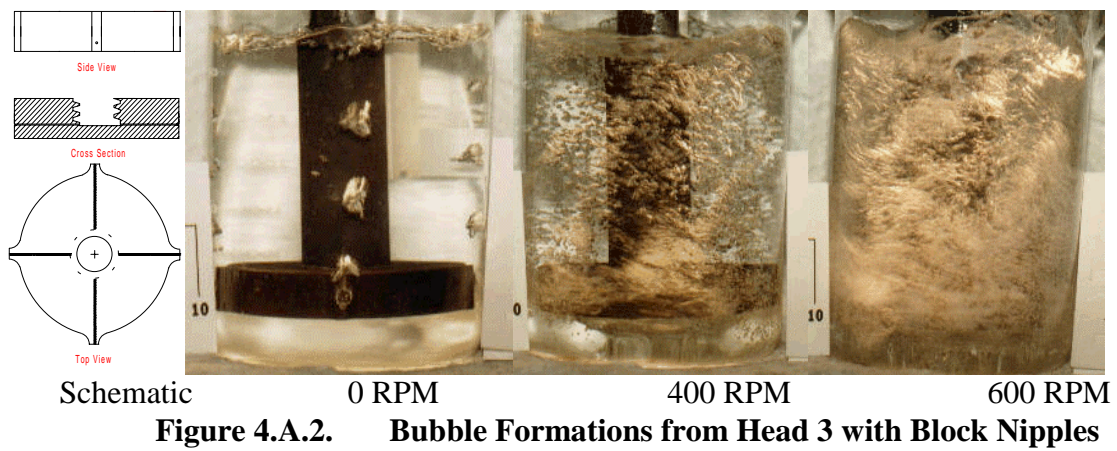
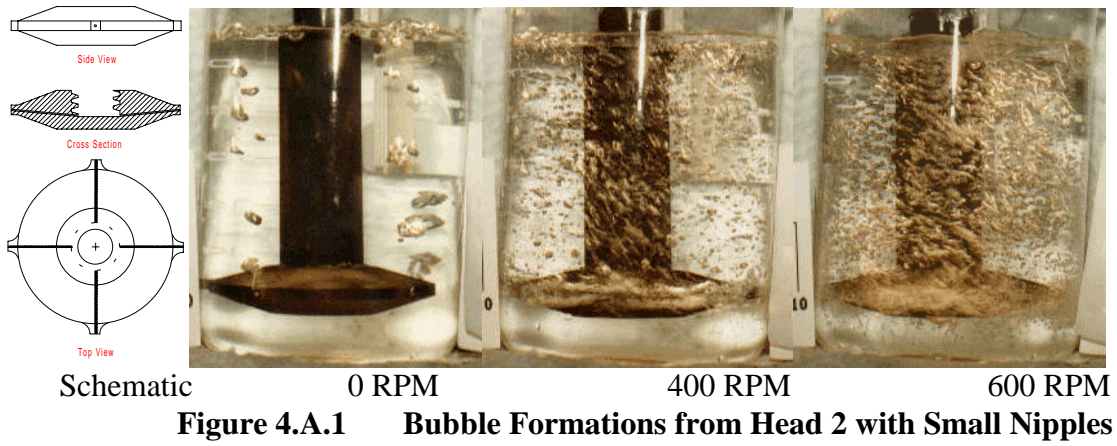
A. Water Model Studies

This study involved a set of experiments in which the carbon agitator heads were photographed while spinning in a water bath at various rotation speeds and gas flow rates. This water model study was made in an effort to characterize the size of the bubbles as they exited the carbon head. By replacing the refractory crucible with a water-filled glass beaker of almost the same size, the bubble dispersion produced by the impeller heads could be observed. The figures given below show examples of the findings.

Careful observation shows that due to the tremendous amount of mixing, a baffle had to be added in most of these water model experiments. The baffle reduced the vortex and allowed pictures at higher rotary speed and gas rates to be taken. A baffle was sometimes required when fluxing molten aluminum, although less often. Because molten aluminum has a higher density than water, the tendency to form a vortex is less.

The water model studies showed that all three heads produced relatively small bubbles, having a diameter of 2-3 millimeters. Heads two and three produced slightly smaller bubbles at higher rotation speeds (bubbles closer to 2 mm diameter, compared to the c. 2.5-3 mm bubbles with Head 1). The main difference between the heads was the amount of gas that we could admit, before 'flooding' the liquid with large bubbles. With heads two and three, we could admit more than 2 lpm of gas, and still maintain good bubble size and dispersion. The maximum gas flow with head No. 1 was considerably less. At 400 rpm we could admit c. 0.5 lpm and obtain small bubbles, but as the gas flow increased, so did the bubble size. Increasing the rotation speed to 600-700 rpm changed this transition point to about 1 lpm. Head 4 produced bubbles finer even than Heads 2 and 3. However, at the contact point between the metal and the exiting gas, a large conical bubble is formed at the bottom of the head. This occurred at all of the rotary speeds and gas flow rates that were tested. From the poor grain refining results obtained in fy-Gem with this head, it seems that this relatively stagnant bubble greatly affects the nucleation reaction. And so, the final bubble size is not material for this head design.

A detailed theoretical study was made of the role of stirring and mixing during gas fluxing. This conclusions are summarized in the technical paper entitled "The Role of Mixing During Degassing of Molten Aluminum," which was published in the journal Aluminum Transactions. A copy of this paper is included in Appendix C of this report.



The specific mixing energy produced was determined by measuring the temperature rise of water in a thermos, produced by mechanical agitation with each of the impeller heads. A typical plot of the results obtained in these trials is shown in Figure 4.A.4. The results of the measurements are summarized below in Table 4.A.1.

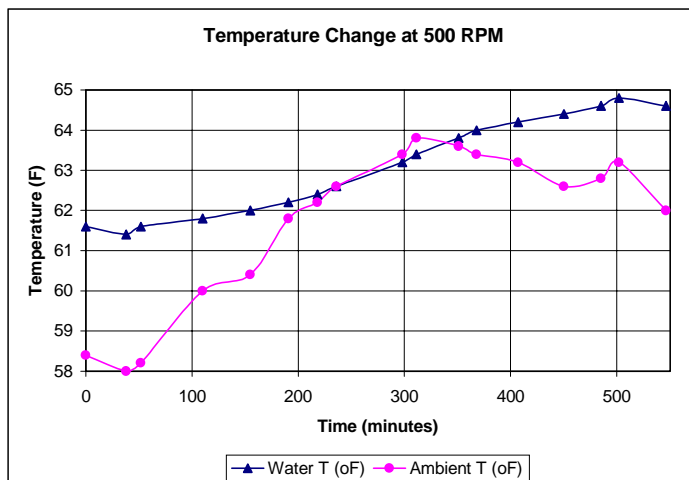


Figure 4.A.4. Temperature Rise of Water During Stirring

Table 4.A.1. Stirring or Mixing Intensity Produced With the Three Heads

Head	Stirring (watts/m ³)	Rotation Speed (rpm)
1 (No Nips)	150-250	600-750
2 (Small Nips)	600-1200	500-750
3 (Block Nips)	2000-5000	300-550

In order to determine the stirring intensity imparted by the agitator (without gas flow) in water, the temperature rise of the water produced by the stirring was recorded and the stirring intensity was then calculated as follows.

First, insulating refractory was placed around the beaker used for the water model studies, and the water was stirred with Head 2, for this example, at a speed of 456 rpm. This produced a temperature rise of 9.3×10^{-3} C/min. In this experiment there was 2750 ml of water. The beaker weighs 1.08 kg, and the portion of the carbon shaft in contact with the water weighs 550 g. The total specific heat of the system is therefore:

water	2750 cal/C
beaker ¹	1,080 g x 0.18 cal/g-C = 195 cal/C
carbon	550 g x 0.17 cal/g-C = 95 cal/C
total	3040 cal/C

Thus, the power delivered to this system by the rotating head is:

¹ Potassium silicate and silica both have a specific heat of 0.18 cal/g-C; and this value has been used here for the beaker.

$$P = 3040 \text{ cal/C} \times 9.3 \times 10^{-3} \text{ C/min} = 28.3 \text{ cal/min} = 0.471 \text{ cal/sec}$$

One watt-second is equal to 0.2389 cal/sec, and the volume of the system is 2.75 liters, so the specific energy dissipated is equal to:

$$\varepsilon = P/V = 0.471 / (0.2389 \times 2.75 \times 10^{-3} \text{ m}^3) = 717 \text{ watts/ m}^3$$

This analysis was made for each impeller head and a short summary is given in the Table shown above.

B. Model of Boron Diffusion from Bubble

Our experience with the fy-Gem process has made it clear that the design of the rotary impeller head, and the size of bubbles produced, have a major impact on the efficiency of the process. To better understand what was happening, a study was undertaken to model the kinetics of the reaction between the boron-containing gas and the metal. This study is given below.

Model of Boron Transfer from Bubble into Molten Aluminum

Introduction

The geometry and operating parameters of the rotating head dispersing BCl₃/Ar gas into the molten aluminum was found in this work to affect the grain refining effectiveness of the fy-Gem process. To assist in visualizing the nuclei formation process the model described herein was developed.

The diameter of a bubble in molten aluminum is found to be about twice that found in a water model under the same rotor operating conditions.[19] Therefore, based on the water model studies described in the body of this report, the bubble size produced in the fy-Gem experiments would be in the 2 – 10 mm range. A 2 mm bubble with a 15% BCl₃ –85% argon mixture therein has 8.3×10^{-8} grams boron in it. When a BCl₃ molecule contacts molten aluminum metal at the bubble metal interface the following reaction occurs:



The reaction has a very high negative free energy of reaction (i.e. 59 Kcal/gmol at 1000 K).[10] At the temperature of the molten aluminum the rate of reaction can be considered fast compared to diffusion rates. At 1000 K the diffusion rate of BCl₃ in argon is calculated from the modified Hirschfelder equation [11] to be 2.4 cm²/sec. This means the BCl₃ diffuses to the wall in about 1 millisecond for a 2 mm bubble and somewhat slower for larger bubbles as shown in Figure 4.B.1. At the Argon/BCl₃ flowrates typically used in the JDC thirty pound reactor experiments (~1 liter/at STP min.) the flow rate of gas out of the 4 each 1/16 inch holes in the rotor is on the order of 0.5 cm/millisecond at 725 °C. Thus, for small bubbles nearly all of the boron enters the molten aluminum near the tip rather than in the bulk of the molten aluminum.

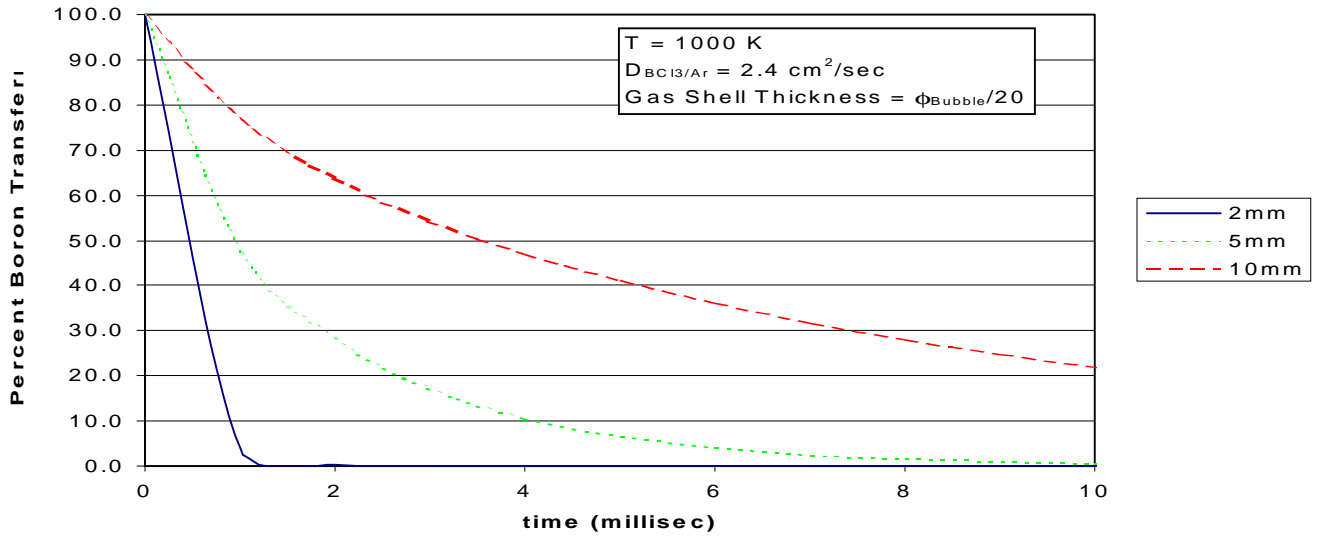


Figure 4.B.1: Percent Boron Transferred into Metal

The values in this figure were calculated from the onion layer model described as follows.

The Model

According to J. Crank [12], the diffusion equation for a sphere with a constant diffusion coefficient can be written as:

$$\frac{\partial C}{\partial t} = D \left(\frac{\partial^2 C}{\partial r^2} + \frac{2}{r} \frac{\partial C}{\partial r} \right) \quad (3)$$

In the case of steady state diffusion, Crank suggests this equation becomes:

$$\frac{d}{dr} \left(r^2 \frac{dC}{dr} \right) = 0 \quad (4)$$

In this study, it was determined that the boron bubble and subsequent metal should be broken down into spherical layers so that the amount of boron at any point could be recorded and analyzed. Using a as the radius of the inner sphere which is at concentration C_1 and b as the radius of the outer sphere at concentration C_2 , then Crank suggests this equation becomes:

$$C = \frac{aC_1(b-r) + bC_2(r-a)}{r(b-a)} \quad (5)$$

By rearranging this equation, the amount of diffusing substance, Q_t , which passes through the spherical wall, can be described as:

$$Q_t = 4\pi D t \frac{ab}{b-a} (C_2 - C_1) \quad (6)$$

where D is the diffusion coefficient and t is the time interval. The computer model used ten layers in the gas bubble and many metal layers, up to the limit of the spread sheet program we were using. The equations were then solved for successive time intervals.

Results and Discussions

The diffusion rate of boron in molten aluminum from data for similar systems summarized in Richardson is estimated to be about $5 \times 10^{-5} \text{ cm}^2/\text{sec}$ at 1000 K. The nuclei that are formed in the fy-Gem experiments in this report are nominally 0.5 microns (i.e. 0.00005 cm). Metal onion shell thicknesses of this size are relevant to visualizing the forming nuclei. The time to diffuse boron out of this layer to reduce its concentration by half is approximately less than a millisecond, about the same time as the transfer of boron from the gas bubble to the aluminum. Thus, for a 2 mm bubble containing 15% BCl₃ in argon, if all of the boron went into the first metal layer of 0.5 • m thickness the boron concentration would reach about 5000 ppm boron. The boron diffuses out of the 0.5 • m layer while it diffuses in from the bubble and the onion peel model shows it only reaches a maximum of about 700 ppm after a fraction of a millisecond. Figure 4.B.2 shows the boron profile for the first five layers over time, assuming boron in pure aluminum. A dotted line on the

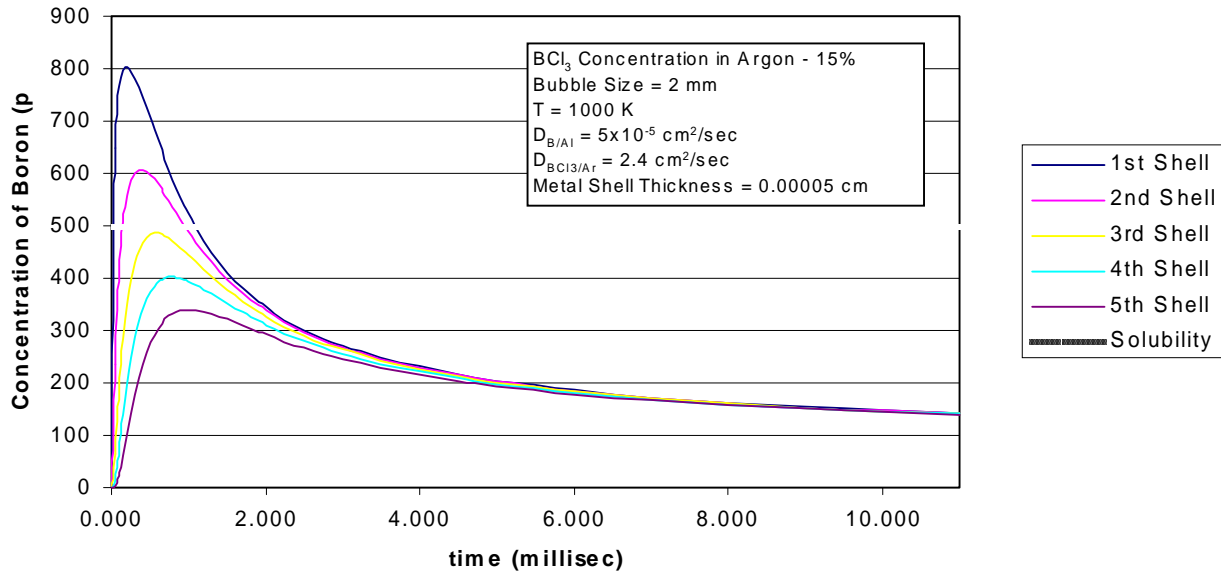


Figure 4.B.2: Boron Profile in Molten Aluminum at Low Input

figure shows the solubility of boron in pure aluminum at 730 °C.[7] As the boron builds up in the metal at the bubble interface, AlB₂ can form, if boron concentration in the aluminum exceeds saturation, which occurs with large bubble size and/or high BCl₃ concentrations in the bubble. If all the aluminum at the interface is converted to AlB₂, then further reaction with BCl₃ would be impeded and it would simply stay in the bubble and exit the melt. This is evidenced by dense BCl₃ clouds observed in early lance experiments, which had large bubbles, particularly when the BCl₃:Ar ratio was high.

Using more dilute gas feeds (e.g. <15%) and smaller bubbles (e.g. <0.2 cm) allows almost all of the boron to enter the melt. In this case boron is still considerably in excess of the

available titanium in the first layer. At 1500 ppm titanium, such as found in foundry alloys, about 750 ppm B would react to form borides in this layer; consuming only about 1/7, which arrives into the layer. As the boron continues to enter the layer you would expect it to react with any solute atom that could incorporate itself into the boride nuclei. EDAX of the nuclei shows this to be the case as discussed in the report as vanadium, manganese, iron, zinc, and copper are found in the nuclei. In foundry alloys using 2 mm bubbles and 15% BCl_3 in argon, there is enough titanium to convert all the boron to nuclei in the first seven layers (e.g. $3.5 \cdot$) which the model shows occurs in about 2 milliseconds.

With larger bubble sizes and higher BCl_3 concentrations the concentration of boron in the first shell goes far above AlB_2 solubility and extends much further into the molten aluminum. Figure 4.B.3 shows the case with 100% BCl_3 in a 5 mm bubble.

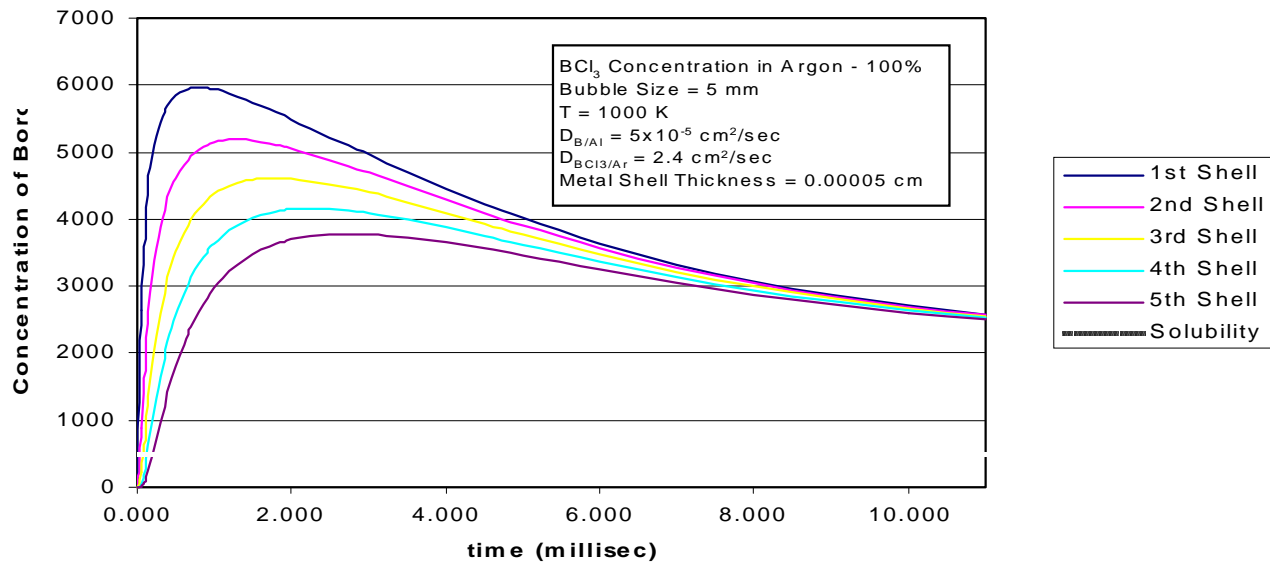


Figure 4.B.3: Boron Profile in Molten Aluminum at High Input

In wrought alloys typical titanium levels are on the order of 200 ppm and the boron must travel an order of magnitude farther into the metal solution from the interface.

As the time frame over which the boron diffuses in the metal phase in this case is on the order of tens of milliseconds, turbulence in the metal must play a heightened role in bringing together the boron and reactive solutes outside the first metal layer. Due to the complexities of diffusion/mixing the model building was stopped at this point.

After the nuclei form, incorporating a blend of solutes (i.e. Fe, Mn, V, etc.), they then float around in the bulk aluminum where dissolved titanium is present. It is expected that the less stable boride formers might exchange with titanium on the surface of the nuclei. This "maturation" may make the nuclei more effective. As explained in the text, a small

but persistent improvement in grain refining was typically observed in TP-1 castings made after twenty minutes compared to those made after five minutes.

The picture that emerges from this model is one of dense, rapid formation of fy-Gem nuclei in the thin layer adjacent to the metal surface with additional nuclei formation as the boron, titanium, and other solute nuclei formers are brought together by metal phase diffusion and convection mixing.

The consistent, uniform size of the nuclei that are formed in the fy-Gem process are a feature of the process. But it appears they are formed under very abrupt conditions (a couple of milliseconds). The reaction used to make Al-Ti-B rod by conventional technology is batch and quite turbulent and exothermic. Nevertheless the nuclei grow and mature on multiple minute time scales rather than milliseconds. One possible explanation for the variable effectiveness of the fy-Gem nuclei in wrought products may be that their rapid non-equilibrium formation may make small nucleating areas on the nuclei that are significantly smaller than the entire nuclei.

The third important observation is that a maximum concentration is reached in a fraction of a millisecond in small bubbles. After this, the concentration drops as boron concentration is reduced in the bubble. For a 2 mm diameter bubble the reaction is largely over in 1 msec. Larger bubbles take longer to react, but the time is still small. The importance of this fact is best considered by example. Using one of the larger gas flow rates employed in this study (2 lpm) it is possible to calculate that 2 mm bubbles are produced at each of the four orifices, and released into the melt, every 0.5 msec. The time to form a larger, 3mm diameter bubble increases to 2 msec. This suggests that a major portion of the chemical reaction, which produces the boride nuclei, occurs at the bubble while it is forming at the orifice of the impeller, and before it is released into the melt. The local conditions at the orifice may thus be expected to have an important influence on performance. This inference is confirmed by the observation that heads 2 and 3 gave different levels of performance, even though the bubble sizes produced by each were nearly the same.

V. Equipment and Procedures

The equipment and procedures used in the fy-Gem process research have evolved gradually over the nearly two years of work. Early experiments utilized gas bottles connected to a lance for distribution of various carbonaceous gases in an effort to produce *in-situ* grain refinement. Current experiments and pilot-scale production equipment utilize boron trichloride liquid in tanks with a vaporizer running into an in-line gas delivery system, with specially designed carbon heads which control the bubble size entering the melt. As time has passed the fy-Gem system has become more intricate, as discussed below.

In order to simplify the presentation of a somewhat complicated story, each type of equipment used (melting furnace, gas delivery system, etc.) is considered in a separate section. The presentation of information is also chronological.

A. Melting Equipment

An aluminum melting facility was constructed by building a furnace shell from fire brick, and placing two natural gas burners in the bottom of the furnace. A heavy steel grate was placed on top of the burners, and supported in place with an inner lining of brick. Insulated covers for the top of the furnace were manufactured from steel plate and an insulating refractory (Kaowool). Hot gases and any fumes from the melt were carried out of the top of the furnace by two 4" diameter steel ducts at either side of the furnace. The entire furnace assembly is enclosed in a larger steel hood, and exhaust gases are removed from the top of the hood by a centrifugal fan to the outside of the building. In order to melt metal, a monolithic silicon carbide crucible is placed on top of the steel grate. The furnace assembly is shown below in Figure 5.A.1.



Figure 5.A.1. The Gas-Fired Aluminum Melting Furnace

B. fy-Gem Gas Delivery Systems

The fy-Gem cart houses the source of carbon or boron-containing gas necessary for nucleation. In early experiments, the cart consisted of a bottle of carbon or boron-containing gas immersed in a refillable hot water cylinder (Figure 5.B.1). A separate water tank with a controllable heat source provided hot water to trace the stainless steel tubes from the carbon or boron-containing material to the control box. The control box was illuminated and heated by a 200-Watt light bulb to prevent cold zones, which would allow the BCl_3 gas to condense. Within the box was a Matheson proportional flowmeter/mixer assembly. This instrument had the capability to measure and control the flow of up to three gases. The instrument also included a gas mixing chamber, so that the gases were measured and mixed before being sent to either a lance (in early work) or the

CILGAR unit for distribution to the melt held in the aluminum melting furnace shown above.



Figure 5.B.1 Fy-Gem V1.0 Gas Delivery Cart

A chlorinator unit was constructed for Fy-Gem version 2.0. The premise behind this design, shown in Figure 5.B.2, was that it might be cheaper and safer to produce boron trichloride on site as needed from boron carbide and chlorine (which is typically already present in the cast house) rather than stockpiling boron trichloride. However, boron trichloride is believed to be a safer source of chlorine than chlorine gas due to its lower vapor pressure. Although the prototype chlorinator worked, this research was not continued as purchased liquid boron trichloride became the preferred option, at this stage of development. This work is described in more detail in Appendix F.

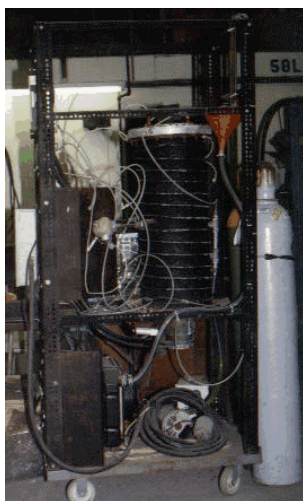


Figure 5.B.2 Chlorinator Unit – fy-Gem Version 2.0

Prior to trials at Alcoa Technical Center, ATC, a fy-gem delivery system utilizing liquid boron trichloride was designed. In this design, fy-Gem version 3.0, argon pressurized a bottle of liquid boron trichloride, pushing the liquid out of the bottle and into a rotameter. The liquid boron trichloride and argon were metered, and then mixed before being sent to the vaporizer unit. Upon vaporization, the gas exited the fy-Gem unit and was distributed to the molten aluminum through the rotary degassing unit. Figure 5.B.3 shows the working prototype for this unit, which was used during the ATC trials.

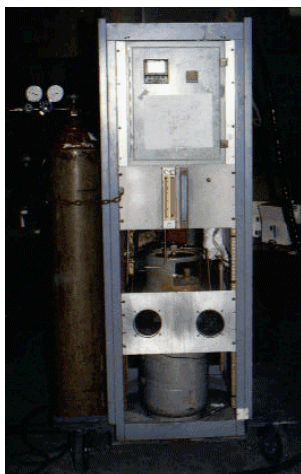


Figure 5.B.3. Fy-Gem Version 3.0

The fourth generation of fy-Gem cart, shown in Figure 5.B.4, which is currently in use, utilizes a more compact cart to house a bottle of liquid boron trichloride and is operated much like fy-Gem Version 3.0. The major difference with version 4.0 is that the boron trichloride flow is monitored after vaporization. With this method, the accuracy to which the gas can be distributed to the melt is increased substantially. Additional changes included the construction of a more compact and more efficient cart as well as the implementation of several new safety features.



Figure 5.B.4 fy-Gem Cart Version 4.0

The most significant problem with the past fy-Gem carts has been the ability to isolate the system from outside contaminants, such as water vapor. Swagelok fittings have been used to reduce leaking at the point of connection between stainless steel tubes and the hardware. However, flowmeters were installed to monitor the flow of the gases into the melt, and these have proven to be inefficient at sealing the glass tubes from the outside air. It has become apparent that the Viton and even the Teflon elastomer seals cannot exact a tight connection between the glass flow meter tube and the metal flow meter assembly body. This has led to a significant amount of leaking and flowmeter clogging. The next

The photograph on the left shows a physical Tri-Clamper sanitary end construction. It features a cylindrical body with a circular top cap and a flange at the bottom. The top cap has a logo and some text. The flange has a label that reads "Tri-Clamper" and "Model 100".

The technical diagram on the right illustrates the dimensions of the sanitary end construction. The dimensions are labeled as follows:

- A**: Total length of the assembly.
- B**: Length of the main body.
- C**: Diameter of the main body.
- D**: Diameter of the top cap.
- E**: Diameter of the bottom flange.
- F**: Height of the top cap.
- G**: Distance from the top of the main body to the top of the top cap.
- H**: Distance from the bottom of the main body to the bottom of the bottom flange.
- I**: Distance from the top of the main body to the top of the bottom flange.
- J**: Distance from the bottom of the main body to the bottom of the top cap.
- K**: Distance from the top of the main body to the top of the top cap.
- L**: Distance from the bottom of the main body to the bottom of the top cap.
- M**: Distance from the top of the main body to the top of the bottom flange.
- N**: Distance from the bottom of the main body to the bottom of the bottom flange.
- O**: Distance from the top of the main body to the top of the top cap.
- P**: Distance from the bottom of the main body to the bottom of the top cap.
- Q**: Distance from the top of the main body to the top of the bottom flange.
- R**: Distance from the bottom of the main body to the bottom of the bottom flange.
- S**: Distance from the top of the main body to the top of the top cap.
- T**: Distance from the bottom of the main body to the bottom of the top cap.
- U**: Distance from the top of the main body to the top of the bottom flange.
- V**: Distance from the bottom of the main body to the bottom of the bottom flange.
- W**: Distance from the top of the main body to the top of the top cap.
- X**: Distance from the bottom of the main body to the bottom of the top cap.
- Y**: Distance from the top of the main body to the top of the bottom flange.
- Z**: Distance from the bottom of the main body to the bottom of the bottom flange.

Additional dimensions shown in the diagram include:

- 4-1/2" (top width)
- 1/2" NPT (top thread)
- 4-9/16" (top height)
- 2 1/4" (top cap diameter)
- 2" ± 1" plus E (main body diameter)
- 3/4" up to 4" tri-clamp (bottom flange)
- 3/4" to 4" (bottom flange diameter)

C. Lance Unit

$$\frac{D_b}{D} = \left[\frac{6\sigma}{D^2(\rho_l - \rho_g)} \right]^{1/3} \quad (1)$$

19



Figure 5.C.1 Lances Used in Early Experiments

D. CILGAR Unit

The term CILGAR is an acronym for Compact In Line Gas Aluminum Refiner. The unit is a version of present day commercial rotary degassers, scaled down to fit into a 30 pound melting crucible. A small variable speed electric motor was connected to a stainless steel drive shaft by a V-belt and pulleys. The stainless steel shaft was hollow, and had a rotary union on the top end. This assembly was used to admit gas into a rotating carbon flux tube. The end of the flux tube was threaded so that impeller heads of various designs could be mounted and removed for various tests. Five different heads have been used for trials in this program. These are shown in Figure 5.D.1. The head labeled Head 1 was used first. This head design minimizes the amount of stirring associated with the head rotation. In spite of the minimal stirring, however, it produced a good dispersion of small bubbles, presumably because of the metal velocity at the periphery where gas enters the melt. Later, Heads 2 and 3 were used to produce greater amounts of stirring, in order to study the effect stirring had on the grain refining process. During the scale-up trials Heads 4 and 5 were used at Alcoa Technical Center and Reynolds, respectively. Head 4 is a scaled-down version of the impeller used in the Alcoa 622 unit. Due to the comparatively large opening on the bottom of the head, the gas first collected in a large conical bubble directly underneath the impeller. This conical region is believed to be the reason that Head 4 is the only impeller design that never produced grain refinement beyond approximately 600 μm . Head 5 is a scaled-down version of the impeller currently used in some Reynolds plants. The major differences between this impeller and Heads 1-3 are that the diameter of the gas ports is twice as large, and the nipples are much wider than on previous heads. This head was also found to produce significant grain refinement.

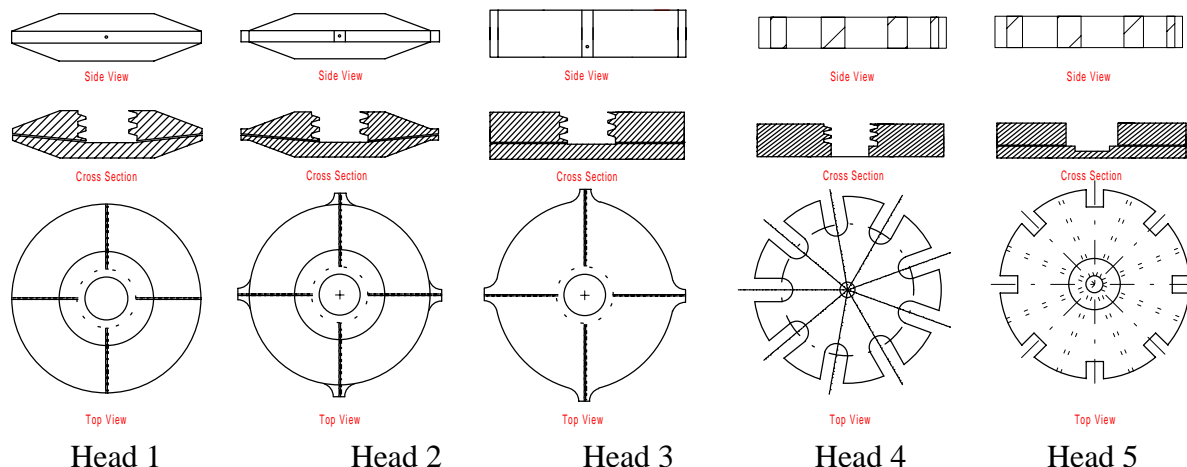


Figure 5.D.1. Five Head Designs Used in fy-Gem Study

F. Sampling Equipment

Three standard sampling procedures were used during this study. They were the spectrographic coupon, Aluminum Association test, and an Alcoa test. In addition to these three, Liquid Aluminum Inclusion Samples and thermal analysis were also made during the course of this work.

The spectrographic coupon sampler, shown in Figure 5.F.1, consists of an approximately 1.5" diameter and 1/2" deep scissor mold. Molten metal was poured into a 1/4" diameter hole on top of the closed mold. The metal then freezes and the mold can be opened like a scissor, which shears off the metal above the 1/4" hole.

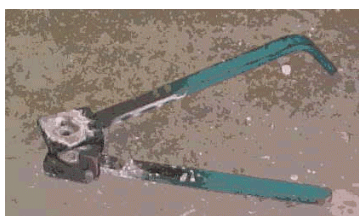


Figure 5.F.1 Spectrographic Coupon Mold

The second test casting has been established by the U.S. Aluminum Association (AA). This grain size sample, labeled TP-1, uses a small conical sample of liquid metal, which is placed into a water bath. The sample then freezes from the bottom to the top by conduction of heat. The resulting sample is conical in shape, 1" diameter at the bottom, 2-3/8" diameter at the top, and 2-1/2" in height. A picture of an AA test sample being taken is shown in Figure 5.F.2. Details of the complete AA TP-1 test procedure are given in Appendix B.



Figure 5.F.2 Aluminum Association Grain Size Test Sample

Another grain size test was developed by Alcoa to simulate the solidification conditions found in ingots. It consists of dipping a cylindrical steel ladle into the melt. The sample is placed into a heated furnace, and a copper chill is used to freeze the metal directionally from the top towards the bottom. The object is to produce a fine equiaxed structure in 100% of this test ingot. The equipment used is shown below.



Alcoa Sample Mold



Alcoa Furnace

Figure 5.F.3 Alcoa Sample Equipment

In addition to the above standard tests, a large number of LAIS (Liquid Aluminum Inclusion Sampler) samples were examined during the course of this study. These samples helped to determine the size and chemical composition of boride particles produced by the fy-Gem process. To obtain these samples, a carbon filter was attached to a stainless steel vacuum cylinder, and placed into the molten aluminum. Then, after pre-heating, the vacuum was turned on and approximately 500 grams of metal were sucked across the filter. In this way borides and other inclusions became trapped in the filter, where they could be examined during subsequent metallographic analysis. The LAIS sampling assembly is shown in Figure 5.F.4.



Figure 5.F.4 LAIS Sample Assembly and Pump

Due to the significant time and labor involved in grain size analysis using the AA or Alcoa test, some investigation into an easier, less costly, real time analysis of grain size was conducted. For many of the early tests in this project, GKS Engineering contributed a DPM gas analyzer and thermal analysis tester to the project. With this unit, it was possible to do a relatively sophisticated thermal analysis of the metal during solidification. Two instrumental approaches have been tried in thermal analysis. One technique uses a single thermocouple placed into the bottom of a sand cup. This method of analysis is used commercially [14] in casting alloys (such as 356 alloy), but it has not found use in wrought alloys (such as 6063 and 3004). The other method of analysis uses two thermocouples [15]. The two thermocouple method has been used to evaluate structure formation in both wrought and casting alloys [16,17], but it has not been used to evaluate grain size. From the experiments made, we concluded that thermal analysis is probably not a reliable indicator of as-cast grain size in wrought alloys, and the tests were discontinued. Figure 5.F.5 shows the thermal analysis equipment used.



Sand Cup

Sand Cup on Mounting Stand

Two TC Analysis

Figure 5.F.5 Thermal Analysis Equipment.

G. Experimental Procedure

The typical experimental procedure was to charge a suitable amount of ingot to the furnace, up to 30 pounds as dictated by the size of the crucible. The gas burners were then lit to heat the furnace and its charge. Once the metal was fully molten, the desired

alloying elements were added to the bath, and then the melt was 'fluxed' or degassed with an Ar-1%Cl gas mixture for an hour or more. The flux treatment removed any particles suspended in the melt, so that a large grain size could be produced. When fluxing was complete, "blank" AA and Alcoa grain size tests, and two Spectrographic coupons were taken. The fy-Gem refinement process was then performed using either a lance or the CILGAR unit at the desired rotary speed. After a set amount of time, the delivery unit was pulled out of the melt and the dross was skimmed off of the surface of the metal. One minute after the inoculation with the carbon- or boron-containing gases, an AA sample was taken. In early experiments, another AA sample was taken after 2 minutes to further study the effect of time on nucleation. Five minutes after inoculation, a full set of samples was taken including AA and Alcoa tests, and two Spectrographic coupons. At this time, the LAIS sampler was placed into the melt and allowed to pre-heat. Following 5-10 minutes of pre-heating, the LAIS sample was drawn. Then, a final set of samples was taken 20-25 minutes after inoculation. These included AA and Alcoa tests, and two Spectrographic coupons.

H. Grain Size Analysis

The standard examination procedure specified by the Aluminum Association is to make a horizontal cut 1.5" from the bottom of this test casting. This surface is ground and polished, and then etched to reveal the grain size at this location. At times, however, it is more instructive to split the small casting down the center, from top to bottom, and to examine that surface. Both procedures were employed in this study.

The Alcoa sample was cut in half along the length of the sample. Then the surface was ground and polished before being etched to reveal the grain structure.

The polished sample was normally treated with Poulton's etch, which contains 60% HCl, 30% HNO₃, 5% HF, and 5% H₂O. This etch is used to reveal the grain structure of the casting. For alloys which contain copper, another etch is required. For some alloys, a 10% HF solution was used to etch the surface, while for others, Fennel's solution was the best choice. Fennel's solution is a two part etching process. The first is an etching step, which uses a solution that contains 30 cc H₂O, 7.5 g FeCl₃, 15 cc HCl, and 45 cc HNO₃. The second is a brightening solution, which consists of 60 cc H₂O, 6 cc HF, 9 cc HCl, and 15 cc HNO₃.

The standardized procedures established to measure grain size on the etched samples are outlined in ASTM E112. The grain structure can be reported in one of several units:

- average intercept distance
- calculated average grain diameter
- ASTM grain size number, and
- grains per unit area

Table H.1 below gives values for different units of measurement, for the sake of comparison. The easiest procedure is to measure the average intercept distance. All grain

sizes in this study were measured and reported in this way. The units employed are microns (μm or 10^{-6} meters).

Table H.1 Comparison of Various Grain Size Measurements

<u>Average Intercept Distance</u>			Average	ASTM		
<u>inches</u>	<u>mm</u>	<u>microns</u>	<u>Diameter (μm)</u>	<u>grain No.</u>	<u>grains/cm²</u>	<u>grains/in²</u>
0.008	0.2	200	252	14.5	1890	12,200
0.015	0.4	400	504	12.5	496	3,200
0.031	0.8	800	1008	10.5	112	724
0.047	1.2	1200	1512	9.5	56	362
0.079	2.0	2000	2520	8	20	128

The average intercept distance was determined in the following way: The etched sample was placed under a stereo zoom microscope (Figure 5.H.1) where it was illuminated from one side by a red light and from the other by a green light, so that each grain has a different color. A calibrated vernier scale was placed in one of the eyepieces, and the average intercept distance was measured by counting the number of grain boundaries along the length of the line. The average intercept distance (AID) was determined from the following equation:

$$\text{AID} = L/(N-1)$$

where the length of the line in the vernier is L, and the average number of grain boundaries lying on this line is N.

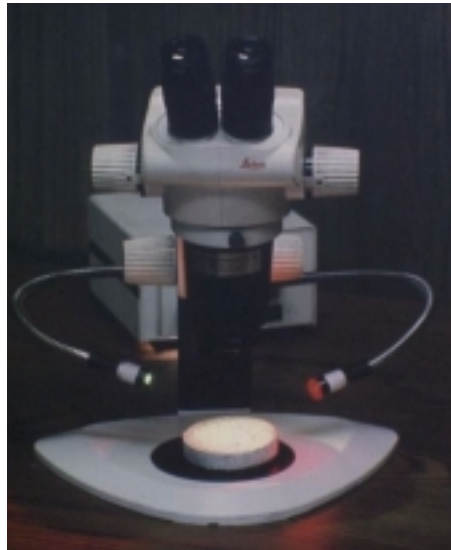


Figure 5.H.1 Stereo Zoom Microscope Used to Measure Grain Size

VI. Experimental Results and Discussion

A large number of different experiments were conducted over the course of this research and development program. All of this information represents a significant body of complex information. To assist the reader in understanding the significance of this material, a chronological presentation of the results is given below. Also, a detailed discussion of the data in each section is given together with the experimental results.

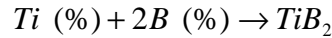
A. Use of Carbonaceous Gases

Both boron and carbon may be reacted with Ti to produce grain refining nuclei Ti-C or TiB₂. In many respects carbon is the preferred element to use. It is more abundant, easily obtained, and the cost is lower. Consequently, a significant number of survey experiments were conducted with commercially available carbonaceous gases. These experiments, and a literature survey of other published work, is given in appendix A. No significant grain refinement was obtained in any of these trials. This is presumably because carbon is virtually insoluble in aluminum (less than 1 ppm) at normal casting temperatures. Thus, the only way Ti-C can form is by reaction with dissolved Ti at the surface of the bubble. If the Ti content is 0.1%, then one atom in 1000 at the surface of the bubble will be Ti. The kinetics of the reaction is therefore unfavorable.

We then proceeded to study the use of boron-containing gases.

B. *In-Situ* Refinement with Boron

The next process to be examined was an *in-situ* grain refinement with gaseous boron-containing reagents. This reaction was felt to be more favorable from a kinetic and chemical viewpoint, and would be more likely to produce positive results. Boron has a considerable solubility in liquid aluminum, about 500 ppm at normal casting temperatures [6]. Thus, boron can easily dissolve into aluminum from the bubble, and then move by diffusion and convection to react with dissolved titanium. The titanium diboride is also much more stable chemically than Ti-C. Then solubility product is given by [18] as:



$$K = (\%Ti)(\%B)^2$$

where

$$\text{Log}_{10} K = -\frac{16,200}{T} + 5.22$$

At a temperature of 725°C (998 K) the solubility product K is equal to 10⁻¹¹. This means that, if you placed Ti and B into solution in the melt, in stoichiometric proportion to form the diboride (that is, so %Ti = 2.2%B), the final equilibrium melt composition would be equal to 1.6 ppm B and 3.6 ppm Ti. The chemical reaction can thus be seen to be extremely favorable. At titanium concentrations typical of wrought alloys (i.e. 200

ppm/Ti) and particularly foundry alloys (i.e. ~1400 ppm/Ti) the solubility of boron in molten aluminum in equilibrium with the boride nuclei is far less than 1 ppm.

This chemical reaction with boron-containing gases produced excellent grain refinement. The grain structure observed was qualitatively comparable to that found with commercial product available today, a 3Ti-1B alloy. A number of tests were made with this new process, in melts containing high purity metal and dissolved titanium levels between 50 and 1300 ppm. Melt compositions ranged from pure Al to various alloy types, such as 3004 and 6061. Grain refinement was found in all tests. A typical example of the internal structure found (before and after the *in-situ* refinement) is given below in Figure 6.B.1. Examination of this figure shows that the new process gave results that might be commercially acceptable as far as grain size and grain structure are concerned.

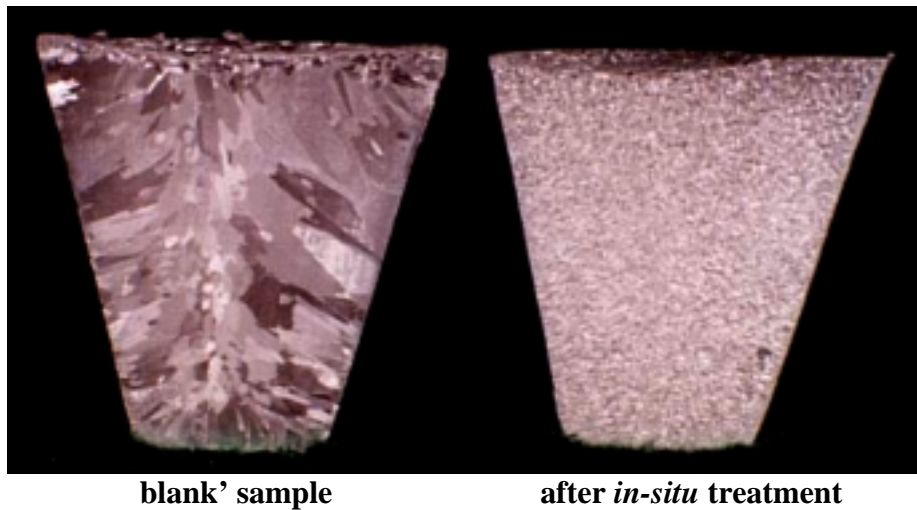


Figure 6.B.1 **Samples Before and After Treatment with BCl₃**

A detailed chronological description of the entire development program with boron-containing gases is now given, starting at the very beginning.

1.Initial Experiments

The first experiments using boron-containing gases to produce *in-situ* grain refinement were conducted in much the same way as the earlier work with carbonaceous gases. About 24 pounds of 99.9% aluminum ingot was melted down and alloying additions were made. The additions typically consisted of 50-250 ppm of titanium, and in some experiments, 1% magnesium and/or 0.5% silicon were added. The melt was then fluxed with an argon-1% chlorine mixture to remove dissolved gases in the metal, and also to help remove any inclusions, such as oxides left over from the melting process. Then, the boron gas, either boron trifluoride or boron trichloride, was administered via one of two types of lances. One was a $\frac{1}{8}$ " diameter stainless steel tube, which was protected from dissolving in the molten metal by a sheath of castable refractory. The other lance was a $\frac{5}{8}$ " graphite tube approximately 14" long. Both were placed at the bottom center of the crucible, so that the gas bubbles would float up through the entire height of the bath (8-9 inches). In these

early experiments, gas delivery times varied, but typically consisted of 2 inoculations of 30 minutes each. The notebook entry for a typical experiment is given below.

Heat 98-28 BCl₃ into an Al-0.025% Ti Melt

We intended to flux for two 25 minute periods with a mixture of argon and boron trichloride at a flow rate of 200 sccm and 24 sccm respectively. This would give an Ar-11% BCl₃ mixture. This gas composition was chosen primarily to give a convenient boron addition rate (of 1 ppm per minute at 100% recovery).

We had a number of difficulties maintaining the flow of BCl₃ gas during this experiment. After eight minutes of fluxing the BCl₃ gas flow dropped. It finally became apparent that the 1/8" diameter stainless steel lance was plugged. We removed the lance and examined it. The chlorides had eaten away a good portion of the hot end of the tube, and molten aluminum blocked off the small diameter (0.035") orifice. We replaced the stainless steel lance with a carbon lance, which contained a porous plug on the end, and resumed fluxing. We fluxed for another 15 minutes with this lance.

In the middle of the second 15 minute fluxing period (with the carbon lance) the BCl₃ gas flow went off scale of the rotameter. We believe this happened when we hit a pocket of condensed liquid in the tube with our propane torch. The flow was off scale for about 5-6 minutes. During this time, the BCl₃ gas flow was greater than about 190 sccm, so the gas composition was more than about 50% BCl₃. During this time there was a visible white fume above the melt. We finally shut off the BCl₃ gas valve, and let the system empty out of reactive gas.

The blank sample had an AA grain size of > 3000 μm . A sample taken at the end of fluxing had a grain size of 340 μm . Also, no columnar grains were observed in the refined sample.

Approximately 6 exploratory experiments were run by introducing boron trichloride and boron trifluoride into the melt through a lance. These experiments showed a significantly greater level of success in grain refining than was achieved in the carbon study. Table 6.B.1 summarizes the results of these experiments.

These exploratory experiments were seen as encouraging. Excellent grain refinement was obtained in nearly all of the samples with the average experiment improving the grain size from 3000 μm in the 'blank' to 220 μm after the second inoculation. However, boron recovery was low and the bubble size was large and could not be controlled. This prompted the construction of a Compact In-Line Gas Aluminum Refiner (CILGAR) unit following the trials at Littlestown Hardware and Foundry.

2. Trials at Littlestown Hardware and Foundry

The objective of these experiments was to validate the viability of the new fy-Gem process in a commercial scale batch melting furnace and to gain valuable operating knowledge necessary for the design of a commercial delivery system. An additional objective was to establish scale-up factors necessary to translate the laboratory results to a commercial scale. A detailed description of all experiments conducted at Littlestown are given in Appendix D. A brief summary of the results is given here. Table 6.B.1

Table 6.B.1 Summary of Initial Experiments with Boron-Containing Gases

<u>Heat No.</u>	<u>Gas Composition</u>	<u>Metal Composition</u>	<u>Temperature</u>	<u>Observations</u>
98-28	Ar-11% BCl ₃	0.025% Ti	750 °C	Grain refinement observed. Stainless lance plugged. Condensation of BCl ₃ resulted in uncontrolled gas flow.
98-29	Ar-11% BCl ₃	0.025% Ti	740 °C	Repeat of 98-29 with hot water tracing on gas lines. Grain refinement observed. 25 & 25 ppm B added.
98-30	Ar-11% BCl ₃	0.013% Ti-0.5%Si	740 °C	Repeat of 98-29 with lower Ti content. Some Si added for growth restriction factor. Grain refinement observed.
98-31	Ar-11% BCl ₃	0.005% Ti-0.5%Si	745 °C	Repeat of 98-30 with lower Ti content. Grain refinement observed. 20 & 20 ppm B added.
98-34	Ar-11% BCl ₃	0.050% Ti	725 °C	180 ppm B added.
98-38	Ar-11% BCF ₃	0.005% Ti-0.5%Si	750 °C	Grain refinement observed. Problems with gas regulator. 20 & 20 ppm B added.

Three experimental heats were made in a crucible melting furnace at Littlestown Hardware and Foundry. The results showed that RID (rotary impeller degasser) treatments in this furnace remove a significant amount of grain refining particles. The removal rate observed in one heat was 15 ppm B per hour. Depending on the boron addition rate, this removal may have prevented any desired grain refinement. There did not appear to be a significant chemical reaction between the melt and gas mixtures containing BF_3 . Only a small portion of the reactive BF_3 gas, less than about 15% of the total, was able to react to form boride. It is possible that a thin layer of solid aluminum fluoride coats the surface of the gas bubbles, preventing further chemical reaction.

A flux treatment with a 5% BCl_3 gas mixture appeared to produce little observable reaction as well, although a treatment using 3% BCl_3 produced a significant grain refinement, and a boron recovery of 115%.

The original design concept was that a small amount of reactive gas would be fed into an existing rotary degasser. The results at Littlestown suggested that a completely different method of introduction may give much better results. Further development then focused on the construction and development of a laboratory analog for industrial furnaces (CILGAR unit). The construction of the CILGAR unit is described above in section V.D. All subsequent laboratory experiments were made with the CILGAR unit. We began with head No. 1, and gradually increased the amount of stirring introduced into the melt by changing rotary head design.

3. Boron Trifluoride

Through the course of this work, a total of 15 experiments were run using boron trifluoride. It was believed that due to its high electronegativity and disassociation properties that boron trifluoride would be a good source of boron for the fy-Gem process.

Grain refinement, as a whole, was better than that achieved with carbonaceous gases. However, the boron trifluoride could not produce grain refinement on the level of commercial grain refiners.

The observed low boron recoveries are consistent with the formation of aluminum fluoride. This compound is solid at casting temperatures¹ and could form a thin layer, which may coat the bubble and prevent reaction of the gas with the metal. There is some evidence in the literature to support this view. In an attempt to reduce chloride emissions, Alcan researchers [19] replaced chlorine with SF_6 in a 6.25 ton laboratory tilting furnace, and in a SNIF unit. In the tilting furnace less than 2% of fluorine reacted with dissolved Ca in the melt. Most wound up in the dross. A lot of inclusions were also generated, especially in Mg-containing alloys. In the SNIF unit half of the SF_6 reacted with Ca (compared to 78% of the Cl_2) at concentrations of approximately 10% in the flux gas. Of most interest, however, is the fact that the degassing efficiency in the SNIF dropped from 81% to 61% when SF_6 was used. This suggests very strongly that some kind of solid layer is formed on the bubble surface.

¹ The Handbook of Chemistry and Physics says that AlF_3 sublimates at 1291°C

4. Boron Trichloride

Following the tests at Littlestown, an extensive set of trials began at the JDC laboratories in New Cumberland, WV. These experiments helped to characterize the fy-Gem process in great detail.

The first step was to construct and design a CILGAR unit for the small, gas fired, crucible furnace as described in Section V.D.

Tests made with BCl_3 gave better grain refinement, but the results and boron recovery tended to be somewhat erratic. The reason for this behavior was not obvious at first. However, as the results of the kinetics experiments (found in Appendix C) became available, the cause of the difficulty became reasonably clear. Up to this point the reactive gas had been administered over a fairly long period of time, typically 10-20 minutes, or longer. From the kinetic studies, it was clear that the boron had reacted with the melt. During this relatively long time a substantial amount of boride particles would float out with the bubbles.

Considering this situation, it was clear that shorter treatment times were necessary. Also, it was decided at this point to simulate conditions typically found in commercial in-line degassing systems. For this purpose tabulated data was used from a recent paper by Alcoa workers [20]. This information is reproduced below in Table 6.B4.1.

Process	Company	Number of Stages	Rotor Diameter (in)	Rotor Speed (rpm)	Typical			Metal Retention Time (min)	Gas per lb Metal (scf/lb)	Gas Loading (scf/lb)	Alloy	Typical Ca Removal (%)
					Metal Flow (lb/hr)	Size (lb)	Process Gas (scfh)					
A622	Alcoa	3	12	180	75600	9651	360	7.66	0.0048	0.04	5454	77
High Efficiency A622	Alcoa	3	6 (triple)	650	75600	2412	540	1.91	0.0071	0.22	5454	85
GBF Rotary System	Foseco	2	7 (estimated)	950	80940	2446	403	1.81	0.0050	0.16		
SNIF	Foseco	2	7.5	500	80000	3700	684	2.78	0.0086	0.18		
Alpur	Pechiney	1 (with 2 rotors)	10	150	67000	3300	636	2.96	0.0095	0.19		
HI-422 Metal Refining System	Hydro Aluminium	2	10 (estimated)	725	44000	5859	254	7.99	0.0058	0.04	5754	75
GFS	Noranda	2	10	300	82540	3800	278	2.76	0.0034	0.07		

Table 6.B4.1 Comparison of In-Line Degassing Systems [20]

From the information in the above Table, the gas loading in industry is found to be between 0.0034 and 0.0095 SCF per pound of metal. These are all two stage units, so the amount of gas going into each stage is 1/2 this amount, 0.05-0.13 liters/lb. The JDC crucible contains 24 pounds of metal during experiments, so the total flux gas should be in the range of 1.2 to 3.1 liters. The residence time for one stage of the above units is between 1 and 1.5 minutes, with the exception of the HyCast 422 unit, so the treatment time for the JDC laboratories was established to be between 1 and 1.5 minutes, and the gas flow rate was calculated to be between approximately 1 and 1.5 lpm.

In addition, the gas delivery system was modified to remove most of the uncertainties associated with the delivery rate of the reactive gas. The piping was changed so that the reactive gas lines could more effectively be cross-purged with argon. All of the lines containing BCl₃ were then heat-traced, including the line running to the rotary union above the furnace. Finally, the flow meters were placed inside a heated cabinet to prevent condensation there.

At this point, a series of preliminary experiments were run to compare the fy-Gem process to commercial 3:1 TiBor rod. While not matching the grain refinement achieved with the TiBor rod, the fy-Gem process did show enough promise to constitute continuation along this new line of testing. Table 6.B4.2 shows the results from these experiments.

Table 6.B4.2. Results of Preliminary Experiments

Heat #	Addition	Head	RPM	Ar (lpm)	BCl ₃ (ccm)	Dtime	T (°C)	B _{add}	Ti	V	Mg	AID(μm)
98-68	0.025 Ti	2	685	0.96	268.4	1.5	735	0.0010	0.034	0.015	0.00	300
98-69	0.025 Ti	2	760	0.96	268.4	1.5	735	0.0007	0.037	0.015	0.00	375
98-70	1Mg-0.015Ti	2	685	0.96	268.4	1.5	750	0.0014	0.017	0.011	0.89	425
98-71	1Mg-0.015Ti	2	685	0.96	268.4	1.5	770	0.0010	0.017	0.011	0.89	425
98-72	3.3ppm 3Ti-B	-	-	-	-	-	719	0.0004	0.028	0.015	0.00	375
98-73	6.6ppm 3Ti-B	-	-	-	-	-	731	0.0007	0.034	0.016	0.00	250
98-74	10ppm 3Ti-B	-	-	-	-	-	726	0.0011	0.035	0.015	0.00	190
98-75	0.025 Ti	2	685	0.96	268.4	1.5	711	0.0010	0.042	0.015	0.00	275
98-76	1Mg-0.015Ti	2	685	0.96	268.4	1.5	727	0.0007	0.019	0.013	0.89	650
98-77	0.025 Ti	2	685	0.96	268.4	0.5	713	0.0004	0.029	0.016	0.00	425
98-78	1Mg-0.015Ti	2	685	0.96	268.4	0.5	717	0.0002	0.026	0.013	0.93	425

Although the target titanium level was not supposed to fluctuate, the actual titanium level was somewhat hard to control due to the variability in composition of a titanium master alloy produced in the JDC laboratory. Analysis run by the Jamegy lab using an AA showed that the titanium level tended to fluctuate along the length of the master alloy. This provided a source of error throughout the length of this study until miniature titanium compacts produced by Jamegy, Inc. were implemented in Heat Number 00-207.

What these experiments showed was that the fy-Gem process could produce grain sizes within approximately 100 μm of commercial grain refiners. Moreover, the grain size improved with time in all heats. The five minute grain size is reported in the above table, but at 20 minutes the fy-Gem process gave results nearly equivalent to that found with the TiBor rod. These results are plotted below in Figure 6.B4.1. This served as a milestone in the fy-Gem project, since the process had not previously yielded such positive results.

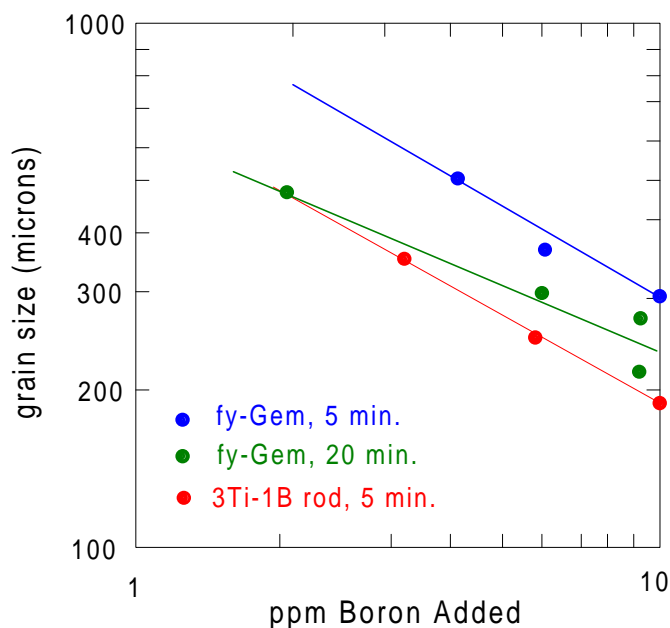


Figure 6.B4.1 Grain Refining Comparison in 99.7% Al

A series of survey heats were then run in several alloys: 99.7% pure Al, 356, 2024, 3004, 5182, 6061, 6063, and 7050 alloy. The results are summarized in Table 6.B4.2 below.

Table 6.B4.2 Results of Survey Experiments

Heat No.	Addition	Head	Agit (RPM)	Ar (lpm)	BCl ₃ (ccm)	Deliv time (min)	Temp (°C)	B _{add}	Ti	Mg	Mn	Zr	AID (μm)
98-79	5182 Alloy	2	685	0.96	268.4	1	706	0.0001	0.010	4.00	0.37	0.00	425
98-80	3004 Alloy	2	685	0.96	268.4	1	718	0.0006	0.039	0.75	1.19	0.00	425
98-83	5182 Alloy	2	560	0.96	268.4	1	714	0.0005	0.009	4.01	0.36	0.00	740
98-86	3004 Alloy	2	685	0.96	268.4	1.75	701	0.0004	0.026	0.77	1.18	0.00	600
99-89	A356 Alloy	2	685	0.96	268.4	1.5	640	0.0000	0.030	0.31	0.00	0.00	660
99-90	6063 Alloy	2	685	0.96	268.4	0.75	710	0.0002	0.039	0.53	0.00	0.00	330
99-91	A356 Alloy	2	685	0.96	268.4	1.5	652	0.0003	0.128	0.26	0.00	0.00	480
99-92	6063 Alloy	2	685	0.96	268.4	0.5	715	0.0001	0.042	0.53	0.00	0.00	350
99-94	2024 Alloy	2	685	0.96	268.4	0.75	712	0.0000	0.035	1.37	0.59	0.00	450
99-96	6061 Alloy	2	685	0.96	268.4	1	703	0.0000	0.083	0.76	0.03	0.00	480
99-97	7050 Alloy	2	685	0.96	268.4	1	703	0.0002	0.024	1.68	0.00	0.10	790
99-98	7050 Alloy	2	685	0.96	268.4	1	721	0.0004	0.022	1.32	0.00	0.13	580

These experiments showed that the fy-Gem process was capable of refining most alloys, with the notable exception of 7050 alloy.¹ 6063 alloy, in particular, seemed to be well suited for the fy-Gem process, at least at the high titanium levels that these experiments were run at.

5. Size and Composition of nuclei from Various Aluminum Alloys

The LAIS sampler was purchased and put into service just prior to the tests reported in table 6.B4.2. Preliminary research showed that the nuclei which were collected on a millipre filter after dissolving away the aluminum alloy matrix with acid gave the same

¹ This was due to the zirconium present in the alloy. This will be discussed in more detail below.

nuclei diameter measurement as that obtained by cutting, polishing and etching the LAIS sample directly. This work was done on a microprobe coupled to image analysis software at Touchstone Laboratory and is reported in detail in Appendix G.3.

Following this work the nuclei size of a number of alloys was determined. As presented in table 6.B4.2A. EDAX analysis to determine the semiquantitative analysis of the nuclei was also taken on each of the aluminum alloys as described in the Touchstone reports given in Appendix G.3. The raw x-ray data was analyzed with ZAF software. The results are also presented in table 6.B4.2A which shows the ratio of the solute (e.g. Mg, Mn, V, Si, Fe) to titanium in the bulk molten aluminum as showed by chemical analysis of cast spectrographic coupons by the Alcoa Technical Center compared to the EDAX/ZAF correction results from Touchstone Labs.

Note that the fy-Gem nuclei tend to be somewhat smaller than the TiBor nuclei for these tests. A more detailed look at the Touchstone reports show the nuclei are more uniform in size with fewer oversize nuclei.

The EDAX analysis show the nuclei incorporate vanadium from the molten aluminum and to a lesser extent manganese, iron, chromium, copper and zinc. They tend not to incorporate silicon and magnesium and surprisingly very little zirconium.

Table 6.B4.2A: Transfer of Solute Elements from Molten Aluminum into Nuclei

<u>Alloy</u>	<u>Sample No.</u>	<u>Element</u>	<u>Ratio W% Element to W% Ti</u>		<u>Nuclei Diameter, •</u>
			<u>In Bulk</u>	<u>In Nuclei</u>	
A 356	9991	Si	44.5	~0	1.195
• B=3 ppm		V	0.10	~0.20	
• GS=480		Mg	2.0	~0	
• Aero W/Nipples		Fe	1.6	~0.10	
6061	99124	Si	56.1	~0	1.074
* B= 4 ppm	99125	V	1.1	~1.10	0.825
* GS = 1500,900		Mn	1.5	~0	
• Block w/Nipples		Cr	4.6	~0.20	
		Mg	81.5	~0	
		Fe	27.7	~0.10	
18% Si in pure Al	99129	Si	876.5	~0	1.032
• B = 7 ppm		V	1.0	~0.50	
• GS = 650		Fe	11.1	~0.10	
• Block w/Nipples					
1.2% Mn in pure Al	99131	Si	9.4	~0	0.508
• B = 10 ppm		V	0.8	~0.60	
• GS = 500 •		Mn	49.40	~0.40	
• Block w/Nipples		Fe	9.4	~0.10	
7050 ¹	9997	Si	4.6	~0	0.960
• B = 2 ppm		V	0.5	~0.60	
• GS = 790 •		Mg	70.0	~0	
• Aero w/Nipples		Zr	41.7	~0.10	
		Fe	3.3	~0.20	
Pure Al	9875	Si	4.0	~0	0.594
• B = 2 ppm		V	1.0	~0.40	
• GS = 425 •		Fe	7.1	~0.10	
• Aero w/Nipples					
1% Mg in pure Al ²	9878	Si	1.9: 2.5	~0	0.588
• B = 2 ppm, 55 ppm	9888	V	0.50:0.69	~0.80	1.066
• GS = 425• , 340•			Mg, 35.8:50.6	~0	
• Aero w/Nipples		Fe	2.5: 4.4	~0.15	
3004	9886	Si	1.5	~0	0.723
• B = 4 ppm		V	0.6	~0.70	
• GS = 600 •		Mn	45.4	~0.80	
• Aero w/Nipple		Mg	29.6	~0	
		Fe	3.1	~0.15	
300 ppm V in pure Al	99130	Si	31.6	~0	0.753
• B = 8 ppm		V	2.0	~1.80	
• GS = 500 •		Fe	8.4	~0.20	
• Block w/Nipples					
0.2Cr in pure Al	99133	Si	2.8	~0	0.780
• B = 9 ppm		V	0.8	~0.70	
• GS = 700 •		Cr	5.6	~0.80	
• Block w/Nipples		Fe	8.9	~0.25	

1. Significant Cu and Zn also transferred to the nuclei in this alloy.

2. Two different levels of Ti addition

3. TiBor nuclei size averaged ~1.2 • with a significant number of large particles.

At this time, discussions began with Alcoa personnel concerning the fy-Gem process, and how it might best be tested and implemented within the Alcoa system. At Alcoa's suggestion, a series of 'matrix' experiments were run in 3004 alloy. The intention behind these experiments was to map out the region of optimum performance for the fy-Gem process before conducting the first large scale trials at the DC casting pit at Alcoa's Technical Center in Pennsylvania.

One of the most important commercial alloys, 3004 alloy contains magnesium, and so the introduction of BCl_3 into this alloy will produce MgCl_2 . In some of the preliminary experiments, a 'synthetic' Al-1%Mg alloy was used to simulate reaction conditions expected in the commercial 3004 alloy. Lagowski [21] has reported that the removal of Mg by fluxing with chlorine in molten aluminum becomes inefficient at temperatures below 710°C . The MgCl_2 salt is solid at these temperatures, and by analogy one might expect the fy-Gem process to become inefficient at low casting temperatures. (A similar effect was observed with BF_3 , because of the solid salt forming at the bubble surface.) Therefore, it was decided to investigate this possibility by using a variety of reaction temperatures.

While temperature was an important variable, the main variables in the Matrix experiments were agitator speed, titanium level, and boron addition. These variables were then compared to what would be expected from commercial grain refiners in Heats 99-113 and 99-114. The results can be found in Table 6.B4.3.

Table 6.B4.3 Results of Matrix 1 and Matrix 2 Experiments in 3004 Alloy

								Average Percent Composition											Grain Size
Heat No.	Addition	Head	Agit (RPM)	Ar (lpm)	BCl ₃ (ccm)	Deliv time (min)	Temp (°C)	B _{add}	Ti	V	Mg	Mn	Si	Fe	Cu	Cr	Zn	Zr	(μm)
99-99	Matrix 1-3004 Alloy	2	300	0.96	268.4	0.5	715	0.0000	0.005	0.016	0.93	1.35	0.05	0.09	0.00	0.00	0.01	0.00	2000
99-100	Matrix 1-3004 Alloy	2	300	0.96	268.4	1	711	0.0003	0.012	0.016	0.80	1.24	0.04	0.08	0.00	0.00	0.01	0.00	2000
99-101	Matrix 1-3004 Alloy	2	300	0.96	268.4	1	706	0.0003	0.023	0.016	0.75	1.28	0.05	0.08	0.00	0.00	0.01	0.00	1100
99-102	Matrix 1-3004 Alloy	2	500	0.96	121.8	1	705	0.0000	0.011	0.016	0.78	1.30	0.05	0.08	0.00	0.00	0.00	0.00	2000
99-103	Matrix 1-3004 Alloy	2	500	0.96	121.8	1	710	0.0000	0.027	0.016	0.80	1.27	0.05	0.08	0.00	0.00	0.00	0.00	2000
99-104	Matrix 1-3004 Alloy	2	500	0.96	268.4	1	720	0.0002	0.013	0.016	0.88	1.27	0.05	0.08	0.00	0.00	0.00	0.00	1800
99-105	Matrix 2-3004 Alloy	3	500	0.96	268.4	1	714	0.0009	0.026	0.015	0.94	1.25	0.05	0.08	0.00	0.00	0.00	0.00	450
99-106	Matrix 2-3004 Alloy	3	300	0.96	121.8	1	709	0.0005	0.013	0.016	0.95	1.29	0.05	0.09	0.00	0.00	0.00	0.00	1200
99-107	Matrix 2-3004 Alloy	3	300	0.96	121.8	1	705	0.0003	0.027	0.016	0.92	1.29	0.05	0.09	0.00	0.00	0.00	0.00	400
99-108	Matrix 2-3004 Alloy	3	500	0.96	268.4	1	718	0.0011	0.010	0.016	0.84	1.27	0.05	0.08	0.00	0.00	0.00	0.00	1400
99-109	Matrix 2-3004 Alloy	3	500	0.96	121.8	1	723	0.0004	0.022	0.016	0.97	1.27	0.05	0.08	0.00	0.00	0.00	0.00	1100
99-110	Matrix 2-3004 Alloy	3	500	0.96	121.8	1	717	0.0005	0.010	0.016	0.88	1.27	0.05	0.08	0.00	0.00	0.00	0.00	2000
99-111	Matrix 2-3004 Alloy	3	300	0.96	121.8	1	727	0.0005	0.010	0.016	0.93	1.27	0.05	0.09	0.00	0.00	0.00	0.00	2000
99-112	Matrix 2-3004 Alloy	3	300	0.96	268.4	1	729	0.0003	0.020	0.016	1.25	1.00	0.05	0.09	0.00	0.00	0.00	0.00	950
99-113	3Ti-B Rod/3004	-	-	-	-	-	728	0.0008	0.013	0.016	0.91	1.27	0.05	0.09	0.00	0.00	0.00	0.00	325
99-114	3Ti-B Rod/3004	-	-	-	-	-	765	0.0004	0.024	0.016	0.88	1.28	0.05	0.09	0.00	0.00	0.00	0.00	325
99-115	Matrix 2-3004 Alloy	3	300	0.96	268.4	1	705	0.0006	0.011	0.016	0.90	1.27	0.05	0.09	0.00	0.00	0.00	0.00	1100
99-116	Matrix 2-3004 Alloy	3	300	0.96	268.4	1	708	0.0006	0.022	0.016	0.79	1.25	0.05	0.08	0.00	0.01	0.00	0.00	375
99-117	Matrix 2-3004 Alloy	3	300	0.96	113.0	2.5	700	0.0010	0.022	0.016	0.86	1.27	0.05	0.08	0.00	0.00	0.00	0.00	240

As can be seen in Table 6.B4.3, the titanium and boron levels are extremely low in most Matrix 1 experiments. In some cases, there was no reportable boron addition. This means the resulting poor grain refinement was intentionally produced, in order to define where the operating boundary of the fy-Gem process was located. It turned out that this somewhat backfired in that all of the grain sizes were very similar to the blanks. Thus, no optimum could be found. However, it is important to note that at this point, the agitator

head was placed into the melt with argon flowing. Once the melt reached the target temperature, the boron trichloride valve was opened and the gas was admitted to the melt. After careful inspection of the gas delivery system, it was determined that there was a significant amount of dead time between the opening of the boron trichloride valve and when the gas finally began inoculating the melt. So, instead of receiving BCl_3 over the full 1 minute delivery time, the melt was actually only inoculated for approximately 10-15 seconds at the higher flow rates and probably not at all at the lower flow rates. After this discovery, the gas cart was modified to reduce the total dead time. First, the gas bottle was repositioned closer to the rotameters. Then, all of the stainless steel and Teflon lines were shortened to reduce the overall distance the gas had to travel. Once these modifications were completed, the dead times were determined experimentally and factored into all delivery times starting with the Matrix 2 experiments. At the low flow rate in the matrix experiments, an extra 34 seconds were added to the delivery time to allow for the dead time, while 10 seconds were added at the high flow rate. In the following tables, the reported gas delivery times reflect only the amount of time that boron was administered to the melt. Also, another important change is the use of a new head design. Beginning with these experiments, Head 3 (shown in Figure 5.D.1, page 19) was used to take advantage of the higher level of stirring that this head imparted.

The Matrix 2 experiments showed improved results as compared to Matrix 1 trials. The most obvious conclusion from this analysis of the Matrix 2 experiments is that the grain size achieved via the fy-Gem process is extremely dependent on the titanium level of the melt. This is seen most clearly in the figure below.

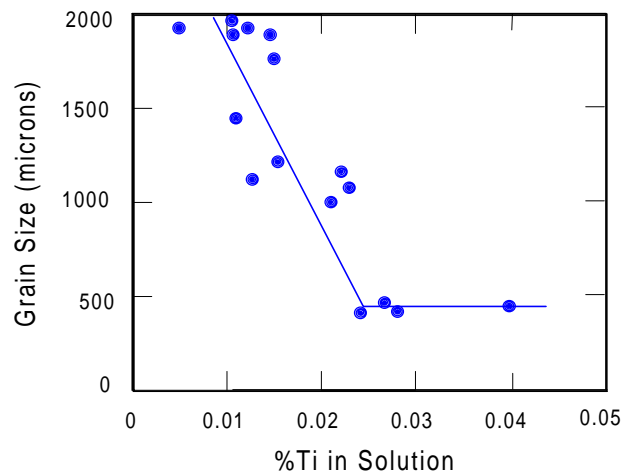


Figure 6.B4.2 Fy-Gem Grain Size versus %Ti in 3004 Alloy

It became apparent during these tests that although fy-Gem grain refined 3004, it did not give as fine a grain size as an equivalent amount of conventional Al-3Ti-1B refiner at a given titanium level.

It is useful to consider in some detail the possible reasons which may have caused the grain size to depend so strongly on the titanium content, as shown in Figure 6.B4.2.

One possibility is that the added Ti reduces the grain size, as a result of growth restriction. This may be determined by calculating the growth restriction factor (GRF) as proposed by Backerud [4]. The elements which contribute to slowing grain growth in 3004 alloy are, in order of potency, Ti, V, Si, Mg and Mn. When these calculations are made, we find the following results from Backerud's theory:

<u>Alloy Composition</u>	<u>Calculated GRF</u>	<u>Estimated Grain Size</u>
3004 + 0.005% Ti	5.1	350 μm
3004 + 0.025% Ti	10.0	225 μm
3004 + 0.05% Ti	16.1	195 μm

At an addition level of 0.025% Ti, the grain growth restriction factor almost doubles, and the grain size is reduced considerably. At higher addition levels, however, there is less of an effect, as a 'saturation' phenomenon of some kind is reached.

The results predicted by Backerud's theory are qualitatively in agreement with the results shown in Figure 6.B4.2. However, there appears to be a titanium, concentration grain refining factor over and above the "growth restriction" phenomenon indicated above, which affects the fy-Gem grain refining effectiveness. While our work was not able to clearly determine what this factor was, several theories have been discussed internally that may be useful to future investigators of the fy-Gem process. These theories are the :

1. Nuclei composition theory,
2. The duplex theory, and
3. The nuclei formation rate theory.

These theories are developed in more detail the results section.

A multi-variable statistical analysis was also performed on the results from the Matrix 2 experiments. The results of the statistical analysis are shown in Figure 6.B4.5.

The analysis shows that, as expected, higher boron and titanium levels resulted in improved, or finer, grain sizes. In addition, lower agitation speeds (with head No. 3) produced somewhat finer grain sizes. This result was surprising as higher rotational speeds clearly help the No. 2 head (e.g. nipped disc type). It may be that the block type head may actually develop less turbulence at the exit of the gas into the aluminum with higher speed due to the flow pattern with the thick disc. Finally, lower temperatures seemed to produce finer nuclei. However, the analysis shows this to be a rather weak effect.

One final important observation from the Matrix experiments is that the last experimental run using the fy-Gem process produced a grain size finer than that produced by Al-3Ti-1B rod in similar melt conditions. It is not clear why this may have happened, but it may be due to the inoculation of boron at a slower flow rate, perhaps in conjunction with the lower metal temperature during reaction.

At this point, further discussions with personnel at Alcoa Technical Center shifted the focus of the fy-Gem study to 6061 alloy. It was determined that due to the high volume and established qualification procedures involved with the production of can stock, fy-Gem would be difficult to implement in 3004 alloy. So, the study refocused its efforts on 6061 alloy. According to Alcoa, the production facilities for the 6000 alloy series would be a better fit for the fy-Gem system, at least initially.

Several preliminary experiments were run in 6061 alloy. The fy-Gem process was used for grain refinement in 5 of these experiments and 3:1 TiBor rod was used in another. The results can be found in Table 6.B4.6. It is also important to note that with experiment 99-124, the experimental procedure for inoculation shifted again. Following the initial multi-variable analysis conducted on the Matrix experiments, it was determined that temperature was not a major factor in controlling grain size. So, the boron trichloride was turned on and the flow was adjusted before the agitator was lowered back into the melt. After several experiments, it was determined that this procedure could be followed while still keeping the temperature of the melt within 10°C of the target. This allowed for better control of the boron trichloride feed into the melt.

Response: 5 Min GS

Summary of Fit

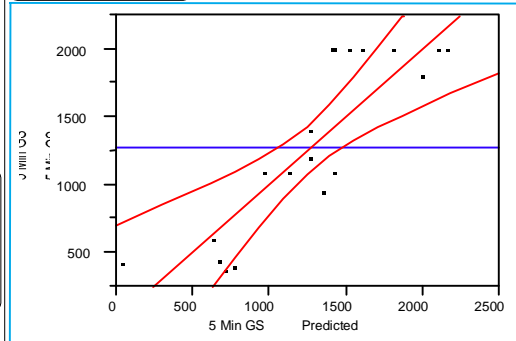
RSquare	0.777291
RSquare Adj	0.708766
Root Mean Square Error	348.326
Mean of Response	1272.222
Observations (or Sum Wgts)	18

Parameter Estimates

Effect Test

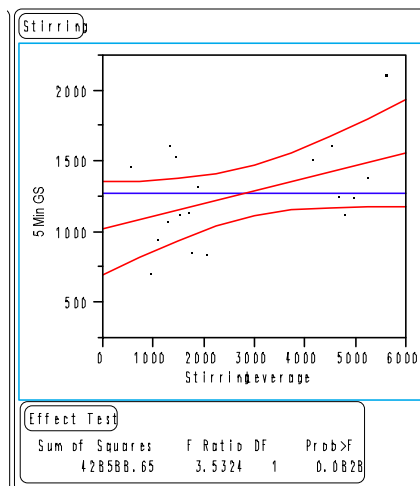
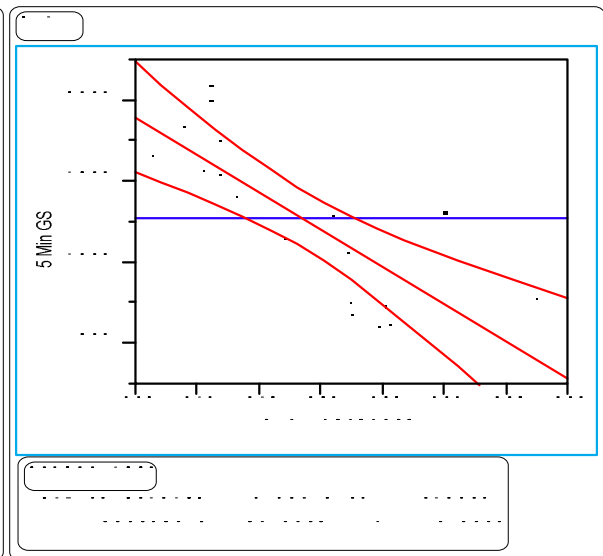
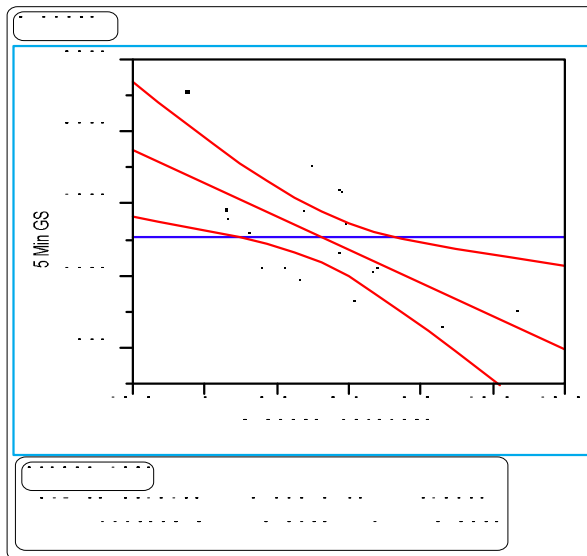
Source	Nparm	DF	Sum of Squares	F Ratio	Prob>F
Stirring	1	1	428588.7	3.5324	0.0828
Temp (C)	1	1	120802.7	0.9956	0.3366
B added	1	1	1118002.5	9.2145	0.0096
% Ti	1	1	2588693.8	21.3358	0.0005

Whole-Model Test



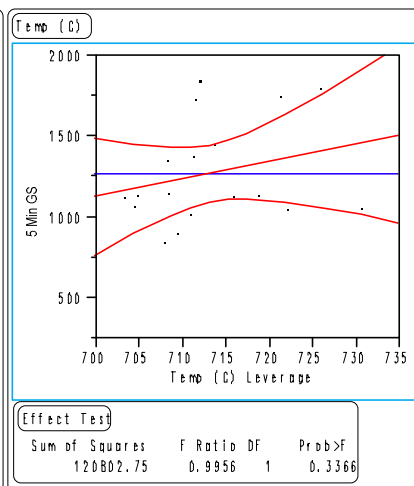
Analysis of Variance

Source	DF	Sum of Squares	Mean Square	F Ratio
Model	4	5505058.1	1376265	11.3431
Error	13	1577303.0	121331	Prob>F
C Total	17	7082361.1		0.0003



Effect Test

Sum of Squares	F Ratio	DF	Prob>F
428588.65	3.5324	1	0.0828



Effect Test

Sum of Squares	F Ratio	DF	Prob>F
120802.75	0.9956	1	0.3366

Figure 6.B4.5 Statistical Multi-Variable Analysis of Matrix Experiments with 3004 Alloy and Block Head (No. 3)

Table 6.B4.6 Results of Preliminary 6061 Alloy Experiments

Heat No.	Alloy	Head	Agit (RPM)	Ar (lpm)	BCl ₃ (ccm)	Deliv time (min)	Temp (°C)	Average Percent Composition											Grain Size (μm)
								B _{add}	Ti	V	Mg	Mn	Si	Fe	Cu	Cr	Zn	Zr	
99-118	3Ti-B Rod-6061	-	-	-	-	-	726	0.0010	0.022	0.014	0.98	0.02	0.74	0.30	0.30	0.07	0.00	0.00	240
99-119	6061 Alloy	3	300	0.96	268.4	1	702	0.0009	0.019	0.013	1.01	0.02	0.74	0.30	0.29	0.07	0.00	0.00	220
99-120	6061 Alloy	3	300	0.96	268.4	1	703	0.0011	0.010	0.013	1.03	0.02	0.73	0.30	0.31	0.07	0.00	0.00	840
99-124	6061 Alloy	3	500	0.96	268.4	1	706	0.0004	0.010	0.014	0.99	0.02	0.73	0.28	0.28	0.06	0.00	0.00	1500
99-125	6061 Alloy	3	500	0.96	268.4	1	705	0.0004	0.013	0.014	1.06	0.02	0.73	0.36	0.27	0.06	0.00	0.00	900
99-127	6061 Alloy	3	500	0.96	268.4	1	714	0.0005	0.016	0.015	1.09	0.02	0.73	0.35	0.27	0.06	0.00	0.00	800

As shown in the above results, it was determined that the fy-Gem process was capable of producing grain refinement equivalent to that of commercial grain refiners, at least in one heat. Compare the results of experiments 99-118 and 99-119. The other 4 experiments did not produce as fine a grain size, but the lower titanium level in these experiments (and B in 99-127) are important factors.

The reason for the excellent grain refinement in heat 99-119 is not obvious, but examination of the experimental notebook shows that there were some difficulties in the delivery of the boron-containing gas. During the treatment, the boron trichloride condensed in the rotameter. When the agitator was pulled out of the melt following the 1-minute inoculation, no BCl₃ gas was observed coming out of the agitator head. So, once the liquid was boiled out of the rotameter and the gas started emanating from the head, the agitator was plunged back into the metal for a second 1-minute inoculation period. Consequently, the physics of the gas delivery may have been altered, compared to the other experiments in the above table.

The above difficulties in BCl₃ gas delivery were unfortunately fairly common, and probably represents the major source of unexplained variability in our laboratory studies. This problem arises from difficulties inherent in handling a corrosive and reactive gas, which boils at 55°F. It also arises from difficulties associated with the laboratory experiments. We were trying to simulate conditions found in a large flow-through degassing system (c. 500-1,000 lb/min) with a short batch treatment in a small 25 lb. melt. Many of these gas delivery problems could have been eliminated by using the mass flow controller, as discussed above. Unfortunately, we did not identify a manufacturer of a reliable device until the end of our study.

A brief detour was taken from the 6061 research to investigate the effects of different solutes on grain refinement. The findings, listed in Table 6.B4.7, show that it is not clear how these solutes affect grain size using the fy-Gem process. Unfortunately, more experiments were scheduled, but cancelled due to an acceleration in the program's time line.

Table 6.B4.7 Results from Incomplete Solute Study

Heat No.	Addition	Head	Agit (RPM)	Ar (lpm)	BCl ₃ (ccm)	Deliv time (min)	Temp (°C)	B _{add}	Average Percent Composition										Grain Size (μm)
									Ti	V	Mg	Mn	Si	Fe	Cu	Cr	Zn	Zr	
99-129	18% Si	3	300	0.96	268.4	1	712	0.0007	0.017	0.016	0.00	0.00	14.90	0.19	0.00	0.00	0.00	0.00	650
99-130	300ppm V	3	300	0.96	268.4	1	700	0.0008	0.019	0.038	0.00	0.00	0.05	0.16	0.00	0.00	0.00	0.00	500
99-131	1.2% Mn	3	300	0.96	268.4	1	698	0.0010	0.017	0.013	0.00	0.84	0.05	0.16	0.00	0.00	0.01	0.00	500
99-133	0.2% Cr	3	300	0.96	268.4	1	706	0.0009	0.018	0.014	0.00	0.00	0.05	0.16	0.00	0.17	0.00	0.00	700

Note that even at the highest addition rate of alloying elements found in aluminum alloys they all produced grain refining with titanium levels of about 180 ppm!! Experiment 99 – 130 is particularly interesting in that the vanadium in the nuclei was nearly twice as high as the titanium concentration and it continued to grain refine.

From October 6 to October 8, 1999, scale up tests were conducted at the Alcoa Technical Center. fy-Gem v3.0, shown in Figure 5.B.3 of the Equipment Section, was used to deliver the boron trichloride gas to Alcoa's 662 in-line degassing unit.

The first test encountered startup problems, with the aluminum alloy freezing and blocking the tap hole of the furnace. In the second run aluminum alloy 6061 with c. 200 ppm Ti was melted in their No. 4 furnace, and about 525 pounds of metal was transferred to the 622 unit. Argon at 24 lpm and BCl₃ at 0.61 grams of B/min were added through the 622 rotor. This flux continued for 24 minutes, to bring the metal in the 622 unit to 6 ppm B. The 6061 alloy was then tapped through a filter at 22 pounds/min, and DC cast into an 11" ingot. A LIMCA unit was used to measure particles in the melt, and showed the metal was relatively clean. A LAIS sample was also taken after the fy-Gem treatment. The off-gas in the plenum above the metal in the 622 unit was sampled by passing it through a 1N caustic solution in a Smith-Greenburg impinger. The solution was analyzed for the presence of chloride ion and the results showed that more than 99% of the Cl from the BCl₃ had reacted with the metal.

The major result was that Alcoa cold finger tests of the metal treated with fy-Gem showed no grain refinement! Chemical analysis of the metal samples following the Alcoa 622 unit showed that the boron had transferred to the molten aluminum.

A test with 400 ppm of dissolved Ti was then conducted, with the same lack of grain refinement.

This failure was a complete surprise. The LAIS samples were analyzed using an SEM at Touchstone Laboratories, and showed that extremely small particles were made during this test. The borides produced were on the order of 0.1 μm in diameter, as shown below in Figure 6.B4.6. We also ran some of the metal used in the ATC trials in the laboratory reactor at JDC, Inc., with the No. 3 head and found that it grain refined as usual.

We then began laboratory experiments to explain why this failure had occurred. Several scaled-down 622 agitator heads were constructed, and attached to the CILGAR unit in our laboratory. (See head 4 of Figure 5.D.1 on page 19) In a water model study, we found

purge gas exited at the bottom of the agitator head, where it collected as a large, flat bubble. This is shown below in Figure 6.B4.7. We have calculated the volume of the large gas bubble to be about 40 cc. Since the argon-BCl₃ purge gas flow is about 1 lpm, the residence time of gas in this bubble is 2-1/2 seconds. In addition to the large residence time, there is very little stirring or turbulence at the surface of the bubble.

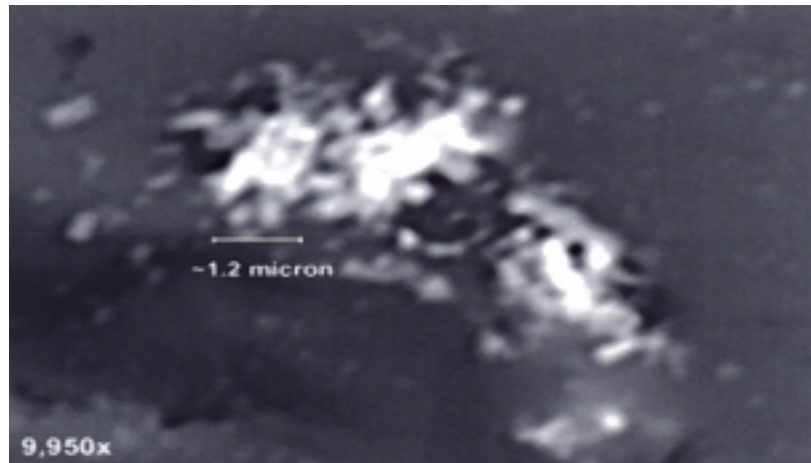


Figure 6.B4.6 Small Nuclei Created During ATC Tests in Alcoa 622 Unit

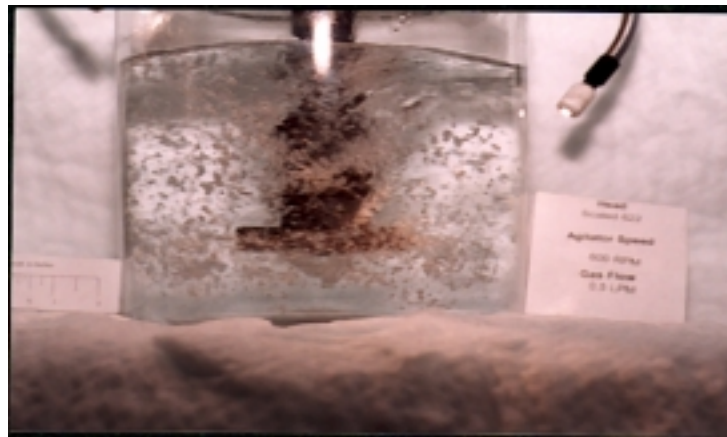


Figure 6.B4.7 Water Model Test of Small Scale Alcoa 622 Rotor Head

The purge gas collects in the large bubble underneath the 622 head, until the bubble becomes large enough to exit, and gas then floats out and up between the vanes at the edge of the head. The gas is 'chopped up' into smaller bubbles by the vanes of the rotor, and so good hydrogen removal is produced. But from the poor grain refining results, it appears that most of the boron reacted at the surface of the large 40 cc bubble.

When the small scale 622 Head was used in the JDC laboratories, the results proved to be just as poor as those obtained at the Alcoa Technical Center. Of the 5 experiments run with this head design, the finest grain size was 1230 μm . The test results are shown below in Table 6.B4.8.

Table 6.B4.8 Results of Experiments in 6061 Alloy with Scaled-Down 622 Head

Heat No.	Head	Agit (RPM)	Ar (lpm)	BCl ₃ (ccm)	Deliv time (min)	Temp (°C)	Average Percent Composition												Grain Size (μm)	Boride Dia. (μm)
							B _{add}	Ti	V	Mg	Mn	Si	Fe	Cu	Cr	Zn	Zr			
99-138	4	100	0.96	268.4	1	705	0.0000	0.015	0.015	1.10	0.02	0.74	0.35	0.20	0.06	0.00	0.00	2000	1.190	
99-140	4	411	0.96	268.4	1	713	0.0001	0.015	0.015	1.04	0.02	0.72	0.35	0.20	0.06	0.00	0.00	1670		
99-142	4	626	0.96	268.4	1	696	0.0001	0.016	0.015	1.12	0.02	0.71	0.36	0.20	0.06	0.00	0.00	1230		
99-144	4	800	0.96	268.4	1	706	0.0002	0.016	0.015	1.06	0.02	0.73	0.35	0.20	0.07	0.00	0.00	1490		
99-146	4	626	0.96	268.4	1	693	0.0001	0.014	0.014	1.07	0.02	0.72	0.35	0.20	0.06	0.00	0.00	1670		

From these results it was apparent that the design of the rotary head is critical for the success of the fy-Gem process. After discussing these findings with Alcoa personnel, we agreed to conduct further studies of head design, and to continue trials later at Alcoa with a head designed by JDC.

At this point, we returned to the original agitator head, so that the differences between all of the designs could be better quantified. A series of 8 experiments were run with the aerodynamic head with no nipples, No. 1 in Figure 5.D.1 on page 19, using varying conditions. The results of this study, shown in Table 6.B4.9, shows that this head is only slightly better at producing grain refinement than the 622 Head.

Table 6.B4.9 Results in 6061 Alloy With Aerodynamic Head (No Nipples)

Heat No.	Head	Agit (RPM)	Ar (lpm)	BCl ₃ (ccm)	Deliv time (min)	Temp (°C)	Average Percent Composition												Grain Size (μm)	Boride Dia (μm)
							B _{add}	Ti	V	Mg	Mn	Si	Fe	Cu	Cr	Zn	Zr			
99-148	1	100	0.96	268.4	1	699	0.0000	0.015	0.014	1.08	0.02	0.73	0.35	0.20	0.06	0.00	0.00	1350	4.850	
99-150	1	411	0.96	268.4	1	694	0.0002	0.016	0.015	1.10	0.02	0.73	0.35	0.20	0.07	0.00	0.00	1500		
99-152	1	626	0.96	268.4	1	705	0.0001	0.024	0.015	1.08	0.02	0.73	0.34	0.20	0.07	0.00	0.00	1130	2.190	
99-153	1	800	0.96	268.4	1	695	0.0002	0.015	0.015	1.08	0.02	0.71	0.35	0.20	0.07	0.00	0.00	1100	1.260	
99-154	1	800	0.96	268.4	1	698	0.0002	0.014	0.014	1.08	0.02	0.72	0.34	0.20	0.06	0.00	0.00	1650	2.500	
99-155	1	626	0.96	279.0	0.5	705	0.0001	0.014	0.014	1.11	0.02	0.73	0.36	0.20	0.06	0.00	0.00	1080	7.140	
99-156	1	626	0.96	98.4	2	703	0.0002	0.015	0.014	1.08	0.02	0.72	0.35	0.20	0.06	0.00	0.00	1130		
99-157	1	626	0.96	268.4	1	703	0.0001	0.014	0.014	1.11	0.02	0.73	0.36	0.20	0.06	0.00	0.00	1500		

The poor grain refinement with this head confirmed our results, found very early in this program in pure aluminum. We then switched to head No. 2, the aerodynamic head with nipples, and began an intensive set of optimization heats. In order to simplify the presentation of data, the experimental results will be grouped below based on the experimental variable studied.

The first optimization variable was agitator rotational velocity. Previous experiments with the head 3 (the block head with nipples) showed that greater rotational velocity resulted in a poorer (larger) grain size. As shown in the table below, with this head higher speeds gave better results. The reason for this difference will be considered later, when we discuss in detail the important role head design plays in the fy-Gem process.

Table 6.B4.10 Results in 6061 Alloy With Head 2 at Different Agitator Speeds

Heat No.	Agit (RPM)	Ar (lpm)	BCl ₃ (ccm)	Deliv time (min)	Temp (°C)	Average Percent Composition											Grain Size (μm)	Boride Dia (μm)
						B _{add}	Ti	V	Mg	Mn	Si	Fe	Cu	Cr	Zn	Zr		
99-160	100	0.96	268.4	1	710	0.0000	0.015	0.014	1.09	0.02	0.73	0.36	0.20	0.06	0.00	0.00	1500	
99-161	400	0.96	268.4	1	699	0.0003	0.015	0.014	1.09	0.02	0.73	0.35	0.20	0.06	0.00	0.00	1000	
99-162	600	0.96	268.4	1	705	0.0005	0.014	0.014	1.09	0.02	0.72	0.35	0.19	0.06	0.00	0.00	680	1.300
99-163	800	0.96	268.4	1	704	0.0006	0.015	0.014	1.14	0.02	0.75	0.36	0.20	0.06	0.00	0.00	430	0.893

Next, the delivery time of boron trichloride was studied. To accomplish this, the boron trichloride flow rate was adjusted according to the delivery time, so that approximately the same amount of boron was added in each run. This method was successful for the most part. Careful review of Table 6.B4.11 shows that the amount of boron added in each run is not constant.

Table 6.B4.11 Effect of Reactive Gas Delivery Time (Head 2 in 6061 Alloy)

Heat No.	Agit (RPM)	Ar (lpm)	BCl ₃ (ccm)	Deliv time (min)	Temp (°C)	Average Percent Composition											Grain Size (μm)	Boride Dia (μm)
						B _{add}	Ti	V	Mg	Mn	Si	Fe	Cu	Cr	Zn	Zr		
99-164	600	0.96	472.7	0.5	707	0.0003	0.016	0.014	1.04	0.02	0.71	0.34	0.19	0.06	0	0	740	
99-166	600	0.96	161.6	2	698	0.0008	0.017	0.014	1.08	0.02	0.72	0.35	0.20	0.06	0	0	540	1.100
99-174	800	0.96	161.6	2	701	0.0008	0.021	0.014	1.14	0.02	0.75	0.36	0.21	0.06	0	0	500	1.990
00-176	800	0.96	268.4	1	706	0.0007	0.027	0.014	1.08	0.02	0.75	0.36	0.20	0.06	0	0	470	0.846
00-177	800	0.96	118.9	3	699	0.0006	0.026	0.014	1.10	0.02	0.75	0.36	0.20	0.06	0	0	410	1.160
00-183	800	0.96	95.5	4	700	0.0007	0.021	0.014	1.11	0.02	0.76	0.36	0.21	0.06	0	0	590	1.120
00-185	800	0.96	78.5	5	712	0.0012	0.022	0.014	1.09	0.02	0.76	0.36	0.21	0.06	0	0	460	0.531
00-190	800	0.96	472.7	1	706	0.0011	0.023	0.014	1.09	0.02	0.75	0.36	0.20	0.06	0	0	440	0.756

From these results, it appears that the results with this head design are not sensitive to the rate of boron delivery. With the exception of heat 00-183, which had a grain size of 590 microns, all heats made at 800 rpm had a grain size of 450 ± 50 microns. This spread represents the probable error ($\pm 10\%$ of grain size) associated with a single test.

The carrier gas flow rate was the next variable studied. The argon flow rate varied between 0.3 and 5.85 lpm. The results are shown below. The main effect is that more boron is absorbed by the melt at higher carrier gas flow rates. (A larger argon gas flow results increases the amount of gas, and the bubble surface area in the melt, so increased efficiency of the boron reaction would be expected.) There is no appreciable effect of the carrier gas flow rate on grain size.

Table 6.B4.12 Effect of Carrier Gas Flow Rate (Head 2 in 6061 Alloy)

Heat No.	Agit (RPM)	Ar (lpm)	BCl ₃ (ccm)	Deliv time (min)	Temp (°C)	Average Percent Composition											Grain Size (μm)	Boride Dia (μm)
						B _{add}	Ti	V	Mg	Mn	Si	Fe	Cu	Cr	Zn	Zr		
99-168	600	0.3	268.4	1	704	0.0003	0.018	0.014	1.05	0.02	0.70	0.35	0.19	0.06	0	0	660	0.994
99-169	600	2.02	268.4	1	698	0.0005	0.018	0.014	1.06	0.02	0.73	0.36	0.20	0.06	0	0	560	0.875
99-175	800	2.02	268.4	1	695	0.0006	0.027	0.014	1.08	0.02	0.75	0.35	0.21	0.06	0	0	470	1.150
00-179	800	2.85	268.4	1	697	0.0004	0.027	0.014	1.11	0.02	0.75	0.36	0.21	0.06	0	0	510	0.784
00-180	800	3.85	268.4	1	700	0.0003	0.025	0.014	1.09	0.02	0.76	0.36	0.21	0.06	0	0	480	0.813
00-182	800	4.86	268.4	1	699	0.0006	0.025	0.014	1.14	0.02	0.76	0.37	0.20	0.06	0	0	440	0.316
00-187	800	5.85	268.4	1	714	0.0008	0.023	0.014	1.05	0.02	0.75	0.36	0.21	0.06	0	0	470	0.961

Immediately following these optimization experiments, four heats were made in 6061 alloy with a commercial grain refiner. These results showed that the fy-Gem process was still not as good as a commercial 3Ti-1B TiBor, for the same boron addition level.

Table 6.B4.13 Tests of Commercial TiBor Grain Refiner in 6061 Alloy

Table 6.2.15c Tests of Commercial Ti-6Al-4V Grain Refiner in 6061 Alloy															
Heat No.	Addition	Average Percent Composition												Grain Size (μ m)	Boride Dia (μ m)
		B _{add}	Ti	V	Mg	Mn	Si	Fe	Cu	Cr	Zn	Zr			
00-191	3Ti-B Rod-6061	0.0003	0.013	0.014	1.11	0.02	0.70	0.36	0.21	0.06	0	0	310	0.453	
00-193	3Ti-B Rod-6061	0.0007	0.022	0.014	1.11	0.02	0.71	0.36	0.20	0.06	0	0	220	1.370	
00-195	3Ti-B Rod-6061	0.0008	0.013	0.014	0.06	0.02	0.75	0.36	0.20	0.06	0	0	220	0.741	
00-196	3Ti-B Rod-6061	0.0003	0.020	0.014	1.13	0.02	0.73	0.36	0.21	0.06	0	0	300		

During the course of the optimization experiments, five additional tests were run in four other alloys: A356, 3004, 5182, and 7050. The results of these experiments are recorded below in Table 6.B4.14.

Table 6.B4.14 Results of Various Alloy Experiments

Table B-11. Results of Various Alloy Experiments																					
Heat	Alloy	Head	Agit (RPM)	Ar (lpm)	BCl ₃ (ccm)	Deliv time (min)	Temp (°C)	Average Percent Composition												Grain Size (μm)	Boride Dia (μm)
								B _{add}	Ti	V	Mg	Mn	Si	Fe	Cu	Cr	Zn	Zr			
99-170	3004	2	800	0.96	268.4	1	700	0.0008	0.026	0.015	0.81	1.16	0.05	0.16	0.00	0.00	0.00	0.00	640		
99-171	A356	2	800	0.96	268.4	1	642	0.0004	0.024	0.014	0.28	0.00	5.99	0.17	0.00	0.00	0.00	0.00	800	2.990	
99-172	5182	2	800	0.96	268.4	1	694	0.0003	0.025	0.003	3.98	0.36	0.06	0.16	0.00	0.00	0.00	0.00	240	4.860	
99-173	7050	2	800	0.96	268.4	1	701	0.0005	0.023	0.015	1.76	0.00	0.11	0.15	1.84	0.00	4.91	0.10	2100	0.927	
00-189	7050	2	770	0.96	268.4	1	695	0.0008	0.021	0.015	1.86	0.00	0.12	0.16	2.08	0.00	5.39	0.01	210	0.593	

The most important observation from the above results is that Zr poisons the fy-Gem process. This is seen clearly in the difference between the two heats, 99-173 and 00-189, which are the same except the Zr addition was omitted in the second heat. This is not an unexpected result, since the same poisoning reaction also occurs in Zr-bearing alloys with conventional TiBor master alloys.

From the nuclei composition table shown earlier (Table 6.B4.2A) the zirconium tends not to incorporate in the nuclei. This means that the effect of the zirconium on the grain refining process must arise from its presence in the bulk molten aluminum and exert itself on the surface of the nuclei during the nucleation event, as it does in conventionally made boride grain refiners.

Note too, that the excellent grain refining results shown in 99-172 and 00-189 occur with nuclei that have high levels of solute elements in the nuclei.

Following the optimization experiments, another set of trials was scheduled at the Alcoa Technical Center. The tests were run in a 50 lb crucible. The impeller head used is shown below. The rotor speed was 550-600 rpm in these trials.

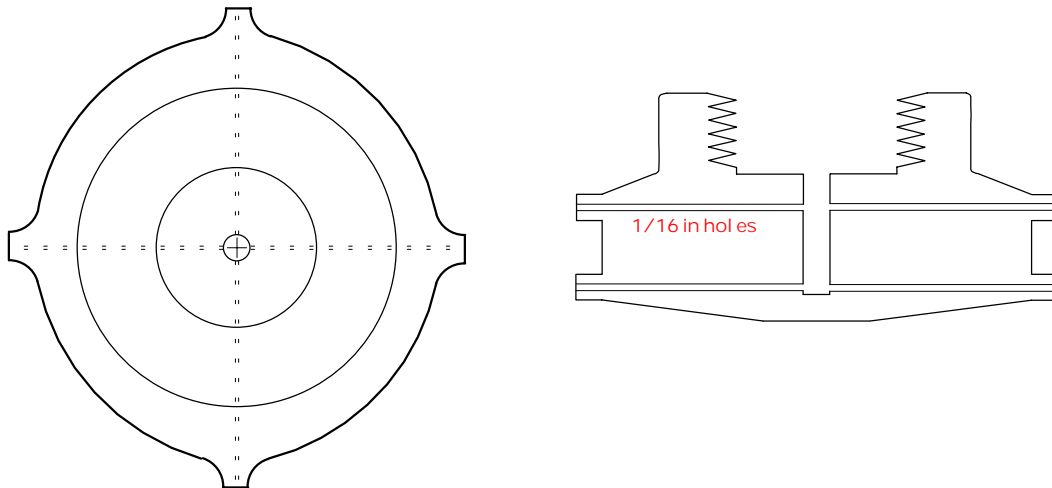


Figure 6.B4.8 Impeller Head Used in Trials at Alcoa Technical Center
Outside Diameter (including nipples) = 4.5"

The first tests were conducted in 6061 alloy which contained 0.025% Ti. The grain refinement at short times was not acceptable. It improved at longer holding times, but the results were marginal at best. A second test was made in metal with 0.04 % dissolved Ti. The grain refinement obtained was excellent. A detailed report of the second Alcoa trials may be found in Appendix D.2.A.

These tests confirmed the results obtained in the JDC laboratory, and showed that the fy-Gem process was indeed capable of producing grain refinement in 6061 alloy. However, an acceptable refinement was obtained only at high dissolved Ti levels. (Similar results were also found in 3004 alloy. (See Figure 6.B4.2 on page 31) The Ti content needed is significantly greater than what is used in normal casting practice today. Thus, although technically feasible, the fy-Gem process loses its economic advantage when the extra Ti must be added.

Based on these results, it appeared that the fy-Gem process is not economically viable for most wrought alloys, at least in its present stage of development. Consequently, we began to focus on casting alloys, which normally contain much higher dissolved Ti levels. The Al-Si-Mg and Al-Si-Cu casting alloys used commercially to produce a wide variety of important products normally contain between 0.08 and 0.15% Ti. Thus, they seemed to be excellent candidates for the fy-Gem process.

During the course of this work, we had a number of discussions with representatives from Reynolds Metals Company. Reynolds has four wheel plants, and they also produce and sell ingot for other foundries. Consequently, A356 was one of the alloys which they considered for fy-Gem trials. JDC received several pigs of A356 alloy from one of Reynolds' cast houses. A series of four experiments were conducted to determine the feasibility of using the fy-Gem process in the foundry alloy A356. In the fourth test a commercial 3Ti-1B TiBor rod was used to refine the metal. Table 6.B4.15 lists these findings.

Table 6.B4.15 Results of First Tests in A356 Alloy

Head	Agit (RPM)	Ar (lpm)	BCl ₃ (ccm)	Deliv time (min)	Temp (°C)	Average Percent Composition											Grain Size (μm)	Boride Dia (μm)
						B _{add}	Ti	V	Mg	Mn	Si	Fe	Cu	Cr	Zn	Zr		
1	800	1.99	95.5	2	702	0.0003	0.100	0.004	0.21	0.00	6.86	0.06	0.01	0.00	0.04	0.00	410	2.200
1	800	1.99	161.6	2	700	0.0004	0.100	0.004	0.22	0.00	6.91	0.07	0.00	0.00	0.03	0.00	380	3.600
1	800	1.99	161.6	4	700	0.0006	0.091	0.004	0.20	0.00	6.79	0.10	0.00	0.00	0.02	0.00	350	2.550
TiBor	-	-	-	-	706	0.0086	0.118	0.005	0.21	0.00	6.99	0.13	0.00	0.00	0.02	0.00	340	0.641

These results were very promising. Even at low boron levels, as compared to much larger additions normally used in foundry alloys, the fy-Gem process produced grain sizes equivalent to those from a commercial TiBor grain refiner.

When these results were reported to Reynolds personnel, a trial run at Reynold's facility in Richmond, VA, was scheduled for early April 2000. A new fy-Gem cart, v 4.0, was constructed and transported to the site. A series of 8 experiments were run over five days in a 400 lb melt. The two impeller heads used are shown below.

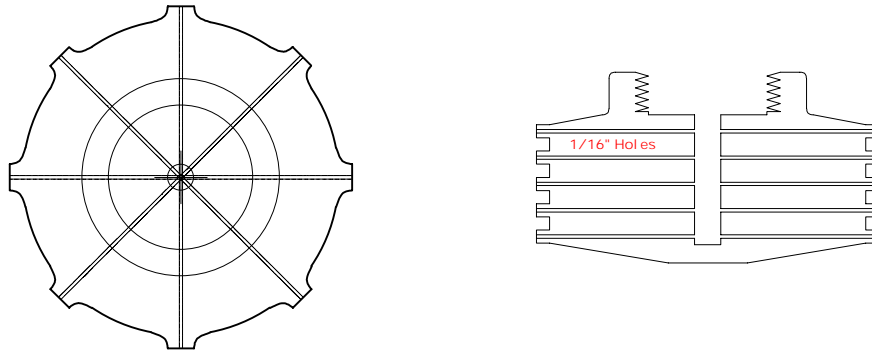


Figure 6.B4.9 The “Megy Head” used in the Reynolds Trials
Outside diameter (including nipples) = 6.5”

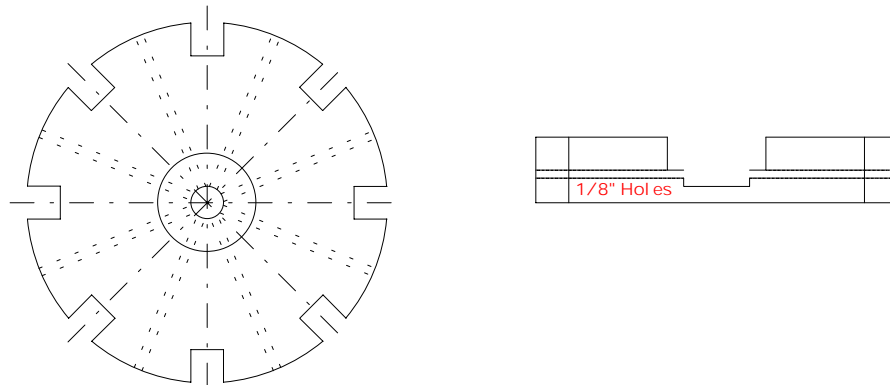


Figure 6.B4.10 The “Mazurek Head” used in the Reynolds Trials
Outside Diameter = 5.5”

The two heads gave similar results, although the grain size with the ‘Megy head’ was usually better. In all trials a grain refiner addition was made, either in the form of TiBor rod or via the fy-Gem process, and grain refining test samples were taken over a two hour time period. Two tests were used to determine grain size. One was the standard

Aluminum Association TP-1 test. The second was the ‘golf tee’ test. The golf tee test is an old Reynolds test procedure, and was employed because the solidification rate with this test is slower than the AA TP-1 test. The golf tee mold gives cooling rates close to those found during the solidification of thick sections in wheels. In some experiments the metal was stirred before taking the grain refining samples. In others, the metal was allowed to sit, without stirring. The two conditions gave different results, as shown below. (In the following figure, the grain sizes reported are an average of all tests made under that condition.) When there is no stirring, the boride nuclei settle out of the melt, and grain size increases slowly with time. When stirring was employed, the borides are not able to sediment. Interestingly, the grain size produced by the fy-Gem process improves with time. We noticed this before, in tests with 3004 alloy. Possible reasons for this effect will be considered in the main discussion given below.

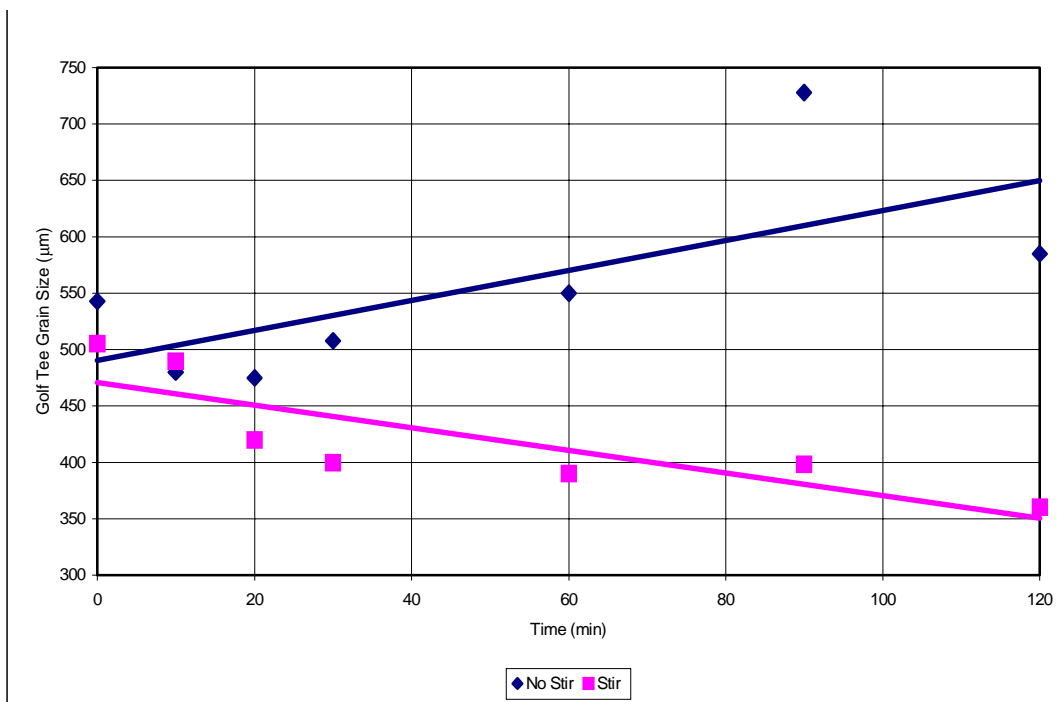


Figure 6.B4.10 Golf Tee Grain Sizes Versus Holding Time in Reynolds Trials

When testing the TiBor refiner, no stirring was employed, and the grain size also increased. From a practical point of view, the tests at 20-30 minutes are probably most relevant. This is because the grain refinement would be made in the ladle, and afterwards the metal would be transferred to the casting furnace. If we average the results of tests taken at 20 and 30 minutes, and where the boron addition is the same¹, we find the results tabulated below.

¹ There were difficulties controlling the boron addition in heat CK, and these results are not included.

Table 10. Average Values for Experiments

ID	HEAD	RPM	STIR	B AIM	Golf T (μm)	TP-1 (μm)
CL	TiBor	-	No	20	380	315
CN	Megy	475	Yes	20	390	245
CO	Mazurek	425	Yes	20	430	260
CP	Mazurek	480	No	20	435	330

It is easily seen that the fy-Gem process is equivalent to the TiBor refiner in A356 alloy, when one compares the results of the golf tee tests. At a faster cooling rate, found with the TP-1 tests, the fy-Gem process is equal to or superior to TiBor. A complete report of the results obtained at Reynolds Metals is given in Appendix D.3.

VII. Discussion of Results

A great deal of experimental information has become available during the course of this study, and it is possible to make a number of interesting and useful observations.

A. Effective Nuclei Form

The fy-Gem process produces heterogeneous nuclei in all alloy systems studied that are of appropriate size and grain refine. Since boron addition levels should be no higher than current practice the dual requirement of having enough particles form to provide a nuclei to every aluminum grain of desired size and large enough to allow growth of a nucleated grain of freezing aluminum means the nuclei must be somewhere in the 0.3-3 micron range. The data from this work show this requirement is met by the fy-Gem process.

B. Composition of fy-Gem Nuclei Varies with Alloy

Another clear result of the work is that the nuclei produced by the fy-Gem process incorporate a significant amount of elements present in the molten aluminum alloys besides titanium. Vanadium, manganese, iron, chromium, zinc, and copper all incorporate into the nuclei and magnesium, silicon and surprisingly zirconium do not. However, all of the heterogeneous nuclei that form show a grain refining capability.

C. Metal Treatment Unit Conditions Appropriate for fy-Gem

The gas flow rates, chlorine flow rates, metal residence times, and agitation rates of Metal Treatment Units are appropriate for the fy-Gem process. As discussed the rotor head geometry is important to fy-Gem nuclei effectiveness.

D. Titanium Levels Important in fy-Gem Process

As with current grain refiners the level of titanium in the molten aluminum is of critical importance to grain refining effectiveness of the fy-Gem process. In conventional grain refining the “growth restriction” mechanism discussed earlier “explains” the role of titanium in the grain refining process. In fy-Gem it appears to be particularly important over and above the “growth restriction” effect.

E. Rotor Geometry Important

The shape of the rotor had the largest effect on the effectiveness of fy-Gem produced nuclei of any variable studied. The tip geometry that produced the smallest bubble and greatest amount of turbulence where it contacted the molten aluminum gave the most effective nuclei.

A number of different head designs were employed in this study. These were described in section 5.D. (See the drawing on page 19.) Head 5 was used at the trials at Reynolds Metals Company. The others were used extensively on the laboratory CILGAR unit at the JDC laboratories in West Virginia. If all of the grain size tests in 6061 alloy are plotted versus head design, the result shown below is found. Heads two and three gave the best results. And between the two impellers, head two gave the smallest and most consistent grain size. The significance of this result should be considered in some detail, because it is of critical importance for the fy-Gem process.

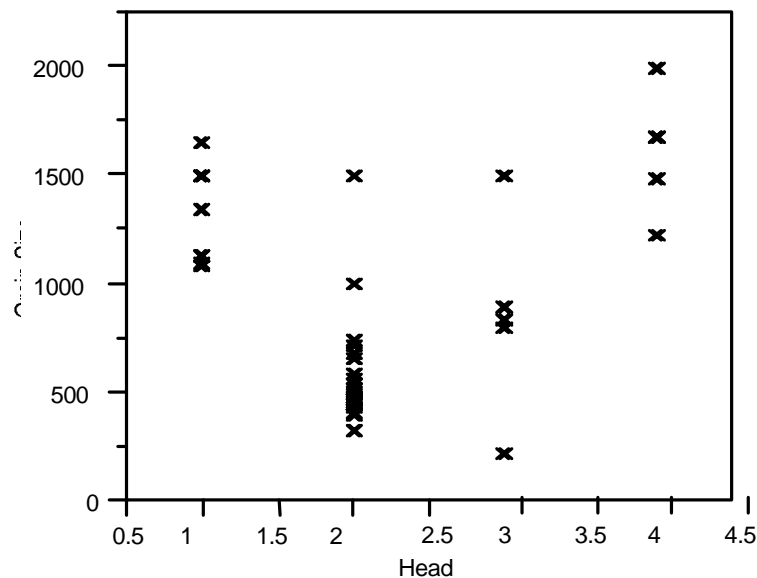


Figure 7.E.1 Grain Size in 6061 Alloy Versus Head Design

It is noteworthy that the bubble size produced by each of the four heads was very similar. What is changing with the head design is the total mixing energy placed into the melt, and the local shear at the point where the reactive gas first enters the melt.

During the course of this program, a theoretical study of mixing during gas purging was conducted. This study has been published in Aluminum Transactions, and a copy of the paper is included in Appendix C.1 for the interested reader. Briefly, Johansen and co-workers [11] developed a simple model, which said the average bubble diameter in the bulk of the solution may be characterized by the energy input of the impeller (in watts/m³). This study shows clearly that Johansen's theory is not valid. The four heads produced roughly equivalent bubble sizes, but the specific energy input varied from about 100 watts/m³ (head 1) to 3,000 watts/m³ (head 3). The local shear at the point where bubbles formed is more important for the fy-Gem process. Head No. 2 has an 'aerodynamic' design, which produces a minimum amount of stirring in the melt. But with this head the gas exits from nipples, which protrude into the melt, where there will be a high local velocity between the head and the metal.

The importance of the local shear is seen clearly when all test results for Head No. 2 in 6061 alloy are plotted as a function of rotation velocity, in the Figure below.

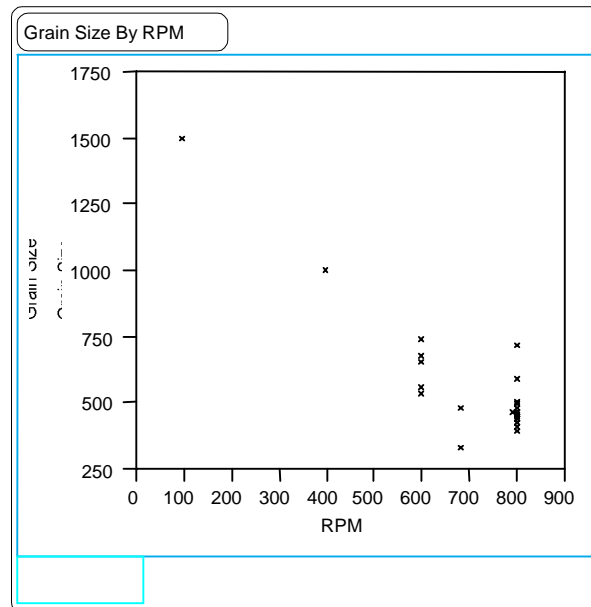


Figure 7.E.2 Grain Size in 6061 Alloy Versus RPM (Head 2)

Now that we know this, it may be possible to further improve the fy-Gem process, by designing new heads to maximize the local shear of metal where reactive gas bubbles are formed.

A statistical analysis of the data set obtained with head No. 2 in 6061 alloy showed that the shaft rpm was the most important variable with an F ratio of 35.7¹. The Ti content of the metal was next, with an F ratio of 4.2.² Other operating variables were not significant from a statistical point of view.

¹ A very high level of significance.

² The Ti content was not varied very much in these trials, or the variance observed probably would have been even greater.

F. Concentration of Boron Introduced

It was a surprising result of this work that the amount of boron added (provided that some was added) did not greatly affect grain refining. In other words additions of one ppm boron were nearly as effective as ten ppm boron additions! It was more important to use an effective rotor and higher titanium additions.

G. Boride Size

Depending on the process operating parameters employed, it is possible to make a variety of boride particle sizes with the fy-Gem process. Moreover, the size distribution tends to be narrower than usually encountered in TiBor refiners. This is because the borides are formed *in-situ*, just before solidification, and at concentrations 1,000 times less than with TiBor rod (c. 0.001% B versus 1% B). Thus, the chance of forming large agglomerates of borides is much less with fy-Gem. This characteristic of the fy-Gem process is potentially one of its inherent advantages. A smaller boride particle size, having a narrower size range, would be desirable for product quality, especially in critical applications, like foil or can stock, where large hard particles are detrimental.

According to a theory published by Greer and co-workers [1], the size of a boride particle is critical to its nucleating potential. Their theory suggests that a narrow size range would give a more potent refiner, and larger particles are better nucleants.

The first test results showed that borides produced with fy-Gem were usually smaller than, or almost the same size as, borides in a commercial TiBor rod. The results of some of these first particle size measurements are shown below in Figure 7.G.1.

As experimental work progressed, it became clear that fy-Gem was usually not as effective as TiBor in the wrought alloys. The particles produced with fy-Gem were usually smaller than with TiBor, and Greer's theory seemed to explain the difference in grain refining ability. Consequently, we spent a great deal of time and energy measuring particle sizes in our tests. Because a large number of conditions were employed in the survey experiments in 6061 alloy, we were able to produce a wide variation in boride particle sizes. (A complete table of all size measurements is given in Appendix G.2.) In some cases, the average particle size was larger than with TiBor. Comparing the particle size measurements to the grain refining observed, we obtain the results shown below in Figure 7.G.2. Contrary to the theory proposed by Greer and co-workers [1], the boride particle size does not appear to have a significant effect on fy-Gem refining ability.

This means that we have to look elsewhere, to explain the comparative performance of the fy-Gem process in wrought alloys.

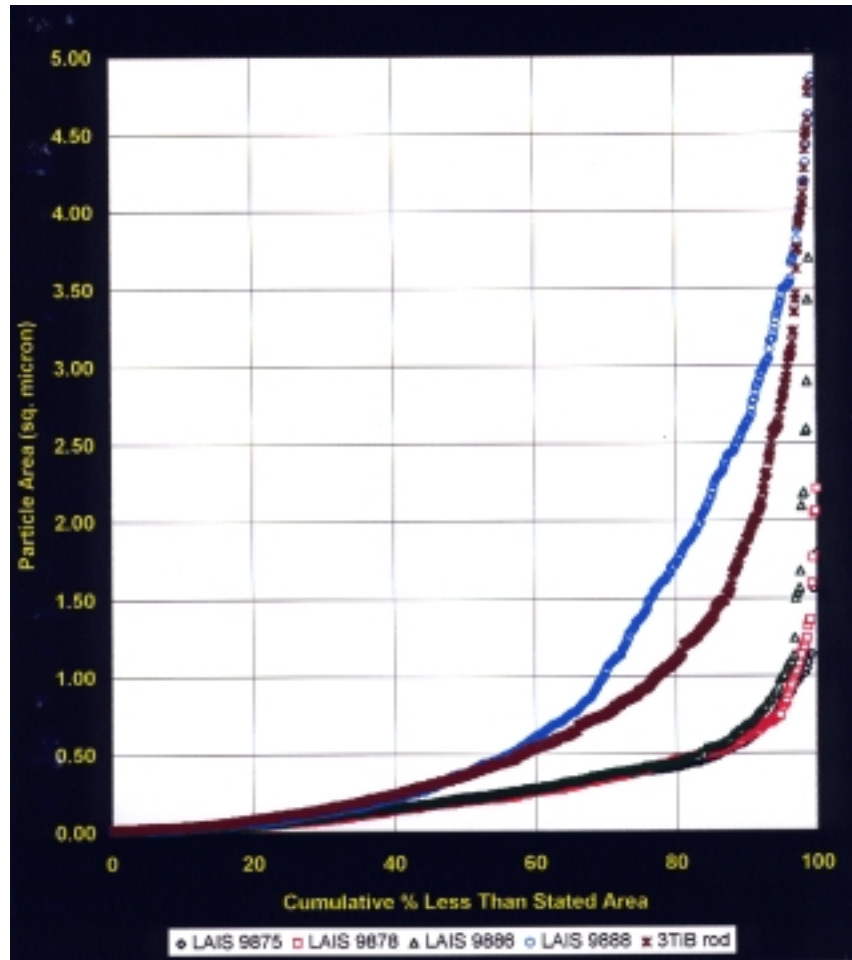


Figure 7.G.1 Plot of Boride Particle Sizes, fy-Gem and TiBor

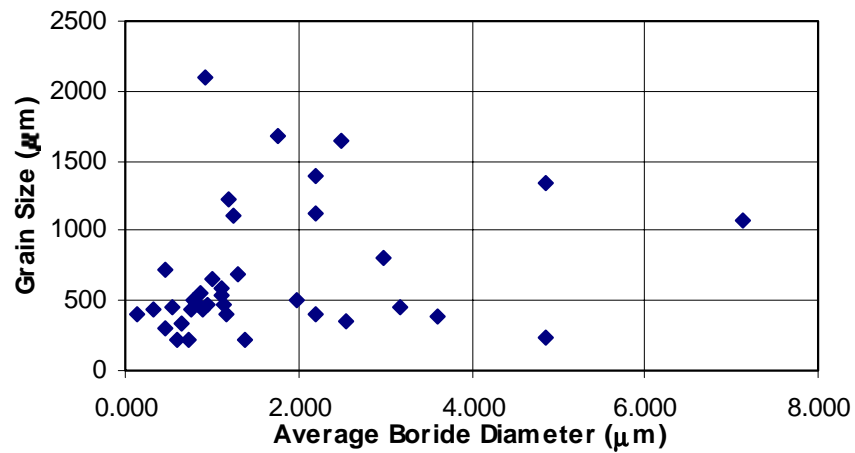


Figure 7.G.2 Effect of Boride Diameter on Grain Size in 6061 Alloy

H. Foundry Process

fy-Gem is as effective in grain refining foundry alloys with high titanium levels (i.e. 1400 ppm) as are conventional grain refiners. The authors recommend that a commercial demonstration of the fy-Gem process be conducted. Verification of expected cost and quality benefits of the fy-Gem process require commercial demonstration prior to open commercial use of the process.

I. Wrought Alloys

Although the fy-Gem process grain refines wrought alloys with their lower levels of titanium (i.e. ~200 ppm) they are not as effective as current commercial grain refiner. Several theories have been discussed by the investigators to “explain” the lower effectiveness of the fy-Gem nuclei in wrought alloys. They are forwarded below in the hope they may contribute to future research to improve the fy-Gem process.

J. The Composition Theory

It has been observed that higher dissolved Ti contents in the metal alloy produce boride particles which are higher in TiB_2 , and these give a better grain refinement. This effect was discussed earlier in some detail, when considering the results of our first matrix experiments in 3004 alloy (pp. 35-37 above), but it is worth reproducing some of those more important results here.

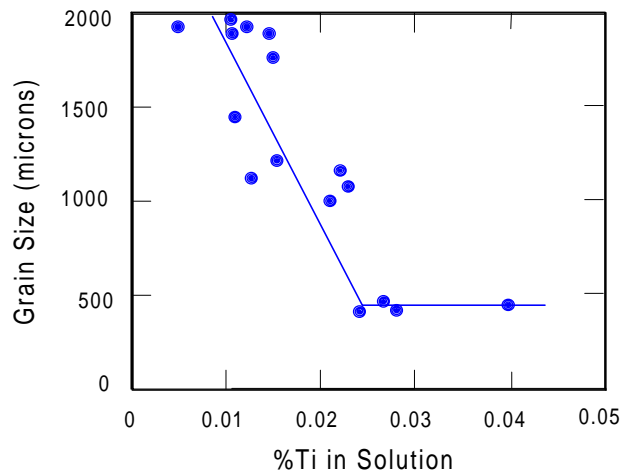


Figure 6.B4.2 Fy-Gem Grain Size versus %Ti in 3004 Alloy

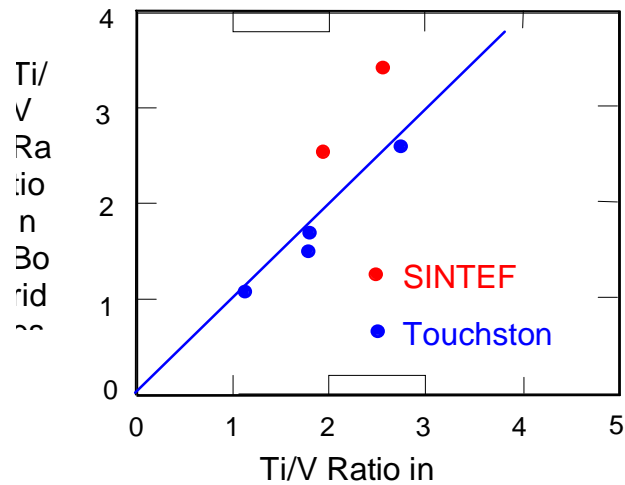


Figure 6.B4.3 Ti/V Ratios in Borides and Liquid Aluminum

The 3004 alloy used in these trials contained 0.016% V. From the first figure, it can be seen that a Ti content of at least 0.025% is needed for optimum grain refinement. This means the Ti/V ratio in the metal, and in the borides, had to be at least 1.6 for best results. This means that the boride particles should contain more than about 60% titanium vis a vis vanadium in the boride nuclei.

It is possible now to describe the probable reaction sequence in the fy-Gem process. The important pieces of evidence to keep in mind are the following:

- the linear relationship shown in Figure 6.B4.3 above,
- the presence of Mn in borides formed in 3004 alloy (Fig. 6.B4.2A on page 34), and
- the rapid build up of B at the bubble surface (Fig. 4.B.1 on page 11)

For a small bubble, the B concentration at the surface increases to a large value in about 0.1 msec. In this very small time, the atoms present in the melt are not able to diffuse to any practical extent. A simple calculation will suffice to illustrate this fact. The diffusion distance, δ , which an impurity can diffuse into a substance may be estimated by the formula:

$$\delta \cong \sqrt{4Dt}$$

where

D is the diffusion constant (c. 10^{-6} cm²/sec), and

t is the time of contact (sec)

When t is 0.1 msec (10^{-4} sec), the diffusion distance, δ , is equal to 2×10^{-5} cm, or 0.02 microns! This suggests that the rapid buildup of boron at the bubble, and the tremendous supersaturation produced, will consume almost all of any boride-forming elements present. Thus, the Ti and V ratios in the boride are about the same as in the metal.¹

¹ Although free energies of formation are not available, it is probable that the manganese boride is much less stable, as compared to TiB₂ and VB₂. This is why only a much smaller amount of Mn, compared to its concentration in the melt, is found in borides formed in 3004 alloy.

In the end, we overcame this technical limitation of the fy-Gem process by going to an alloy (A356) that had a high Ti content. There are other possibilities, however. It would be possible to make an addition of Ti, together with the B, in the fy-Gem process.

The effect of other elements which are incorporated in the fy-Gem nuclei are also reported in Figure 6.B4.2A on page 34.

We were not able to demonstrate clearly that nuclei composition played a clear negative role in grain refining performance for any element we studied. It could be that more sensitive testing in focused experiments would show some effect of nuclei composition. We were quite surprised the effect of composition was limited.

Zirconium in the alloy plays a clearly negative effect, but in the bulk aluminum solution, not as a constituent of the nuclei.

K. The Duplex Theory

The role of dissolved Ti content on the fy-Gem grain size in 3004 alloy is consistent with results published earlier by Guzowski and Sigworth [7]. Commercial TiBor master alloys used to refine wrought alloys contain excess titanium, present in the grain refiner as discrete particles of titanium aluminide (TiAl_3). Guzowski and Sigworth made experimental alloys, whose overall composition was less than the stoichiometric Ti/B ratio of TiB_2 . As a consequence, there was no TiAl_3 in these refiners, and the composition of the borides varied between AlB_2 and TiB_2 . A constant amount of boron was added via these refiners, to 99.7% Al containing different amounts of residual titanium. The results obtained are shown in Figure 7.K.1. The grain size depends slightly on boride composition, but the overriding factor was found to be the Ti content in the metal, similar to results with fy-Gem in 3004 alloy.

Sigworth and Guzowski also offer a possible explanation for the poor performance of fy-Gem compared to commercial master alloys, observed at low residual Ti levels. Titanium aluminide particles present in commercial TiBor refiners may contain numerous small boride particles. This two-phase structure was called a 'duplex' particle by Guzowski and Sigworth, and was found to be an extremely potent grain refiner. At the surface of TiAl_3 there will be a very high local concentration of Ti, until the particle dissolves. Thus, boride particles contained in the duplex particle will be potent nuclei. With fy-Gem there is no TiAl_3 produced, and the grain size is larger with low Ti residuals. At higher Ti contents in the metal, the relative advantage of a duplex particle is lost, and the fy-Gem process behaves similarly to TiBor refiners.

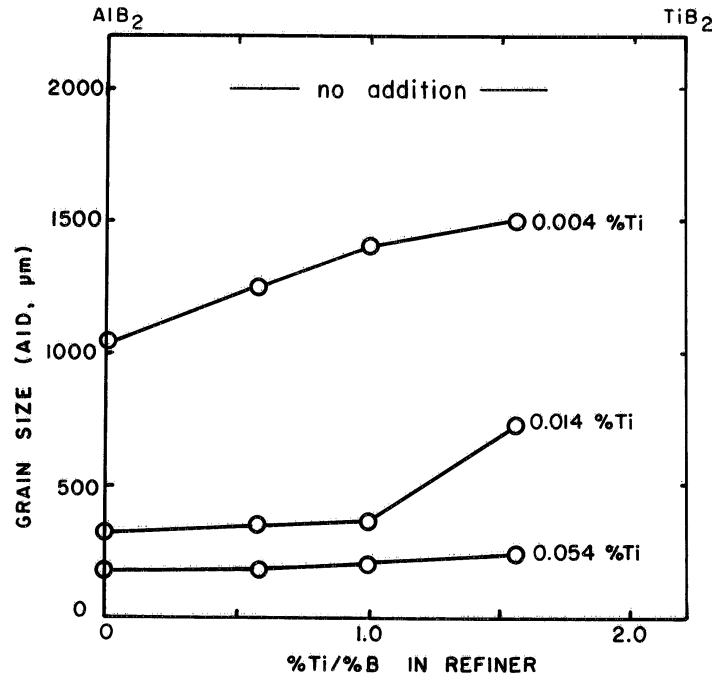


Figure 7.K.1; Two Minute Grain Size in 99.7% Al having Various Ti Levels

L. The Nuclei Formation Rate Theory

In the experiments run in this work, conditions which favor slower formation of the nuclei usually led to better grain refining performance. For example, lower concentrations of BCl_3 in argon were favorable. Also smaller bubbles formed at higher tip speeds were favorable. Turbulence during formation of the bubble when nuclei were forming appeared favorable.

Referring to the “onion skin” model presented earlier, favorable factors were those that lowered the boron supersaturation during nuclei formation.

In support of this theory is the finding that the boride nuclei size does not effect the grain refining efficiency. That is to say that perhaps nuclei that are formed in very non-equilibrium conditions have small areas on their surface which nucleate, but as per Greer do not grow without greater supercooling. Under gentler growth conditions perhaps the size of the nucleating areas are larger.

Another observation in support of this theory is that the nuclei generally become more effective with holding time.

M. Holding Time

We observed that the grain refining potency of the fy-Gem process almost always improved significantly with holding time. (Consider Figures 6.B4.1 on page 30 and 6.B4.10 on page 44) The most probable explanations for this are:

1. The size of the borides is changing with time, and
2. The composition of the boride nuclei surface changes with time

The first explanation is unlikely. TiB_2 has an extremely high melting point, and a very low solubility in liquid aluminum. Thus, it should coarsen by Ostwald ripening only very slowly. In addition, we have seen above that boride size is not an important factor in grain refining performance. The second explanation is more probable.

The nuclei are created in substantial supersaturation and boron excess at the bubble interface. After they form they mix with the bulk aluminum melt where the titanium is in excess of equilibrium on the nuclei surface. Perhaps some of the solute elements like manganese or vanadium exchange with titanium from the liquid aluminum, and surface energy being what it is some of the less thermodynamically stable areas on the nuclei reform. Perhaps this adds its effectiveness as a grain refiner.

N Gas Delivery System

A most important part of the fy-Gem process is the gas delivery system. Several versions of equipment were constructed to deliver a mixture of argon and boron trichloride. These were described in section 5.B above. No design was perfect, but they were certainly adequate for the purpose of this study.

Boron trichloride boils at 55 °F. At room temperature it has a vapor pressure of about 5 psi. The compound is also extremely corrosive, and highly reactive. If air or water leaks into the gas delivery system, a corrosive, sticky yellow liquid forms, which is anathema to correct operation of valves and flowmeters. In addition, in colder weather there is the risk of BCl_3 condensing in the line connecting the gas delivery system and the rotary degasser. Consequently, it is necessary to heat trace the delivery line, or use commercially available heated lines.

Because of the problems inherent with the handling of BCl_3 , as described above, we experienced a sporadic, but continual difficulty in maintaining an accurate delivery of reagent gas. For this reason, the final concentration of boron in the metal was not always as desired. Almost certainly, this situation contributed greatly to the variability we observed in the performance of the fy-Gem process.

Further development work should employ the mass flow controller identified in section 5.B for the gas delivery system. This equipment would make the process much more reliable. It will also give an instantaneous, real time reading of boron delivery rate.

IX Conclusions and Recommendations for Further Work

The fy-Gem process is capable of producing boride particles having a more uniform size range than with conventional TiBor refiners. The average fy-Gem particle size may also

be smaller. These two characteristics mean that the incidence of large, undesirable particles (KAlF clusters, oxides) will be considerable less with fy-Gem.

Greer and co-workers [1] have proposed a theoretical model which suggests that nucleant potency, and grain refining effectiveness, will depend on the size of boride particles. In our experiments the average boride size produced by the fy-Gem process varied from 0.5 to 5 microns, but particle size does not appear to control or significantly effect the grain refining ability.

Tests in A356 alloys, which contained c. 0.1% Ti established that in foundry alloys the refinement with fy-Gem is equivalent to, or better than TiBor alloys for the same addition level of boron. The fy-Gem process is ready for commercial implementation in foundry casting alloys.

The grain refinement produced with fy-Gem improves significantly with holding time. This is probably due to refinement of the nuclei surface by molten aluminum with dissolved titanium therein.

Statistical analysis of matrix experiments has shown that the most important process variable is the design of the rotary impeller head. It is vital to maintain a high degree of shear locally at the surface of the head, where reactive gas bubbles first contact the liquid metal.

These results, and the fact that four different head designs produced equivalent bubble sizes; even though the specific stirring intensity varied from 100 to 5,000 watts/m³; contradict the theory proposed by Johanson and co-workers [9]. In other words, the specific stirring intensity does not control bubble size during degassing. Local conditions, which exist at the surface of the rotary head, are controlling.

A number of useful experiments can be made, to further elucidate the mechanisms important for the fy-Gem process, and to further improve its performance. These recommendations come to mind:

1. Experiments on boride composition and holding time

It would be worth doing experiments in high purity aluminum metal, which has a fairly low V content. To this metal various additions of V, Mn, Fe, Cr, Zn, Cu and Ti could be made, to establish with certainty the effect of the Ti element ratio in the metal, and the corresponding borides, on grain refining performance. LAIS samples should be taken at short and long times in these experiments, to determine if the composition of borides changes with time. It may also be desirable to add Si to some of these melts, in order to maintain a constant value of the growth restriction factor.

2. Development of Impeller Heads

This study has shown that the fy-Gem process works best when a high localized shear is maintained at the point where the reactive gas bubble first contacts the metal. Now that

this requirement has been established with certainty, it may be possible to further optimize the process with different head designs.

3. Gas Delivery System

Any future work should employ the mass flow controller identified in section 5.B, in order to eliminate a significant source of process variability in fy-Gem.

4. Two Stage BCl₃ Addition

It may be possible to check the Nuclei Formation Rate Theory with a two stage BCl₃ addition. In stage one nuclei would be produced using the best head and operating conditions possible. Then a small amount of additional BCl₃ would be added in a second stage (say maybe 5% of the total) under very gentle condition. These would include very dilute BCl₃ in the argon and small bubbles. In the second stage the nuclei would already be present with the titanium concentration surrounding them at bulk levels. Under these conditions a relatively slow growth may occur and make a more perfect surface on the nuclei.

5. Second Generation fy-Gem

It may be useful to explore the possibility of adding Ti together with B in the reactive gas. One possibility is TiCl₄. Although it considerably complicates the gas delivery system, and adds significantly to the load of chlorine that the system must handle, it would be an interesting test of the capabilities of the fy-Gem process. The results would suggest useful directions which may be taken to further optimize the process for wrought alloys.

The Role of Mixing during Degassing of Molten Aluminum

Geoffrey K. Sigworth

GKS Engineering Services

116 Derby Street

Johnstown, PA 15905, USA

e-mail: gkseng@twd.net

Abstract

A number of studies have suggested that increased mixing improves the results obtained during the degassing of aluminum melts. However, the role of stirring has not yet been systematically studied. This paper reviews the available technical information on the role of mixing, and then examines the theoretical basis of the degassing process. The effects of mixing during the degassing of aluminum melts are classified. It appears that mixing is best characterized by a specific mixing intensity, or power density. Equations are given for specific mixing intensity by rotary stirrers and by the flow of gas through a melt, and calculations are made for a commercial degassing system.

Key Words: Degassing, Mixing, Aluminum alloy.

The Role of Mixing during Degassing of Molten Aluminum

Introduction

Commercial experience has established that a relatively high degree of mixing is required to obtain the best results during the degassing of molten aluminum. The history of degassing equipment over the last 30 years is characterized by the continued development of more intense stirring methods. Of course, as the stirring intensity increases, the process designer has to deal with the increased amount of rotational energy placed into the metal. Otherwise, great deals of splashing, vortexing, or air/metal emulsion are produced. Some of the design solutions, which have been used to reduce rotational momentum, either singly or in combination, are:

- Use of baffle plates
- Use of rectangular boxes
- Placing the rotor off center in the box
- Alternating rotor direction in multi-stage units
- Use of 'pumping' heads, to control and direct the metal flow
- Rotor designs having a high-localized shear where gas enters the melt
- Reverse rotation of the rotor assembly

There is a certain cost associated with these techniques. In addition, metal quality deteriorates at some point as the stirring increases. Thus, there is a limit to how much stirring is required for the best results.

This paper attempts to provide an answer to this question by reviewing the available technical information, and then examining the theoretical basis for characterization of the degassing process. It appears that mixing is best characterized by a specific mixing intensity, or power density (g, in watts/m³). Mixing has three effects:

- It breaks up the bubble flume, and distributes the bubbles evenly throughout the liquid.
- It promotes the formation of smaller bubbles.
- It assists in the transport by convection of reacting species to the bubble.

The first effect is characterized by a power ratio proposed by Oldshue and Chen [1, 2]. The second is explained by a theoretical relationship that predicts the maximum stable bubble size.

This relation has been derived by calculating and comparing the surface tension forces and the shear forces acting on the bubble. The third and last effect is described by using a dimensionless Stanton number, which gives the minimum level of circulation required in the melt for rapid mass transport. Correlations are also given for specific mixing intensity by rotary stirrers and by the flow of gas in a melt.

Review of Literature

Several researchers have reported that increased mixing improves the performance of degassing equipment. For example, in the first developmental trials with the Alpur system, Hicter [3] gave the results shown in Figure 1. More recently, Nilmani and co-workers [4] studied four different impellers. They measured the rate of desorption of oxygen in water models, to simulate hydrogen removal from liquid aluminum. In a batch process the hydrogen removal is given by the equation:

$$\frac{\overline{H}}{\overline{H}_0} = \exp\left(-\frac{k\rho A}{M}t\right) \quad (1)$$

Where \overline{H} is the hydrogen content at any time in cc/100g,

\overline{H}_0 is the original, or starting, hydrogen content in cc/100g,

t is the time in seconds,

k is the mass transfer coefficient in the bubble/metal boundary layer in m/s,

ρ is the density of liquid metal in Kg/m³,

M is the mass of liquid metal in the ladle or crucible in Kg, and

A is the surface area of bubbles in the melt in m².

The term $k\rho A/M$ has the dimensions of sec⁻¹, and determines the rate of hydrogen removal. This was called the gas slope parameter by Nilmani and co-workers. A similar expression can be derived for oxygen desorption in the water model study. The degassing performance of the impeller for an inert gas flow rate of 150 liters per minute is shown in Figure 2. It can be seen that the performance of all four heads in the water model improves with increasing rotation speed. Nilmani and his coworkers also calculated the peripheral velocity at the surface of the head and plotted the degassing performance versus this parameter, as shown in Figure 3. Considering this plot, all but the Foseco RDU head give similar results. The Foseco head is

different in shape. It has a triangular cross section, as compared to the rectangular turbine shape of the other heads. It also uses a centrifugal pumping action, see Figure 1 of reference [4].

It is evident from these results that the average bubble size decreases as the rotor speed increases. The average bubble diameter may be calculated from the following expression [4]:

$$kA = \frac{7.87.D_r^{0.5} G.H}{g^{0.25}.d^{1.75}} \quad (2)$$

where D_r is the diffusion coefficient of the reacting species in m^2/sec ,
 G is the gas flow rate in m^3/sec ,
 H is the height of liquid metal in m,
 g is the gravitational constant, 9.8 m/sec^2 and
 d is the average bubble diameter in m.

Johansen et al. [5] examined the forces acting on bubbles in a stirred melt. The surface tension forces keep the bubble from breaking up. Viscous forces, caused by turbulent shear produced by stirring, tend to break up the bubble. Calculating and balancing the two types of forces, they found the maximum bubble diameter that can exist in a stirred melt to be:

$$d = C \left(\frac{\sigma}{\rho} \right)^{0.6} \left(\frac{M}{P} \right)^{0.4} = C \left(\frac{\sigma}{\rho} \right)^{0.6} \left(\frac{\rho}{\varepsilon} \right)^{0.4} \quad (3)$$

where

σ is the surface tension of the metal in N/m,

ε is the specific mixing intensity, or power density, in watts/m^3 ,

P is the total energy of stirring in watts, and

C is a constant which depends weakly on rotor type and gas flow rate.

This simple relation was sufficient to calculate the bubble sizes observed in a large number of water model experiments with the HYCAST rotor and with a six bladed turbine impeller. It also allowed them to deduce that the bubble size in liquid metal will be about twice the size of bubbles observed in water model studies. Figure 4 shows the measured and calculated bubble sizes as a function of rotor speed.

Another approach was taken by Alcoa researchers [6, 7], who conducted a detailed statistical analysis of industrial results obtained with their in-line degassing process. They offered the

following correlation for the kinetics of Ca and hydrogen removal [6, 7]:

$$\frac{k\rho A}{M} = \frac{kA}{V} = Z \left(\frac{N^3 D^5}{V} \right)^{0.1045} \left(\frac{G}{A_r} \right)^{1.136} \quad (4)$$

where V is the volume of liquid metal in the reactor in m^3 ,

Z is a constant, which depends on the impurity element being removed, and the type of alloy being treated,

N is the rotation speed of the impeller head in revolution/sec,

D is the diameter of the impeller head in m,

G is the volumetric flow rate of gas in m^3/sec and

A_r is the surface area of the reactor in m^2 .

As we shall see below, the first term on the right hand side of this equation ($N^3 D^5/V$) is proportional to the power density (ϵ).

Chen [2] conducted a detailed water model study of an Alpur impeller and suggested that the resulting bubble distribution and flow pattern falls into one of the following four types. The type of flow pattern observed can be predicted by the stirring ratio (S). This is the ratio of the power density produced by the rotor (P_r in watts) to that produced by the upward flow of gas inside the liquid (P_g in watts). That is:

$$S = P_r/P_g \quad (5)$$

The four bubble flow regimes are:

For $S < 1$ flooding or channeling

For $S \approx 1$ minimum dispersion of bubbles

$1 < S < 3$ intimate dispersion, or well dispersed

For $S > 3$ uniform dispersion, or recirculating flow

This classification scheme was originally proposed by Oldshue [1]. Without a more detailed study, it is not clear to what extent the results of the above water model experiments may be applied to the degassing of aluminum. In fact, a careful analysis of industrial results [8] suggests that, in most well designed commercial systems, the inert purge gas is saturated with hydrogen when it leaves the metal. In this case, the hydrogen removal process is limited by thermodynamic equilibrium. Thus, only the gas flow rate affects the hydrogen removal. In other words, below a certain size, the bubble diameter no longer affects hydrogen removal. This

statement is true only for in line systems having a fixed metal flow rate. In the general case, the ratio of the gas flow rate to the metal flow rate determines the degassing performance. This was shown clearly in the experiments of Chen and Engler [9], who developed a novel technique to continuously measure the hydrogen content during a batch degassing process. Some of their results are reproduced in Figure 5. In this particular experiment, the rate of gas removal is not improved significantly by increasing the impeller rotation speed beyond 650 rpm.

In some cases, increased stirring may result in a deterioration in metal quality. The most obvious problem is when a vortex forms. This is undesirable because oxides and other impurities at the surface of the melt are dragged into the metal by the vortex. Increased stirring may also result in a more rapid pickup of gas at the surface of the melt. This problem was studied theoretically in some detail by Johansen et al. [5] and by analysis of results obtained in plant trials by Waite [10]. The latter study is particularly illuminating, since it suggests that the adsorption of gas at the metal surface, as it is controlled by relative humidity in the air, often limits the degassing efficiency. This is an important difference between the water model studies and degassing of molten aluminum. As shown theoretically in reference [5], the rate of surface adsorption of gas is up to 10 times greater in liquid metal than in water. The other important difference, as may be calculated from equation 3, is that the bubble diameter in liquid metal will be about two times larger than that observed in water.

It is obvious from the above analysis that stirring and mixing have an important effect on the performance of any degassing process. Unfortunately, the picture that emerges from the information at hand is not very coherent and further analysis is necessary.

The other problem is one that has not been considered by the aluminum community. This is the role that mixing plays in the transfer of reacting species to the bubble. Author's commercial experience has shown that as metal flow rate increases, it becomes increasingly important to have proper mixing. One way to look at the situation is to compare the metal residence time in the reactor to the mixing time. This ratio is a dimensionless Stanton number, which can be used to describe the minimum level of circulation required in the melt for effective mass transport. This question becomes increasingly important as the industry tries to reduce operating costs by

decreasing the size of in-line reactors. In the Alcan compact degasser, for example, the metal residence time is calculated in seconds, not in minutes [10]. In this case, the question of what constitutes proper mixing becomes increasingly important.

Theoretical Analysis of Mixing and Stirring

Prior studies of the degassing of aluminum have assumed that the metal phase is perfectly mixed in the reactor. This assumption focuses only on the diffusion kinetics of the reacting species at the boundary layer surrounding the bubble. In this way, the analytical problem becomes more tractable. André, Robinson and Moo-Young [11] have conducted a detailed numerical study of the reaction mechanisms in gas-liquid reactors. This study is important because it establishes unambiguously when the assumption of perfect mixing is a reasonable one. The model employed in their study used a variable number of process stages, as shown in Figure 6. The volumetric flow of gas upwards through the reactor (Q_G) is shown on the left hand side of the figure. The mole fraction of the adsorbed species in the gas (hydrogen when degassing aluminum) is represented by (y). The volumetric flow of liquid through the reactor is Q_L and the entering and exit compositions are C_{in} and C_M respectively. There is a circulation of liquid inside the reactor, characterized by the internal volumetric flow rate (Q_C).

One important variable that may be used to characterize the in-line reactor is the recycle ratio (R):

$$R = Q_C / Q_L \quad (6)$$

This is the number of times, on average, that the liquid metal recirculates inside the reactor during its residence there. The recycle ratio may also be characterized by the liquid residence time inside the reactor:

$$t_R = V / Q_L \quad (7)$$

and the liquid circulation time:

$$t_C = V / Q_C \quad (8)$$

Thus:

$$R = t_C / t_R \quad (9)$$

The results of the numerical analysis conducted by André, Robinson and Moo-Young [11] are shown in Figure 7. Note that the results are characterized by the dimensionless group:

$$St_c = \frac{k\rho A}{M} t_c \quad (10)$$

The term $k\rho A/M$ has the dimension of sec^{-1} . (Note how this term appears in equation 1.) When multiplied by the circulation time, t_c , it forms the dimensionless Stanton number (St_c) that relates to metal circulation. The number of stages corresponding to in-line metal treatment systems is two ($M=2$). If we allow a maximum error of about 5%, then we must ensure that:

$$St_c = \frac{k\rho A}{M} t_c \leq \frac{0.2}{1 + (1/R)} \quad (11)$$

Alternatively, for a reasonably well mixed reactor, where R is greater than about 10:

$$St_c \cong \frac{k\rho A}{M} t_c \leq 0.2 \quad (12)$$

André, Robinson and Moo-Young also studied the situation involving a batch reactor. In this case for example, when treating metal in a ladle or a crucible furnace, the dimensionless group must be:

$$St_c = \frac{k\rho A}{M} t_c \leq 2 \quad (13)$$

Here the criterion (for a maximum error of 5% associated with the assumption of a perfectly mixed reactor) is different by a factor of ten. This is because there is no flow of liquid through the reactor in a batch process. Thus, there is no way that the liquid metal can somehow slip by the reaction zone, and escape treatment.

The dimensionless group presented above in equations 11 to 13 compares two quantities. The first is the ability of the circulating metal to provide the reactive element to the bubbles by convection. The second is the rate at which the reactive element can be removed by diffusion in the boundary layer surrounding the bubbles. When St_c is greater than 0.2 in an in-line reactor, or 2 in a batch reactor, the rate of reaction is limited by the mixing, or internal circulation of liquid. In this case, the metal stirring needs to be increased.

To use the above equations to evaluate the degassing process, the circulation times in industrial reactors must be determined. There are several possible difficulties in this task. The first problem is that it is usually much easier to measure mixing times (T_M) than circulation times, especially in water-based systems, and this is the data found most commonly in the literature.

Fortunately, there is an excellent correlation between the two, as shown by the experimental and theoretical study of Koen [12]. When measuring the mixing time, an addition is made to the liquid at zero time, and some property (viscosity, refractive index, conductivity, etc.) is measured with time. If the value of this physical property is represented by X , then the response of the liquid with time is given by:

$$\frac{X - X_{\infty}}{X_0 - X_{\infty}} = EXP\left(\frac{-t}{t_c}\right) \quad (14)$$

where X_0 is the initial value of X , at zero time,

X_{∞} is the steady state value, found at very long times and

X is the value at any time (t).

The significance of this equation may be illustrated by a simple example. At time zero a certain amount of salt is added to a tank, which contains distilled water. The electrical conductivity is measured at a certain location in the stirred tank. As the salt dissolves into and mixes with the water, the change in electrical conductivity is given by equation 14.

If the mixing time is defined as the time required for X to reach \exp^{-1} or 63% of its steady state value, then $t_M^{(63)}$ is equal to t_c . Similarly, $t_M^{(87)}$ is equal to $2t_c$ and $t_M^{(95)}$ is equal to $3t_c$. The mixing time is commonly defined as $t_M^{(95)}$, and this is the value used in this study. Thus, equations 11 and 13 become:

$$St_M \cong \frac{k\rho A}{M} t_M \leq \frac{0.6}{1 + (1/R)} \quad (15)$$

and for a batch process:

$$St_M = \frac{k\rho A}{M} t_M \leq 6.0 \quad (16)$$

where t_M is equal to $t_M^{(95)}$ in the above equations.

The mixing time must then be calculated, using the results found by Asai, Kawachi and Muchi [12]. They were interested in characterizing the conditions found in stirred steel ladles, and conducted a number of studies in water models. Various sizes were studied and the diameter of the vessel was equal to the height in all cases. The mixing times found in water models can be

applied to aluminum melts, when the water model results are multiplied by $(\rho_{Al}/\rho_{water})^{1/3}=1.33$. The results corresponding to three vessel sizes, which contain a volume of liquid equivalent to 20, 200 and 2000 kg of molten aluminum, are shown in Figure 8. The single curve on the left-hand side of the figure (at small values of ϵ) corresponds to a flow regime in which the energy dissipation is controlled by viscous forces. For the three separate curves on the right hand side of the figure, inertial forces predominate.

To use Figure 8, it is necessary to develop relations that can be used to calculate the power density associated with mixing.

Stirring by Impeller

There is a significant body of technical information on stirring and mixing by impellers in the chemical engineering literature. This data has been reviewed in detail by Shinji Nagata [14], and also by Bates and co-workers [15]. A dimensional analysis of the problem shows that:

$$f\left(\frac{D^2 N \rho}{\mu}, \frac{DN^2}{g}, \frac{P}{\rho N^3 D^5}\right) = 0 \quad (17)$$

where D is the diameter of the impeller in m,
 N is the rotation speed of the impeller in revolutions/sec,
 μ is the viscosity of the liquid phase in kg/m-sec,
 g is the gravitational constant, 9.8 m/sec² and
 P is the power consumed by the impeller in watts.

The first term in parentheses in equation 17 is the Reynolds number (N_{Re}) which represents the ratio of the inertial forces to viscous forces acting in the stirred system. The second term is the Froude number (N_{Fr}) which is the ratio of inertial to gravitational forces. The last term is the power number (N_P) which is a ratio of the pressure differential producing flow to the inertial forces.

The effect of changes in the Froude number can usually be ignored in all stirred systems operating in the laminar flow regime and in fully baffled reactors. The effect of the Froude number would be observed as a vortex at the surface of non-baffled systems. In effect, the vortex is the liquid's way of restoring the balance between inertial and gravitational forces. In liquid metal systems, we generally wish to avoid vortex formation; thus, the effect of the Froude number can be safely ignored. This means that for dimensionally similar systems, the power number is a function only of the Reynolds number. Figure 9 shows the experimental results for the power number versus the Reynolds number for six different turbine impellers [15]. In the turbulent regime, for values of $N_{Re} > 1000$, the power number is nearly constant, which means that the stirring power delivered to the liquid by the impeller (in watts) is:

$$P = N_p \rho N^3 D^5 \quad (18)$$

In practice, it is often necessary to make small adjustments to equation 18 to fit the experimental data on power consumption. The N_p is often not constant and decreases as the rotation speed increases. For example, see Figures 1.17 and 1.18 in reference [14]. In addition, as larger amounts of gas are admitted to the reactor, the power consumption drops. This is because the viscosity and density of the gas is much less than the liquid.

Johansen and co-workers [5] measured the power input by using a dynamometer and also by measuring the temperature rise of water in model studies. They determined correlations for the power versus rotation speed for two impellers: a Hydro rotor having a diameter of 0.2 m, and a six bladed turbine impeller with a diameter of 0.18m. The power produced by the Hycast rotor in water was:

$$P = \frac{0.895.N^{2.5}}{1+12.25.G^{0.5}} \quad (19)$$

The corresponding equation for the six-bladed impeller is:

$$P = \frac{1.394.N^{2.5}}{1+45.G} \quad (20)$$

From the above results, we find that the decrease in N_p at higher speeds is large enough in these two cases to bring the functional dependence of P from N^3 to $N^{2.5}$. The second effect, a decrease in power caused by the gas phase, is found in the denominator of equations 19 and 20. Calculations for the amounts of gas commonly used in the degassing of aluminum show that this

effect is relatively small.

Combining equation 18 with equation 20, and noting that $D = 0.18$ and $P = 1000 \text{ kg/m}^3$, we find that the power number for the turbine impeller is:

$$N_P = 7.38/N^{0.5} \quad (21)$$

This means:

$$P = \frac{7.38 \cdot \rho N^{2.5} D^5}{1 + 45.G} \quad (22)$$

In the absence of experimental data, this equation may be used as a first approximation to calculate the power generated by turbine impellers. For a more detail, see the study of Nagata [14]. The general equation for the Hydro rotor is:

$$P = \frac{2.797 \rho \cdot N^{2.5} D^5}{1 + 12.25.G^{0.5}} \quad (23)$$

Stirring by Gas Flow

The steady state flow of a gas bubble in liquid aluminum can be simply explained by the gravitational force acting on the bubble:

$$F_g = g\Delta\rho V_b \quad (24)$$

where F_g is the gravitational force in Newton,

$\Delta\rho$ is the difference in density between bubble and liquid ($\approx \rho$) and

V_b is the volume of the bubble in m^3 .

The gravitational force is opposed by the drag forces on the bubble, caused by viscous and momentum phenomena present in the liquid, until a steady state terminal velocity (U_b) is reached. This velocity can be calculated for various bubble sizes by using equations presented in the review by Clift, Grace and Weber [16]. The results are presented in Figure 10.

Most bubbles found in liquid aluminum have an equivalent diameter, D_e , greater than 0.7 mm (0.07 cm). Thus, the Reynolds number describing their flow ($N_{Re} > 100$) falls well into the turbulent regime. The drag coefficient (C_d) for these bubbles is essentially constant and equal to 0.455 [16]. Hence:

$$U_b = \sqrt{4/3 \cdot g D_e / C_d} = 1.71 \sqrt{g D_e} = 2.12 \sqrt{g \cdot (V)^{1/6}} \quad (25)$$

As the bubbles become larger, the shear forces become greater and start to deform the bubble. The bubbles then change from a spherical shape (region 1) into wobbling ellipsoids (region 2). The aspect ratio of the bubble (region 3) increases with diameter until they become spherical caps at a diameter of 6-10 cm (2.5-3"). For spherical caps, the drag coefficient is 8/3 [16], thus:

$$U_b = 0.8\sqrt{g} \cdot (V)^{1/6} \quad (26)$$

If we consider a single spherical bubble rising in the melt, the rate of energy dissipation is given by:

$$\varepsilon = \rho F_d U_b / M \quad (27)$$

If there are many bubbles, but they do not interact in any way nor cause a steady state recirculating flow of liquid, which contributes significantly to the velocity of the bubble, then:

$$\varepsilon = \rho F_d U_b N_b / M \quad (28)$$

where N_b is the average number of bubbles in the melt at any time. It can be shown that:

$$N_b = \frac{GH}{U_b V_b} \quad (29)$$

The drag force acting on the bubble is:

$$F_d = \frac{1}{2} \Delta \rho U_b^2 A_b C_d \quad (30)$$

where A_b is the cross sectional area of the bubble in m^2 and

C_d is the dimensionless drag coefficient for a bubble.

We therefore find that:

$$F_d = 0.552 \rho g D_e^3 = 12,030 D_e^3 = 22,980 V_b \quad (31)$$

Hence,

$$\varepsilon = 1.054 \rho^2 g GH / M \quad (32)$$

A similar relationship can be developed for spherical cap bubbles by assuming that

$A_b = 1.92 V_b^{2/3}$. The result is:

$$\varepsilon = 1.031 \rho^2 g GH / M \quad (33)$$

this equation is virtually identical to equation 32. Hence, we can use the relationship

$$\varepsilon \cong \rho^2 g GH / M \quad (34)$$

for bubbles of any size rising through a bath of liquid aluminum.

In the above analysis, we have ignored the change in pressure that the bubble encounters during its ascent, and the effect of pressure on bubble size. For degassing processes operating at atmospheric pressure, this effect is relatively small and can be ignored without serious error. This would not apply to a process operating under a vacuum or reduced pressure, nor would the above relations be valid in this case.

Effect of Liquid Recirculation

The previous equations are valid when an impeller is used to introduce gas into a melt. This is because the bubbles are spread out evenly into the liquid and they rise without any significant effect on the metal flow patterns. The simple analysis given above is not valid when internal recirculation of the metal results from the flow of gas. Such a case occurs when using a lance or a porous plug, as shown schematically in Figure 11. Here bubbles rise in a plume, causing the metal to flow upwards at this location. Thus, the bubble ascent is no longer at its steady state rise velocity, U_b , but at a larger value. Therefore, the bubbles are in the melt for a shorter period of time, and the total energy released to the metal is less than that given in equation 34.

This case has been studied by Sahai and Guthrie [16]. They have shown that:

$$\varepsilon = \frac{\pi \rho^2 U_b^2 D_e^2 C_d \bar{U} GH}{8 U_c V_b} \quad (35)$$

where \bar{U} is the average recirculation speed of the bath, and

U_c is the rise velocity of the bubble in the plume

Sahai and Guthrie's results show that:

$$\left(\bar{U} / U_c \right) (R_c)^{1/3} = 0.18 M^{1/3} \quad (36)$$

where R_c is the radius of the crucible or ladle. Combining equations 26, 35 and 36 we find:

$$\varepsilon = 0.186 \rho^2 g GH / R_c^{1/3} M \quad (37)$$

Taking this equation and making calculations for a crucible filled with 2000 lb. (750 kg) of aluminum, we find that:

$$\varepsilon = 0.27 \rho^2 g GH / M \quad (38)$$

This is 27 % of the value found in equation 34.

It is now possible to make several useful and interesting calculations. Since the published information regarding specific mixing intensity and bubble size is most complete for the Hydro degasser, calculations will be made for this system, which usually operates at a speed of 700-800 rpm. The Hydro commercial degasser box normally contains 620 kg of molten aluminum. The results of the calculations are tabulated below.

Table I. Calculated Results for the Hydro Degassing System

	Rotation Speed of Impeller Head (rpm)					
	400	800	1,000	2,000	4,000	10,000
ϵ_R (w/m ³)	708	4,100	7,200	40,000	224,000	2.27x10 ⁶
ϵ_G (w/m ³)	38	38	38	38	38	38
T_C (sec)	5.4	3.1	2.6	1.5	0.9	0.4
d (mm)	9.1	4.7	3.7	1.9	0.9	0.4
A (m ³)	1.24	3.43	4.78	13.5	38.1	151
V/kA (sec)	283	87	59	17.5	5.2	1.05
St_c	0.019	0.036	0.044	0.085	0.16	0.39

The stirring power ratio ($S = \epsilon_R/\epsilon_G$) is always greater than one. Even at low operating speeds, the rotor produces more than enough stirring to disperse the bubbles throughout the melt. The area of the bubbles in the melt is calculated from the bubble diameter by using equations 25 and 29. The value of kA/V has been calculated for hydrogen removal using values for the mass transfer coefficient (k) given in reference [18]. The mass transfer coefficient depends on the bubble diameter according to the following equation:

$$k = 2\sqrt{\frac{D_r}{\pi}} \left(\frac{g}{2d} \right)^{1/4} \quad (39)$$

In this equation the reciprocal of kA/V is given. The reciprocal is given in units of seconds and represents the time to remove 63% of the hydrogen (\exp^{-1}) in a batch process.

The Stanton number for circulation is the ratio of the metal circulation time (T_C) divided by V/kA . In all cases, except for 10,000 rpm, the numerical value of this dimensionless group is

well below the critical value of 0.2. Thus, in practice there is sufficient metal circulation to ensure that the usual assumption of a perfectly mixed reactor is valid. Contrary to expectation, the value for St_C increases as metal stirring increases. This is because the term V/kA , which is determined by bubble size, decreases faster than the circulation time.

It is worth noting that the metal circulation time is on the order of a few seconds, whereas the metal residence time in most systems is about a few minutes. This suggests that the size of the degassing chamber can be reduced without seriously hindering the kinetics of the degassing process. This is presumably the basis for the reported success of the Alcan compact degasser [10].

Conclusions

In this paper a detailed model has been presented for the stirring produced while degassing aluminum with rotary impellers. The equations given allow one to estimate the specific stirring intensity (ϵ), the average bubble diameter, and the total bubble surface area in degassing systems. Calculations have been made for a well established commercial system, and show that:

- the gas bubbles are well dispersed, even at low stirring speeds
- there is plenty of stirring, and the assumption of a perfectly mixed reactor is valid
- the metal circulation time is usually only few seconds, while the metal residence time is usually one or two minutes
- the above suggests that the size of most degassing boxes can be reduced significantly

Acknowledgements

The author gratefully acknowledges JDC Incorporated, Reynolds Metals Company, and the U.S. Department of Energy, whose financial assistance have made this study possible.

References

1. J. Y. Oldshue: "Fluid Mixing Technology" (Chemical Engineering), McGraw-Hill, 1983, pp. 141-154.
2. J. J. J. Chen and J. C. Zhao, "Bubble Distribution in a Melt Treatment Water Model," *Light Metals* **1995**, pp. 1227-1231.
3. J. H. Hicter, "Alpur Refining Process," *Light Metals* **1983**, pp. 1005-1022.
4. M. Nilmani, P. K. Thay and C. J. Simensen, "A Comparative Study of Impeller Performance," *Light Metals* **1992**, pp. 939-946.
5. S. T. Johansen, S. Graadahl, P. Tetlie, B. Rasch and E. Myrbostad: "Can Rotor Based Refining Units be Developed and Optimized Based on Water Model Experiments," *Light Metals* **1998**, pp. 805-810.
6. D. C. Chesonis, H. Yu and M. Scherbak, "In Line Fluxing with High Speed Multiple Rotor Dispersers," *Light Metals* **1997**, pp. 843-846.
7. J. G. Stevens and H. Yu, "A Computer Model Investigation of the Hydrogen Removal Rate in the Alcoa 622 Process," *Light Metals* **1992**, pp. 1023-1029.
8. G. K. Sigworth, "Gas Fluxing of Molten Aluminum: Part 1 - Hydrogen Removal," *Light Metals* **1999**, pp. 641-648.
9. X.-G. Chen, F.-J. Klinkenberg and S. Engler: "Optimization of the Impeller Degassing Process Through Continuous Hydrogen Measurement," *Light Metals* **1995**, pp. 1215-1222.
10. P. D. Waite, "Improved Metallurgical Understanding of the Alcan Compact Degasser After Two Years of Industrial Implementation in Aluminum Casting Plants," *Light Metals* **1998**, pp. 791-796.
11. G. André, C. W. Robinson and M. Moo-Young, *Chem. Eng. Sci.*, Vol. 38, **1983**, pp. 1845-1854.
12. C. Koen, *The Chemical Engineer*, February, **1975**, pp. 91-95.
13. S. Asai, I. Muchi and M. Kawachi, "Fluid Flow and Mass Transfer in Gas Stirred Ladlers," in *Foundry Processes: Their Chemistry and Physics*, Plenum Press, New York, **1988**, pp. 261-289.
14. Shinji Nagata, "Mixing: Principals and Applications," Kodansh Ltd., Tokyo, **1975**, pp. 24-56 and pp. 124-164.
15. R. L. Bates, P. L. Fondy and J. G. Fenie, "Impeller Characteristics and Power," in *Mixing*, V.W. Uhl and J.B. Gray, editors, Academic Press, New York, **1966**, pp. 111-178.
16. R. Clift, J. R. Grace and M. E. Weber, "Bubbles, Drops, and Particles," Academic Press, New York, **1978**, pp. 45-206.
17. Y. Sahai and R. I. L. Guthrie, *Met. Trans. B*, Vol. 13B, **1982**, pp. 193-202.
18. G. K. Sigworth and T. A. Engh, *Metallurgical Transactions B*, 13B, **1982**, pp. 447-460.

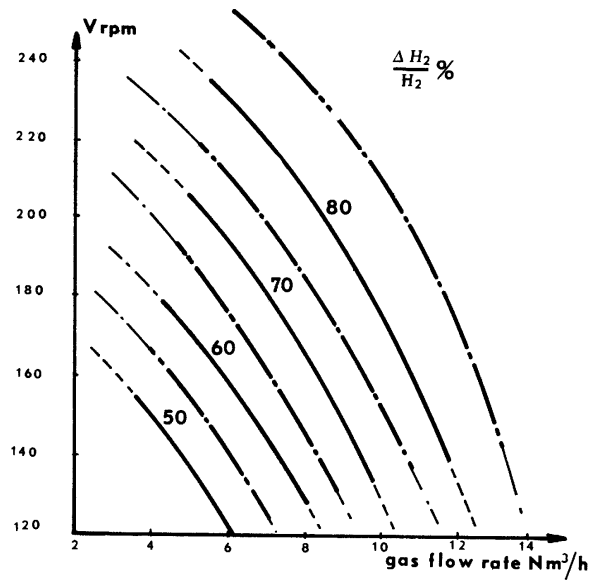


Figure 1. Hydrogen Removal Efficiency in the Alpur Process [1]

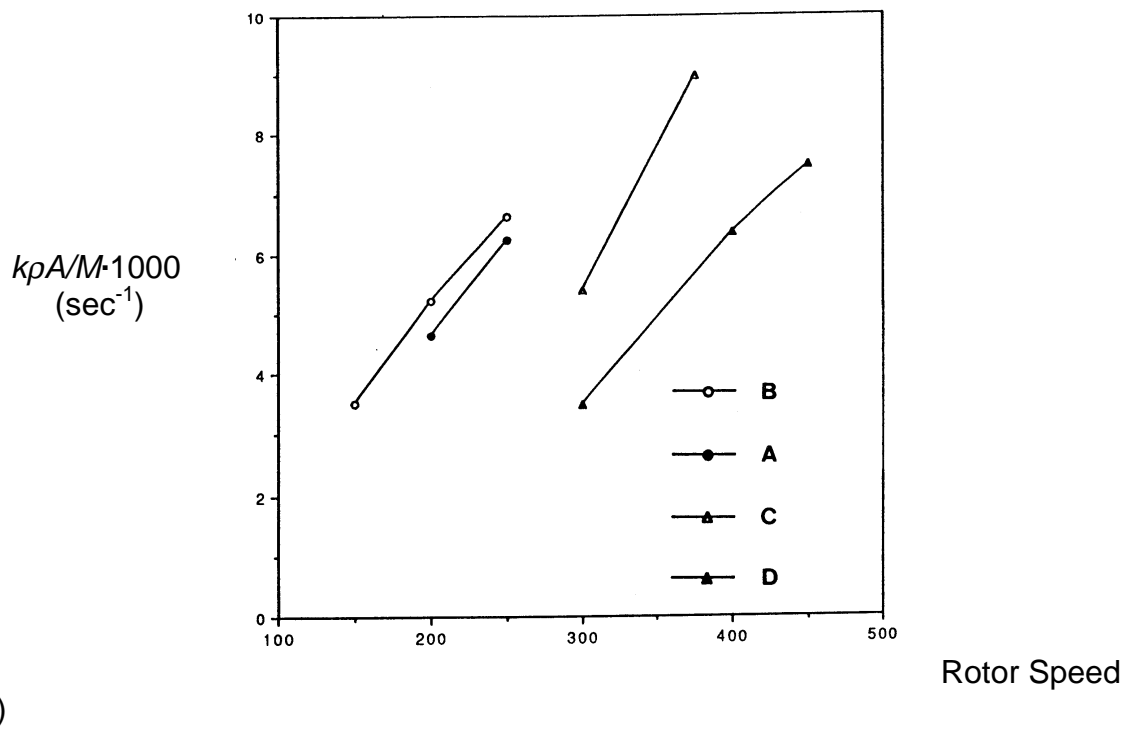


Figure 2. Effect of Rotor Speed on Gas Slope Parameter [4].
(The four rotors studied were: A - Alpur, B - Alcoa 622, C - Foseco RDU, and D - SNIF.)

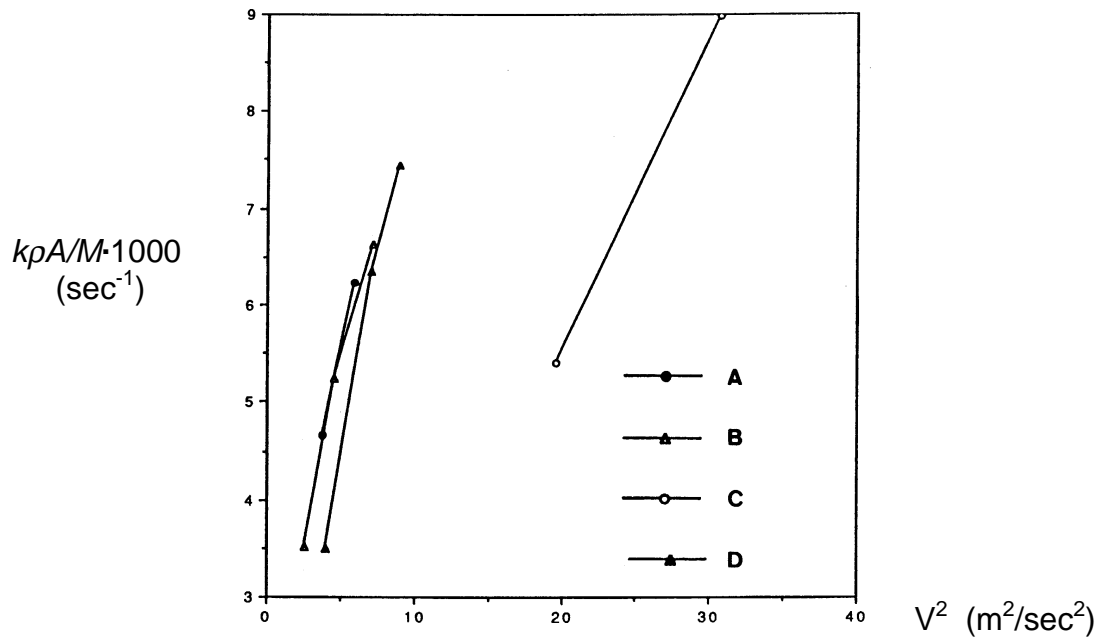


Figure 3. The Gas Slope Parameter Versus the Square of the Velocity at the Periphery of the Rotor Head [4].

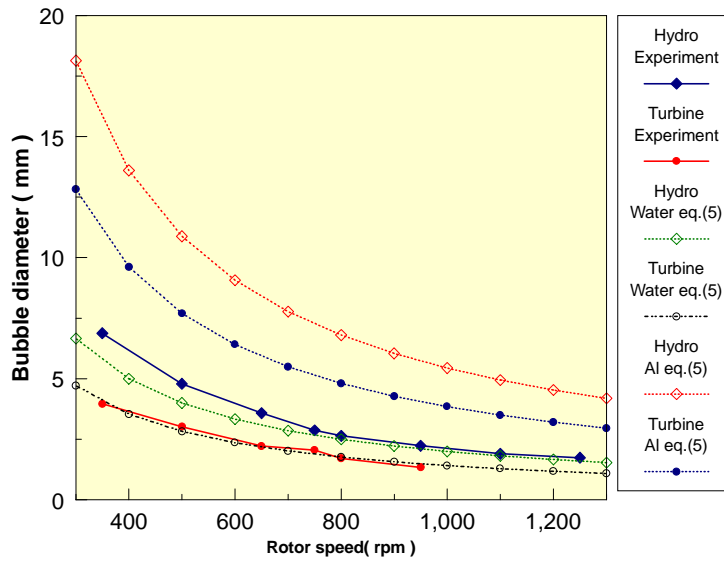


Figure 4. Bubble Sizes Determined from Experimental Results of Water Model Experiments, and From Equation 5 of Reference [5]. (Equation 3 of this paper)

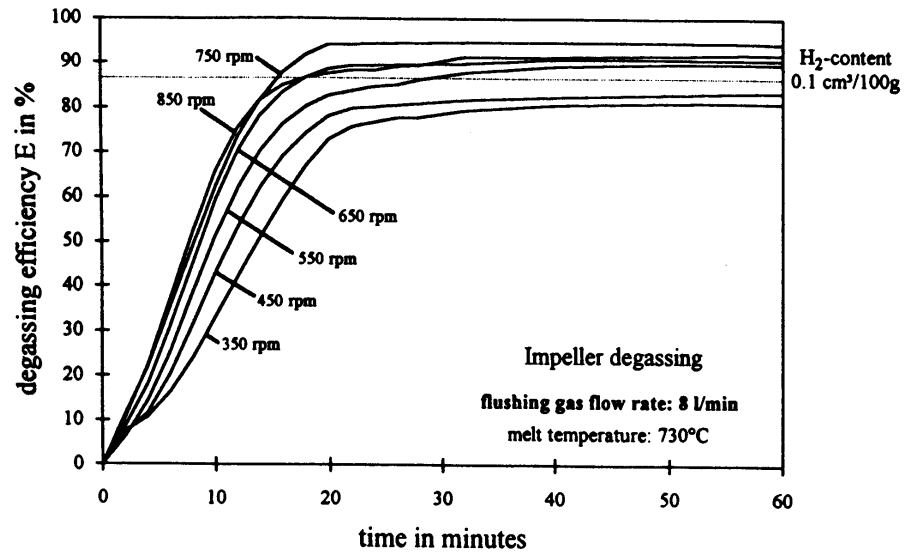


Figure 5. Hydrogen Removal with Time in a 150 kg. Melt [9]
(versus rotation speed with Foseco FDU impeller)

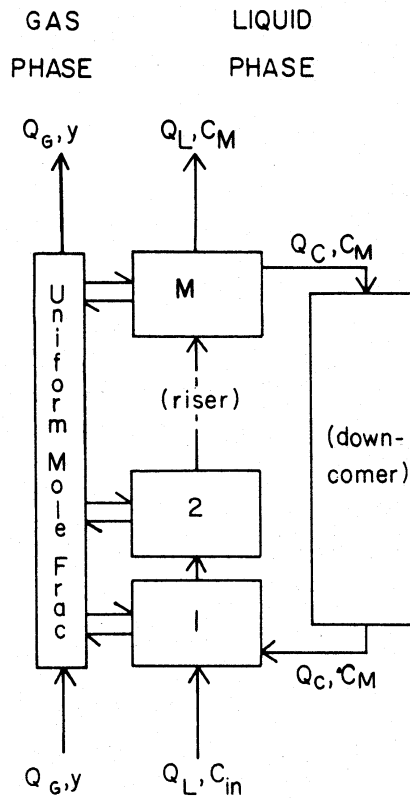


Figure 6. Block Diagram for the Steady State Mixing Model
for a Continuous Flow Reactor [11]

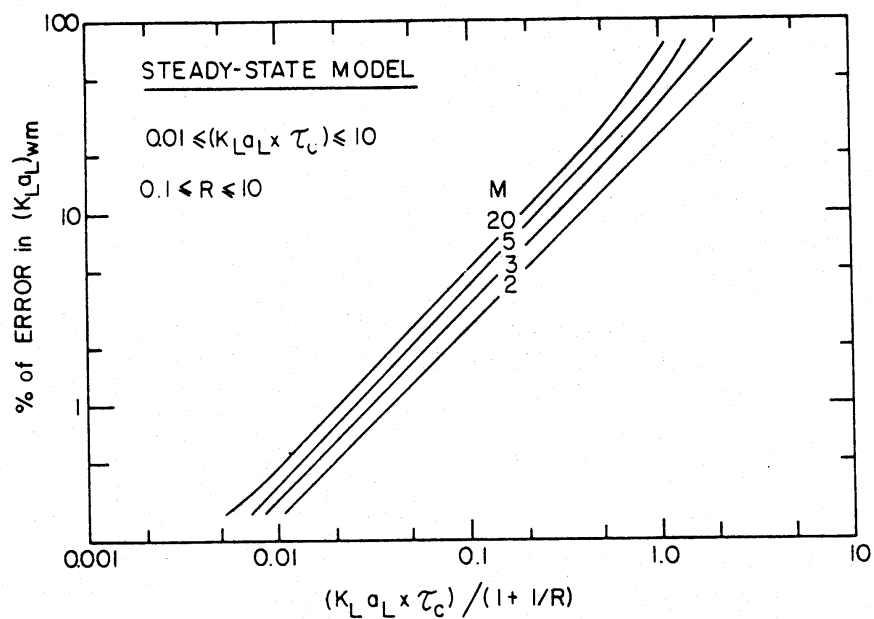


Figure 7. Calculated Percent Error Associated With Assuming a Perfectly Mixed Reactor [11]

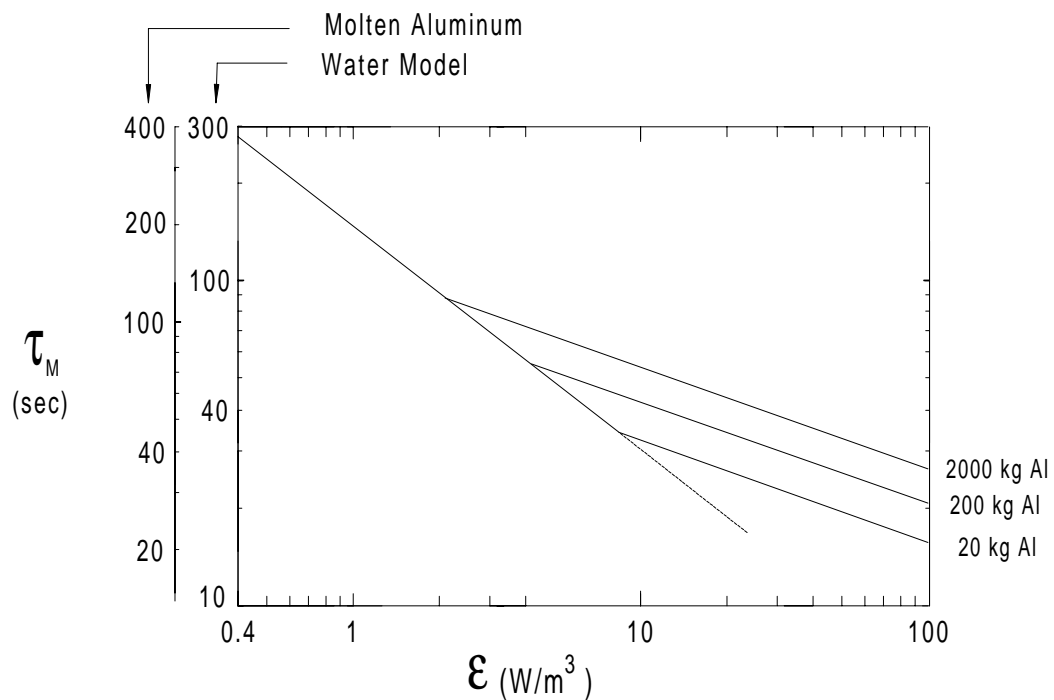


Figure 8. Relation Between Mixing Time and Power Density (Calculated after [13])

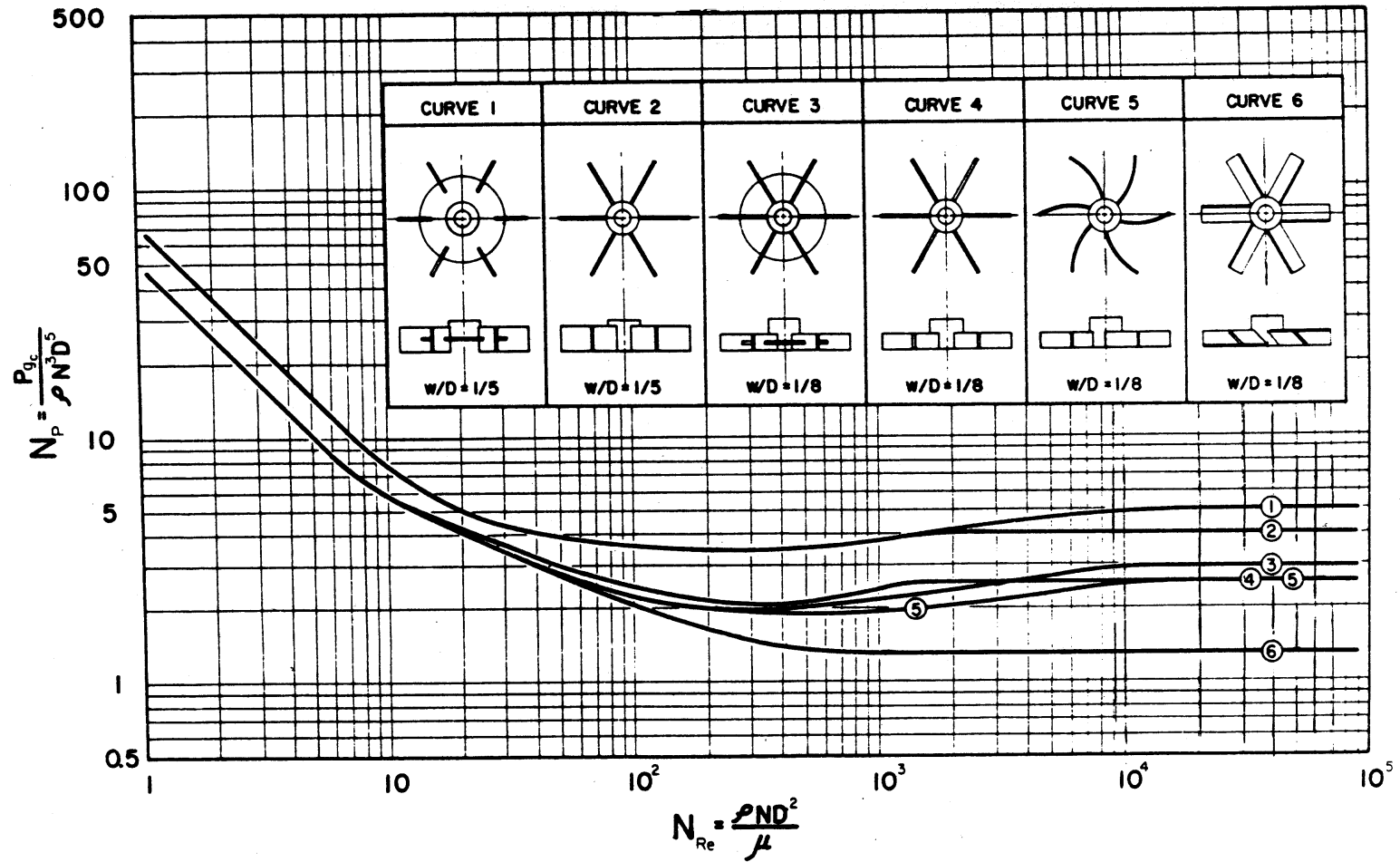


Figure 9. Measured Power Numbers for Six Turbine Impellers [15]

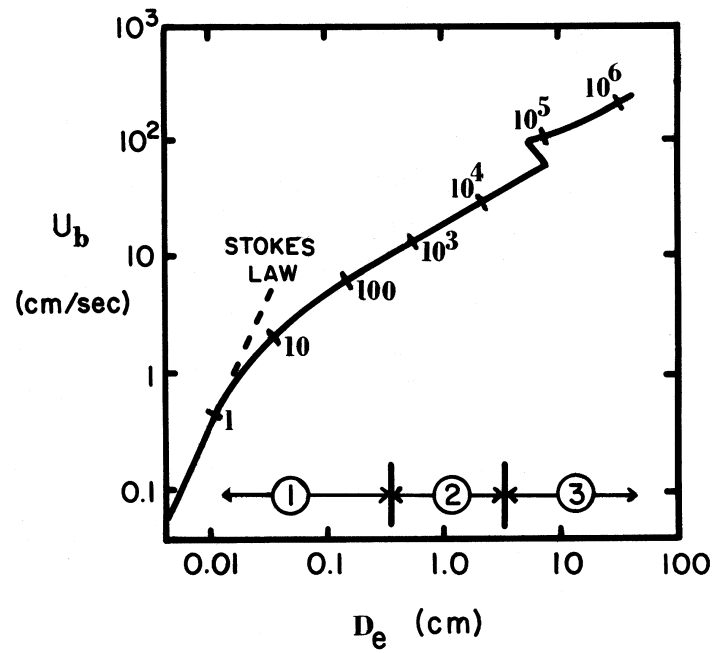


Figure 10. Terminal Rise Velocity for Gas Bubbles of Varying Size in Liquid Aluminum at 1000°K (1370°F).

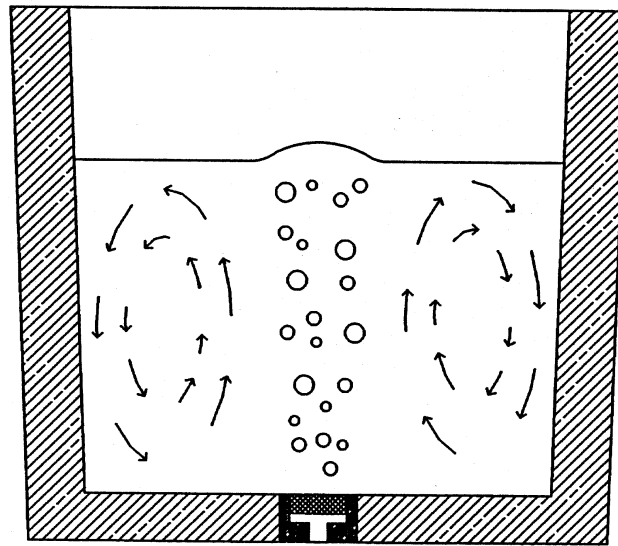


Figure 11. Flow Patterns Observed When Gas is Admitted Through a Porous Plug at the Center of a Crucible or Ladle.

Report of Plant Experiments Conducted at Littlestown Hardware and Foundry

(A New Process for Grain Refinement of Aluminum)

September 11, 1998

Abstract

Three experimental heats were made in a crucible melting furnace at Littlestown Hardware and Foundry. The results obtained show that RID treatments in this furnace remove a significant amount of grain refining particles. The removal rate observed in one heat was 15 ppm B per hour. Depending on the boron addition rate, this removal may prevent any desired grain refinement. There did not appear to be a significant chemical reaction between the melt and gas mixtures containing BF_3 . Only a small portion of the reactive BF_3 gas, less than about 15% of the total, was able to react to form boride. It is possible that a thin layer of solid aluminum fluoride coats the surface of the gas bubbles, preventing further chemical reaction.

A flux treatment with a 5% BCl_3 gas mixture appeared to produce little observable reaction, although a treatment using 3% BCl_3 produced a significant grain refinement, and a boron recovery of 115%.

We need to study the kinetics of the reaction of the two boron-containing gases in more detail. In particular, it is desirable to conduct experiments in pure Al melts, which contain no dissolved Ti, and in Al-Mg alloys.

We also need to think again about the basis for this process. Our original thought was that we would feed a small amount of reactive gas into an existing rotary degasser. The results at Littlestown suggest a completely different method of introduction may give much better results. Further development should focus on the construction and development of a laboratory analog for industrial furnaces (CILGAR unit). In this way, more meaningful experiments can be made in the laboratory.

Three experimental heats were made at Littlestown Hardware and Foundry (LHF) during April, 1998. The procedures employed, and the results obtained, are described below for each trial.

Heat 1 – Preliminary Heat April 20, 1998

Approximately 450 lb. of 99.7% metal supplied by LHF was melted in a gas-fired crucible furnace, and brought to a temperature of 760 C. A spectrographic sample was taken, from which we obtained the following analysis:

<u>Si</u>	<u>Cu</u>	<u>Fe</u>	<u>Mg</u>	<u>Ti</u>	<u>B</u>	<u>Mn</u>
0.056	0.020	0.123	0.0022	0.0003	0.0059	0.007

Ten lb. of lump Si and three five-ounce buttons of 10% Ti alloy were added. This analysis came back:

<u>Si</u>	<u>Cu</u>	<u>Fe</u>	<u>Mg</u>	<u>Ti</u>	<u>B</u>	<u>Mn</u>
2.575	0.020	0.135	0.0022	0.0114	0.0040	0.007

We then fluxed for 30 minutes with the RID unit, and found 107 ppm Ti and 33 ppm B. In other words, the 30 minute flux treatment removed 7 ppm B.

It was clear from these results that the material supplied by LHF was an EC (electrical conductivity) alloy. EC metal receives a sizable boron addition to remove dissolved Ti and V. Since we intended to add only a few ppm B to grain refine the metal, this high level of dissolved B was not appropriate for our tests. We therefore ordered a skid (1000 lb) of 99.9% metal from Belmont Metals for trials the following week.

During these tests we also discovered that the flowmeter we had for the argon was not large enough to deliver the amount of inert gas flow required. We therefore ordered another flowmeter tube for our gas mixing panel.

Although this test would seem to be a "failure", an important observation can be made. This observation is important for understanding the results obtained (or to be more accurate, the results not obtained) in heats two and three below.

This heat showed that a RID treatment in this furnace removed something like 15 ppm B per hour. This result is in line with the inclusion removals published by other researchers. Consider, for example, the paper by Pedersen [1], who reported that from 49 to 63% of TiB_2 particles are removed by the Hydro HA rotary degassing treatment.

Thus, while we are adding boron by the degassing treatment, we are also removing some, or all, of the desirable grain refining particles by the very same fluxing treatment.

Heat 2 – Trial with BF_3 April 29, 1998

We first installed the new flowmeter tube (# 604) in the mixing panel. This tube contains two floats: a glass ball and a stainless steel ball. The calibration supplied by Matheson for air at 70 F and 1 atmosphere pressure is shown below. For the size of crucible and the RID

employed in these experiments, c. 20 SCFH¹ represents the maximum gas flow that can usually be obtained, without "flooding" the melt with large bubbles.

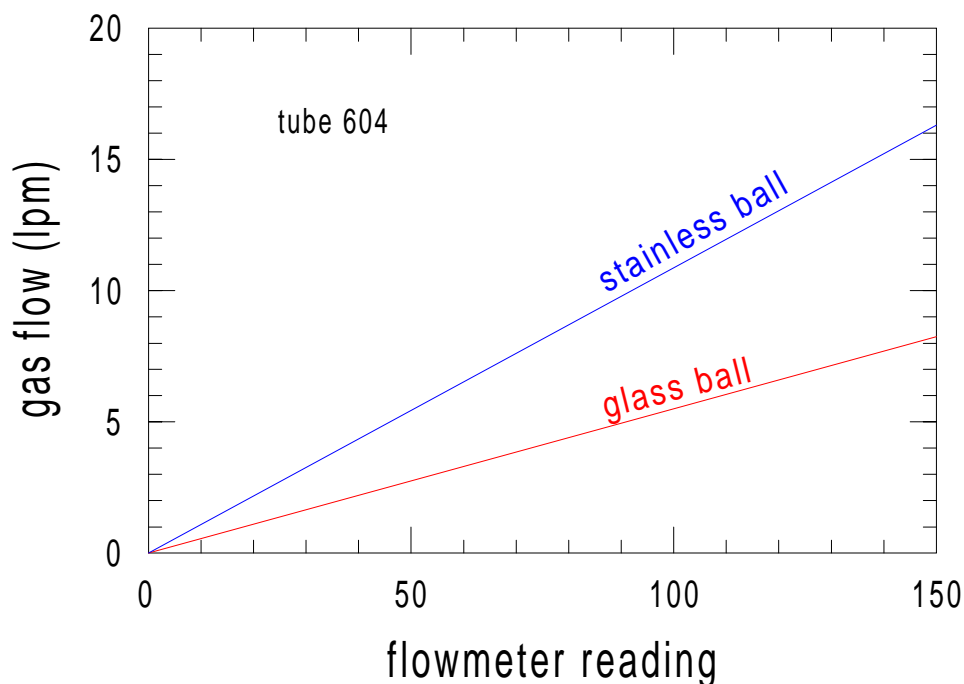


Figure 1. Calibration Curves for Matheson Flowmeter No. 604

The flowmeter tube used to admit boron into the melt (# 601) was calibrated by running argon through the tube, and collecting the gas by bubbling into a beaker filled with water. At a flow indication of 130 on the tube, we collected 200 ml of gas in 2 minutes 45 seconds. This is an observed flow rate of 73 sccm, compared to the expected 70 sccm. This agreement is well within experimental measurement error.

We charged 13 pigs, approximately 400 lb., of 99.9% metal to one of Littlestown's crucible furnaces. When molten the following analysis was found:

<u>Si</u>	<u>Cu</u>	<u>Fe</u>	<u>Mg</u>	<u>Ti</u>	<u>B</u>	<u>Mn</u>
0.059	0.003	0.061	0.0035	0.0036	0.00015	0.005

We then added 10 lb Si and three five ounce buttons of 10% Ti. (These buttons are normally used at LHF to add Ti.) The heat was brought to a temperature of 750 C. A spectrographic sample was taken, from which we obtained the analysis:

<u>Si</u>	<u>Cu</u>	<u>Fe</u>	<u>Mg</u>	<u>Ti</u>	<u>B</u>	<u>Mn</u>
2.61 ²	0.014	0.106	0.0017	0.0172 ³	0.0009	0.006

¹ This is 9.4 lpm, since one lpm = 2.119 SCFH.

The boron was unexpectedly high. After some discussion we were told that the 10%Ti buttons were actually 10Ti-1B alloy! (The total boron added in the buttons should have been 23 ppm, 1/10 the Ti addition, but only 8 or 9 showed up in the analysis. Is B present as TiB_2 less likely to show up on a spectrographic reading, or did some float out?)

We placed a new carbon shaft on the RID and fluxed with 8 lpm of argon for an hour. An analysis taken at this point showed 155 [194] ppm Ti and 3 ppm B. This analysis was much better, but the grain size in AA and hockey puck samples was still very small. We added two more pigs of 99.9 metal to the heat and fluxed for another 45 minutes at c. 9 lpm Ar. Hockey puck grain size samples taken at this time were visibly coarser, and an analysis showed 2.43% Si, 131 [164] ppm Ti, and 2 ppm B.

We fluxed for another 30 minutes and obtained an analysis showing 130 [163] ppm Ti, and 2 ppm B. The grains in the modified⁴ hockey puck sample (1-9) were noticeably larger, so we began fluxing with BF_3 . An AA sample (1-10) and an Alcoa sample (1-11) were also taken at this time. One ppm B in a 400 lb. melt is 380 cc of gas. We began fluxing with a mixture that added 0.13 ppm in three minutes:

BF_3 flow = 50 sccm

argon flow = 6 lpm

In other words, this gas mixture was 0.83% BF_3 . This mixture was added for three minutes and a hockey puck sample and spectrographic coupon were taken. No observable grain refinement was seen. The chemical analysis was 135 [169] ppm Ti and 2 ppm B. We fluxed an additional six minutes (9 total) and found an analysis of 133 [166] ppm Ti and 3 ppm B. No hockey puck was taken. After an additional ten minutes of fluxing, (19 total minutes or 2.5 ppm B added) a slight grain refinement seemed to be evident from the hockey puck samples. The coupon taken was 127 [159] ppm Ti and 2 ppm B.

We then increased the flow of BF_3 to the maximum on this tube; from 140 to 150, but shut down the fluxing after eight minutes because the metal temperature was just under 640 C. We therefore removed the RID unit and heated up the melt. We also changed out the flowmeter tube to allow us to use more BF_3 .

² Two calibration programs were used to analyze these samples: "99" and "test". The 99 program is designed for high purity metals, and showed 1.25% Si. The test program showed 2.61 on the Si2 line. This is the figure reported above.

³ This is the Ti reported on the LHF "99" program. When comparing this value (in earlier test samples) with results obtained at Alcoa Technical Center, the LHF analysis is consistently about 80% of the value reported by ATC. Thus, the actual Ti content here is 215 ppm. In the data which follows, both numbers are reported. The expected values according to the ATC analysis are given in brackets. For this sample, the Ti content is 172 [215] ppm.

⁴ This sample was made by dipping a steel ladle into the melt, allowing it to heat and fill with metal, and then removing the sample and placing it onto a steel plate. The steel ladle produced a sample 2.5" in diameter and 1" high, nearly the same as the KBA hockey puck. The cooling rate in this sample was also similar to the original KBA test. The results are believed to be more reproducible, however, since hot metal is not poured into a cold ring mold. This test has the advantage that a grain size can be obtained in a few minutes after pouring. (It is not necessary to cut and polish the hockey puck.)

We resumed fluxing with BF_3 at 140 on tube 602, and the glass ball at 20% on tube 604. This is a gas flow of:

BF_3 flow = 205 sccm (0.54 ppm B/min)

argon flow = 1.06 lpm

This mixture was 16% BF_3 , which appeared to be too "rich". A significant amount of fuming was observed. The argon flow was increased slowly until the fuming stopped, at a flow of 4 lpm, and held constant at this level for the rest of the test. The resulting gas mixture was 5 % BF_3 , and a flux treatment of 15 minutes (8 ppm B added) was employed. The last chemical analysis was 134 [168] ppm Ti and 3.3 ppm B. The final grain size samples were not significantly different from the starting blanks.

At this point we were three hours past the normal quitting time for this shift, and we decided to call it a day.

Observations on Heat 2

First of all, there did not appear to be a significant chemical reaction between the melt and the BF_3 . A total of 10.6 ppm B was added via the two gas mixtures, but only about 1 or 1.5 ppm B (less than 15% of the total) was found in the melt at the end of the experiment. In addition, the Ti content was essentially unchanged by our treatment. We began with 130-131 [163-164] ppm Ti and ended up with 134 [168] ppm Ti in our last sample. If the 32 ppm B added had reacted with Ti dissolved in the melt, and if the resulting TiB_2 particles were removed by the gas fluxing, then our Ti content should have dropped by 32 ppm x 2.22 or 71 ppm. Since this was not the case, it appears that only a small portion of the reactive BF_3 gas, less than about 15%, was able to react to form boride.

There are several possible explanations for this finding. First of all, BF_3 would react with aluminum to form AlF_3 , a solid at these temperatures. It is possible that a thin layer of solid aluminum fluoride coats the surface of the gas bubbles, thereby preventing further chemical reaction. Secondly, the bubble distribution was far from optimum. The carbon shaft on the RID unit was machined poorly, exhibiting a run out of about 1/2 to 3/4", which preventing us from going to faster rotation speeds with the RID unit. The head design also was poor, in my opinion. The end result was that a significant amount of the gas floated up near the carbon shaft in bubbles that were between 1/2 and 1" in diameter. If the RID had been operating optimally, all of the gas would have been in bubbles less than about 1/8" diameter.

No significant grain refinement was observed, although this observation is clouded by the fact that our starting blank sample was partially refined, because of the accidental boron addition via the 10% Ti buttons.

Heat No 3 – Trials with BCl_3 April 30, 1998

Approximately 450 lb. of 99.7% metal supplied by LHF was melted in a gas-fired crucible furnace. 11 lb. of lump Si and 45 g. of Ti (via a broken ty-Gem tablet) were added. The heat was fluxed for c. 35 minutes with the RID unit, and samples were taken. The chemical analysis was:

<u>Si</u>	<u>Cu</u>	<u>Fe</u>	<u>Mg</u>	<u>Ti</u>	<u>[Ti]</u>	<u>B</u>
-----------	-----------	-----------	-----------	-----------	-------------	----------

2.55 0.034 0.095 0.0036 0.0196 0.0245 0.0002

A fairly coarse grain size was observed, and a ten minute gas fluxing treatment was begun with

BCl_3 flow = 140 sccm (0.37 ppm B/min)

argon flow = 2.5 lpm

This mixture was 5% BCl_3 , which generated a fair amount of fume towards the end of the treatment. Samples taken at the end of the 10 minute (4 ppm B added) treatment exhibited only a slight grain refinement. Chemical samples showed 194 [243] ppm Ti and 2 ppm B.

The results with this "rich" gas mixture appeared to be similar to those found the day before with BF_3 : no significant reaction was observed. As a consequence, we changed the gas composition to 3% BCl_3 . The gas flows used were

BCl_3 flow = 78 sccm

argon flow = 2.5 lpm

for a total of ten minutes (and 2 ppm B). After this treatment a significant grain refinement was observed, and observed chemical analysis was 186 [233] ppm Ti and 4.3 ppm B.

About five minutes into the second ten minute treatment a small amount of liquid BCl_3 was observed to collect in the bottom of the flowmeter tube. Shortly afterwards, the stainless steel ball became wet, and it was not possible to get a meaningful reading of gas flow after this time. The liquid did not appear to be passing through the tube, however, and we decided to continue with the fluxing for an additional five minutes. We felt that as long as the setting of the flow control valve was unchanged, the BCl_3 flow would be constant.

Observations on Heat 3

A flux treatment with the richer gas composition appeared to produce little observable reaction, similar to the case with BF_3 in the second heat. This observation is somewhat puzzling, because BCl_3 will react to form either MgCl (a liquid) or AlCl_3 , a vapor. There should be no impediment to reaction at the surface of the bubble with BCl_3 .

With a treatment using 3% BCl_3 there was a better reaction. Significant grain refinement was found. Also, the total boron recovered in the second treatment was (4.3-2 ppm in melt)/2 ppm added or 115%. Also, there was an observed drop in Ti content of 8 [10] ppm Ti. This small difference could be caused by sampling or analytical errors, but it could also be caused by reaction with BCl_3 to form borides, which then floated out of the melt. In this case, an additional 10/2.22 or 4.5 ppm of B is involved in the chemical reaction. This additional boron is a significant portion of the total added in the second trial: 225% of the total. This suggests that our boron addition was larger than expected, because of condensation of vapor in our gas transfer system, and admittance of the liquid BCl_3 into the furnace during this trial.

Concluding remarks

We need to study the kinetics of the reaction of the two boron-containing gases in more detail. In particular, it is desirable to conduct experiments in melts which contain no

dissolved Ti. In this case, the results are not complicated by the flotation and removal of TiB_2 particles, and the efficiency of the reaction can be determined by a simple chemical analysis. We also need to further determine the role of gas composition (% BF_3 and % BCL_3). These experiments should be made in pure Al and in Al-Mg alloys.

It also appears that we need to think again about the basis for this process. My original thought was that we would feed a small amount of reactive gas (BF_3 or BCL_3 , or a mixture of the two gases, or even an intermediate compound, such as BCl_2F) into an existing rotary degasser. These results suggest that a completely different method of introduction may give much better results.

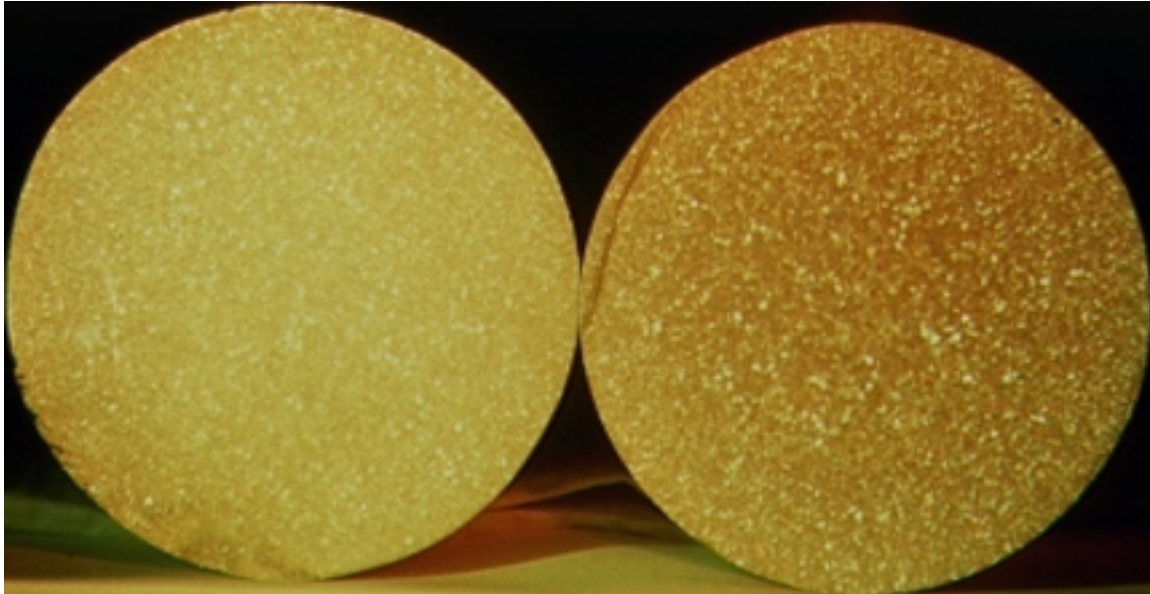
Further development should focus on the construction and development of a laboratory analog for the industrial furnaces used at Littlestown. (This is called a CILGAR unit in our DOE proposal.) In this way, more meaningful experiments can be made in the laboratory.

References

1. T. Pedersen: "Refining Efficiency on Hydrogen, Alkaline Metals and Inclusions in the Hydro Metal Refining System," Light Metals 1991, pp. 1063-1067.

Appendix of Experimental Observations

Heat 1



Sample 1-10
AID = 475 μm
before BF_3 treatment

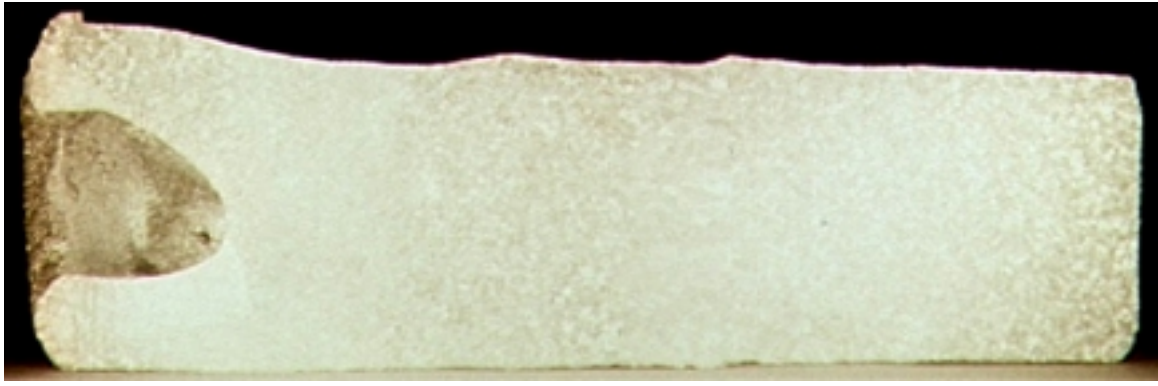
Sample 1-21
AID = 400 μm
after BF_3 treatment

Figure 1. Internal Structure of Aluminum Association Test Samples



Sample 1-11 (before treatment)

Figure 2a. Internal Structure of Alcoa Grain Size Sample



Sample 1-20 (after treatment)

Figure 2a. Internal Structure of Alcoa Grain Size Sample

Fy-Gem Scale Up Trials in 6061 Alloy at Alcoa Technical Center

C.R. Durst
May 18, 2000

Jamegy Development Corporation, Inc.
South Chester Street
New Cumberland, WV 26047

Introduction

On March 24, 2000, a series of experiments were conducted at Alcoa Technical Center in a 60-pound pilot reactor to study the effectiveness of the fy-Gem process in 6061 Alloy. Fy-Gem v3.0, shown in Figure 1 below, utilized a system in which Argon pressurized a bottle of liquid boron trichloride, BCl_3 , pushing the liquid out of the bottle and into a rotometer. The liquid boron trichloride and argon were metered, and then mixed before being sent to the vaporizer unit. Upon vaporization, the gas exited the fy-Gem unit and was distributed to the molten aluminum through the agitation unit.

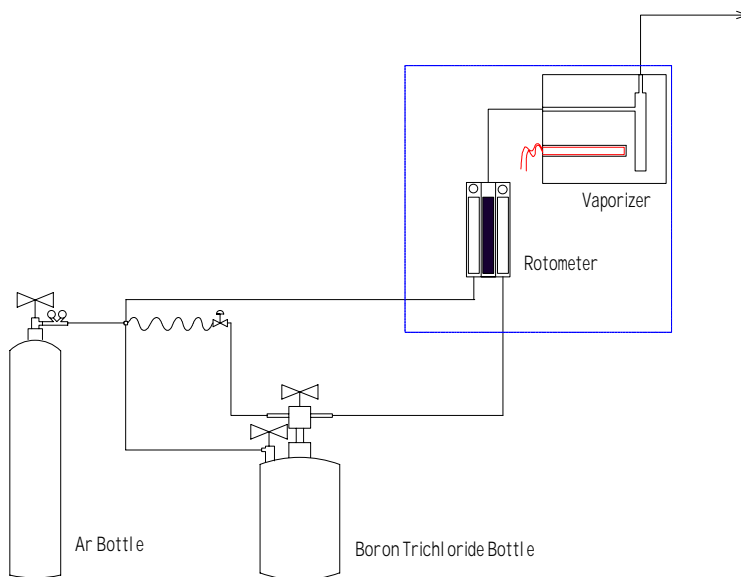


Figure 1. P&ID for fy-Gem v3.0

The agitation unit consisted of a mock 622 rotor with a scaled up version of the agitator head currently used in JDC lab work (Figure 2).

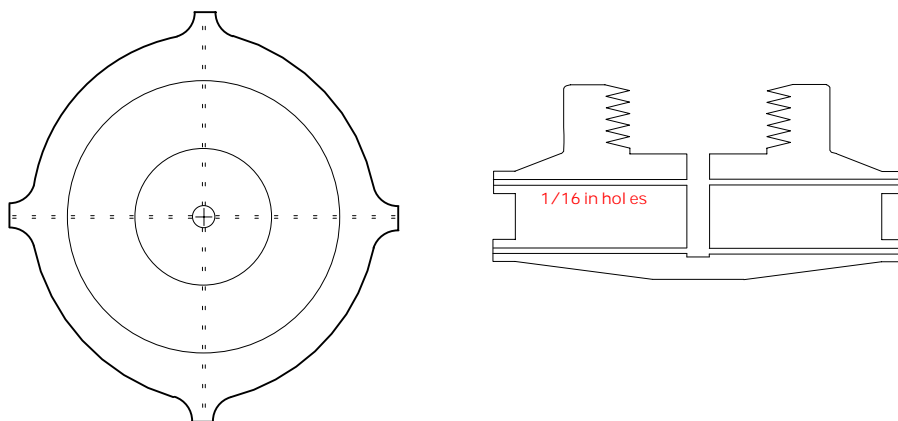


Figure 2. The Agitator Head Used in ATC Trials
Outside Diameter (including nipples) = 4.5"

Procedures

Prior to the start of each experiment, 60 lbs of aluminum were cut, weighed, melted, and alloyed in an induction furnace. At the same time, the fy-Gem unit was turned on to warm up and ensure that the lines were purged from the previous experiment. When the appropriate temperature was reached, the metal was fluxed using argon flowing through a lance. Immediately after fluxing, the agitator unit was placed over the melt and allowed to preheat slightly while a “blank” Cold Finger and chemical analysis sample were taken. Due to the presence of a vacuum hood over the top of the melt, it was possible to turn on the fy-Gem unit and allow it to reach a steady flow prior to the start of each experiment. After steady flow was ensured, the agitator was plunged into the molten aluminum and the boron trichloride was introduced into the metal. Once the desired amount of boron trichloride was introduced, the agitator unit was removed from the melt and the boron trichloride flow was turned off. The metal was then skimmed and a series of samples were taken. The samples consisted of cold finger and chemical analysis samples taken at 1, 5, 10, 20, and 30 minutes upon removal of the agitator and a LAIS sample taken after 30 minutes.

Results and Discussion

The main variable throughout the course of this work was titanium concentration. Table 1 illustrates the parameters as defined prior to each run.

Table 1. Experimental Parameters

Series Number	BCl ₃ Flow (cc/min)	Ti Addition (ppm)	Rotor (RPM)	Addition Time (min)
780211	67.4	250	550-600	4
780211-T	-	150	-	-
780210	67.4	400	550-600	4

In the first experiment, 780211, 250 ppm of titanium were initially added to the melt. It was determined that 250 ppm would be the uppermost limit on titanium levels consistent with current commercial practices. The fy-Gem system was then used to administer boron in the form of boron trichloride to the melt via a scaled-down 622 rotor and the agitator head found in Figure 2. Upon removal of the agitator, the samples were taken and analyzed. The chemical analysis showed that the titanium was very close to the target, while the boron fluctuated between 3 and 4 ppm (Table 2).

Table 2. Percent Compositions of Series 780211 Samples

Sample time after addition (min)	Percent Compositions						
	Ti	B	Si	Fe	Cu	Mg	Cr
Blank	0.025	0.0000	0.57	0.34	0.29	0.95	0.19
1	0.024	0.0004	0.59	0.35	0.28	0.96	0.20
5	0.023	0.0003	0.59	0.35	0.29	0.97	0.19
10	0.024	0.0003	0.58	0.35	0.29	0.96	0.19
20	0.024	0.0004	0.57	0.35	0.29	0.94	0.19
30	0.024	0.0003	0.56	0.34	0.28	0.94	0.19

In Series 780211, the fy-Gem process did not produce sufficient grain refinement, as shown in Figure 3 and Table 3. The grain sizes were read from three points on each sample: 0.75 inches, 2.25 inches, and 3.5 inches from the bottom of the sample. In this series, grain refinement was relatively poor over the first 5 minutes, but did improve with time.

Table 3. Grain Sizes of Series 780211 Samples

Sample Time after Addition (min)	Grain Size (μm)		
	0.75" from Bottom	2.25" from Bottom	3.5" from Bottom
Blank	TCG	TCG	TCG
1	440	TCG	TCG
5	400	930	1130
10	370	600	700
20	390	580	720
30	370	580	890



Figure 3. Cold Finger Samples from Series 780211

At the end of this experiment, an additional mini-compact of titanium was added to the melt to bring the total concentration of titanium up to approximately 350 ppm. The goal of this run, 780211-T, was to determine if the borides could be manipulated after they had reacted with the initial titanium present in the melt. While Table 4 does show that the melt reached 350 ppm titanium, it took 30 minutes to do so. This may be representative of the dissolution time and therefore this experiment may not have been run consistently with its defined goals. The boron level, however, remained relatively consistent with the first part of this experiment, 780211, excluding the sample at 20-minutes.

Table 4. Percent Compositions of Series 780211-T Samples

Sample time after addition (min)	Percent Compositions						
	Ti	B	Si	Fe	Cu	Mg	Cr
5	0.025	0.0004	0.59	0.35	0.29	0.96	0.19
10	0.026	0.0003	0.55	0.33	0.27	0.89	0.19
20	0.033	0.0021	0.58	0.34	0.28	0.95	0.17
30	0.035	0.0003	0.59	0.36	0.29	0.97	0.19

In Series 780211-T, the additional 100 ppm of titanium resulted in some improvement of grain size, especially near the top of the sample as shown in Figure 4 and Table 5. The grain sizes again were read from three points on each sample: 0.75 inches, 2.25 inches, and 3.5 inches from the bottom of the sample.

Table 5. Grain Sizes in μm of Series 780211-T Samples

Sample Time after Addition (min)	Grain Size (μm)		
	0.75" from Bottom	2.25" from Bottom	3.5" from Bottom
5	430	540	640
10	340	540	470
20	380	560	540
30	410	590	560

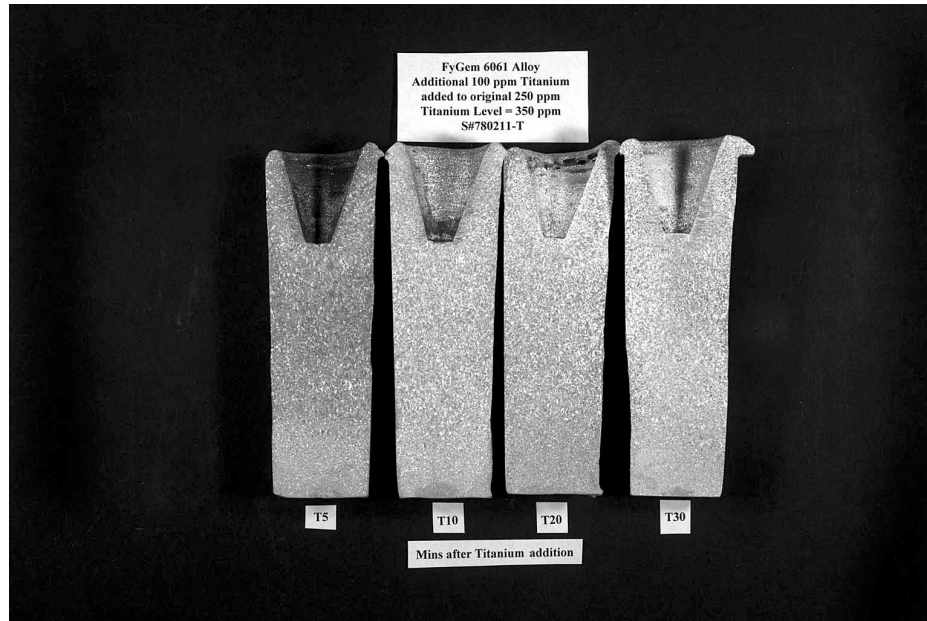


Figure 4. Cold Finger Samples from Series 780211-T

In the final series, 780210, the level of titanium in the melt was targeted at 400 ppm. While within specifications, this may not be cost-effective, but for this set of experiments, it was determined that it was more important to determine if fy-Gem could grain refine wrought alloys than it was to stay within the constraints of current commercial practices. The chemical analysis (Table 6) shows that approximately 450 ppm titanium were initially present in the sample, but the titanium level dropped down to 360 ppm by the end of the experiment. Additionally, analysis shows that 5 ppm boron were added, which is within current commercial constraints.

Table 6. Percent Compositions of Series 780210 Samples

Sample time after addition (min)	Percent Compositions						
	Ti	B	Si	Fe	Cu	Mg	Cr
Blank	0.039	0.0000	0.60	0.37	0.28	0.95	0.19
1	0.045	0.0005	0.57	0.34	0.29	0.93	0.19
5	0.037	0.0005	0.61	0.36	0.30	0.97	0.20
10	0.037	0.0005	0.59	0.36	0.29	0.96	0.19
20	0.037	0.0005	0.58	0.35	0.29	0.95	0.19
30	0.036	0.0004	0.55	0.33	0.28	0.90	0.19

At this composition and using the parameters listed in Table 1, the fy-Gem process did produce significant grain refinement as shown in Figure 5 and Table 7. The grain sizes were read from three points on each sample: 0.75 inches, 2.25 inches, and 3.5 inches from the bottom of the sample. In this series, the grain refinement was immediate and relatively consistent with a slight improvement over time.

Table 7. Grain Sizes in μm of Series 780210 Samples

Sample Time after Addition (min)	Grain Size (μm)		
	0.75" from Bottom	2.25" from Bottom	3.5" from Bottom
Blank	TCG	TCG	TCG
1	310	380	460
5	360	370	410
10	380	300	380
20	310	350	320
30	310	350	370

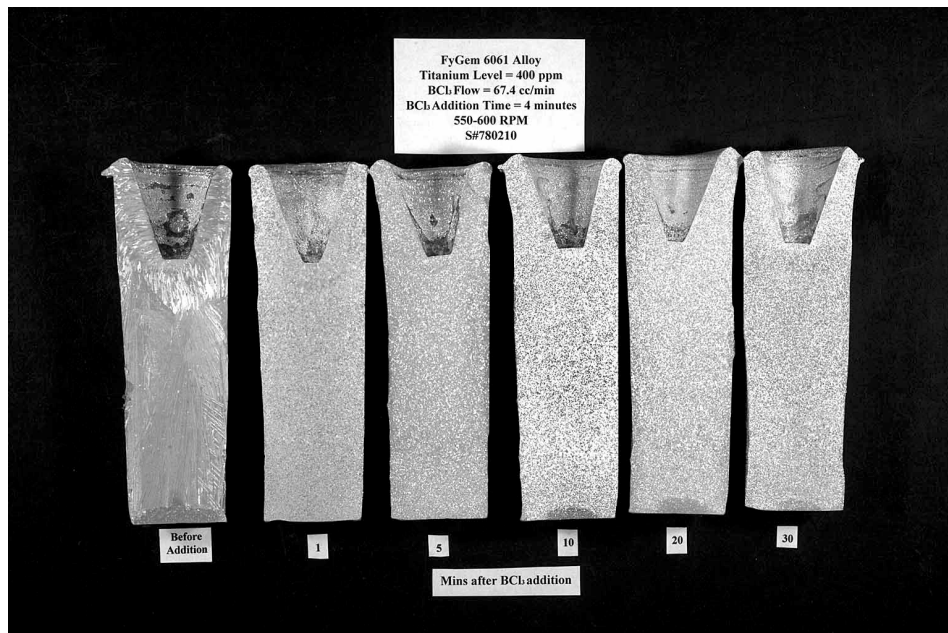


Figure 5. Cold Finger Samples from Series 780210

At the end of each experiment, a LAIS sample was taken for analysis with an SEM at Touchstone Laboratory. Results from Touchstone are given in Table 8.

Table 8. Boride Sizes

Series	Avg Dia (μm)	Std Dev	Min Dia (μm)	Max Dia (μm)	% in Area Range	
					0-0.5	0.5-1
780211	0.689	0.0726	0.600	0.846	83	17
780211-T	0.565	0.0547	0.481	0.681	100	-
780210	0.628	0.0298	0.596	0.681	100	-

Discussion

Results from these tests seem to be mixed. Series 780210 showed that the fy-Gem can produce significant grain refinement. However, this test was run in a melt containing approximately twice the amount of titanium that could be expected commercially. Additionally, even with the elevated titanium levels, the grain size was not as fine as what is currently being produced using TiBor. Series 780211 showed that at this time, the fy-Gem process may not be ready for commercial tests on wrought alloys.

Figure 6 shows the grain size of Series 780210 over the thirty-minute period of the experiment. In this figure, TCG is represented as 2000 μm . Overall, the figure seems to show that there may be a slight improvement in grain size with time, particularly on the top readings.

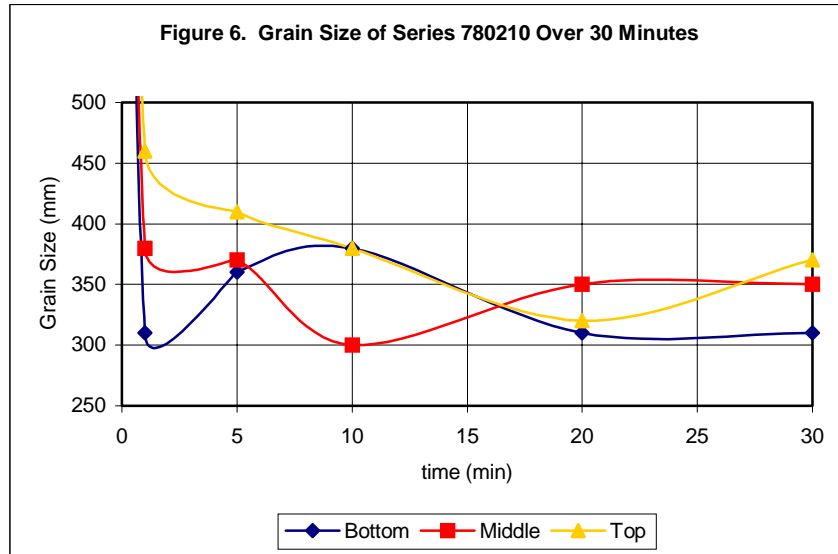
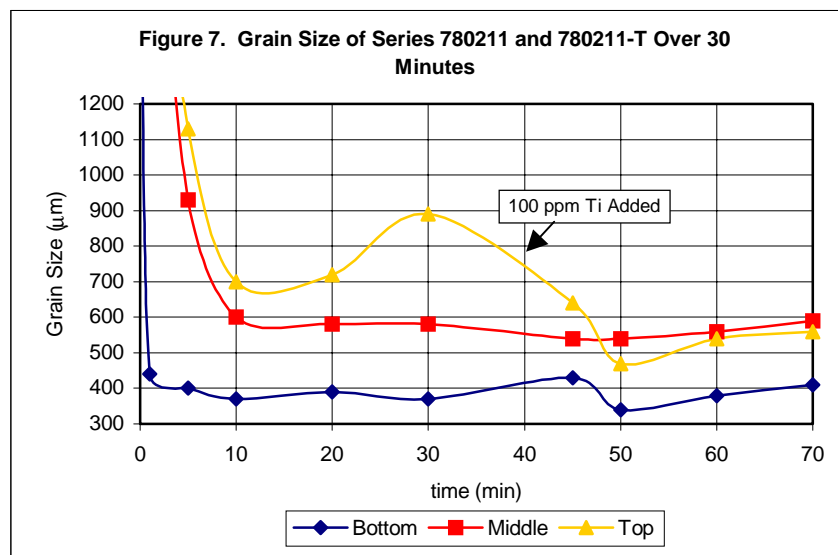
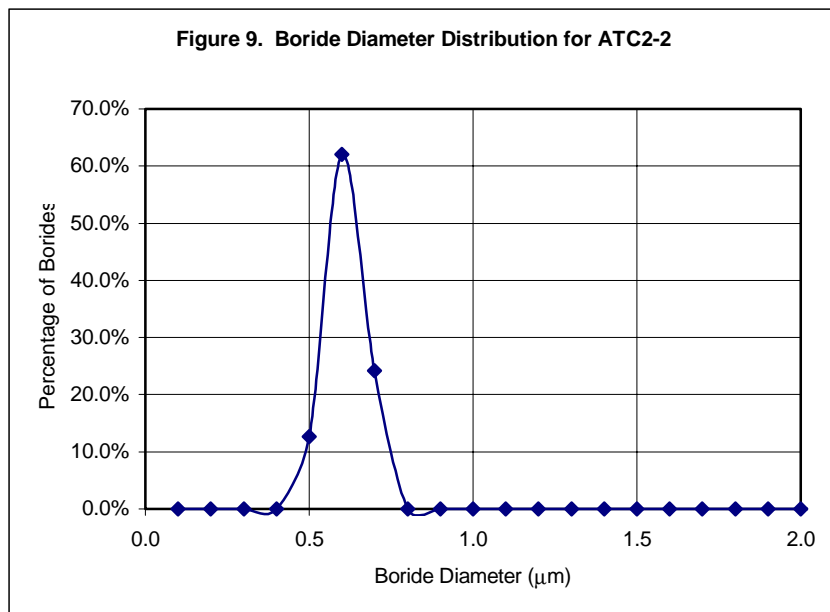
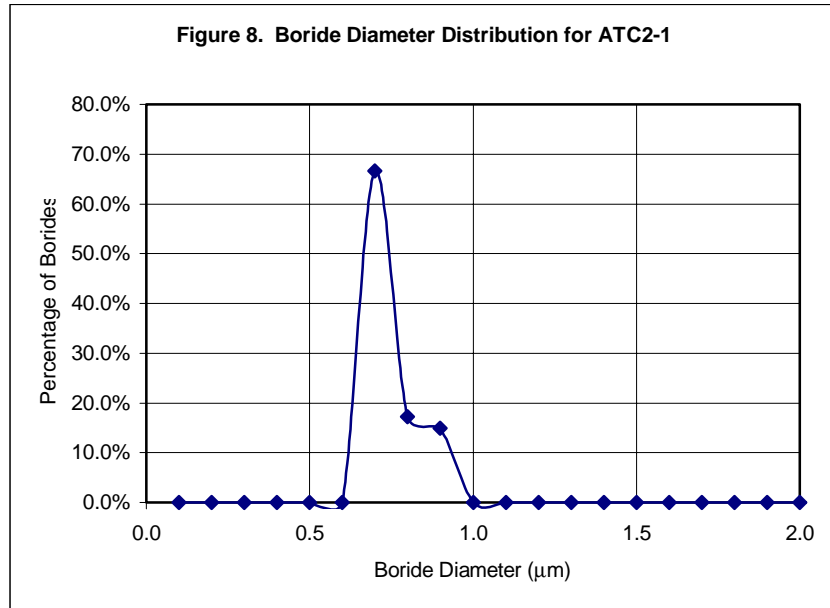
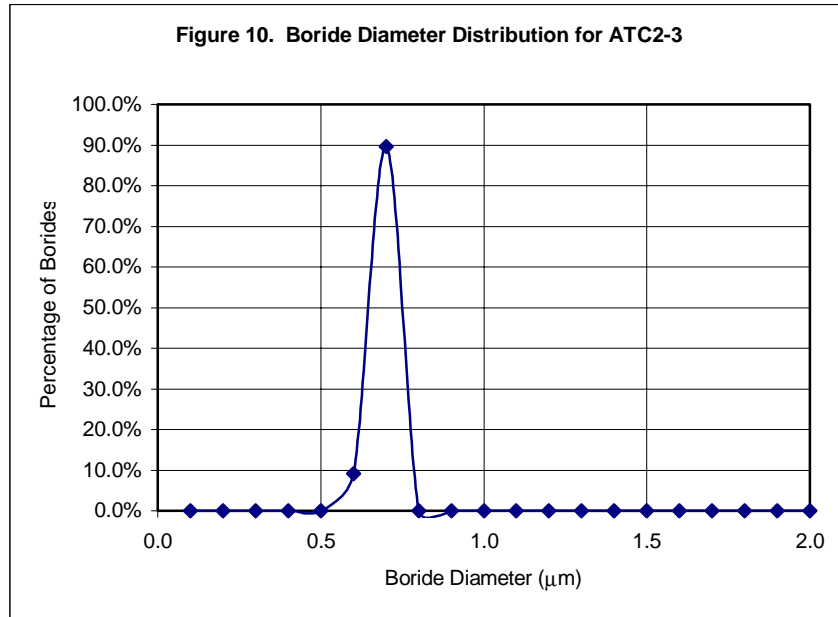


Figure 7 shows the grain size of series 780211 and 780211-T over thirty-minutes. While it is not immediately apparent, there was an improvement of grain size with time, particularly within the first 10 minutes. After the first 10 minutes, grain sizes remained relatively consistent with the exception of the reading taken 3.5 inches from the bottom (labeled “Top” in Figure 6). However, upon addition of an extra 100 ppm titanium, the grain size seemed to improve again. At ten minutes after the second titanium addition, all three grain sizes reached their lowest points for this experiment. However, it is not readily apparent from this experiment whether this is due to improvement with time, titanium, or both.



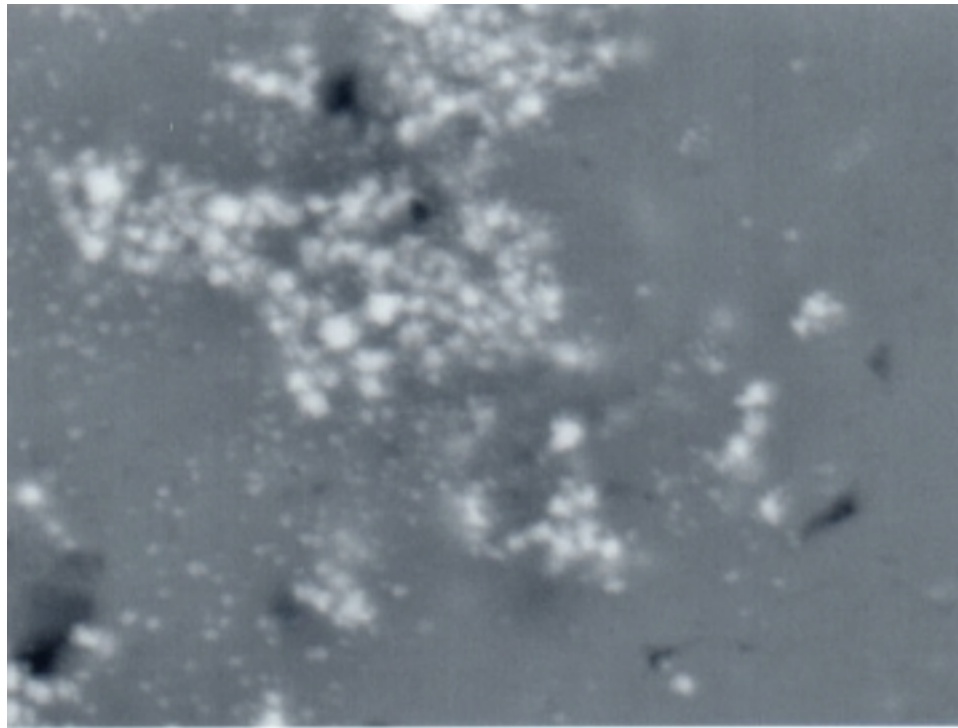
The diameter of the borides, found in Table 8, produced during this set of experiments is approximately half on average of what is produced in the laboratory at JDC. However, the particle distribution is somewhat consistent with what is normally found in the lab (Figures 8-10).





As shown in Table 8, the average boride size is approximately 0.6 μm . This reading is taken from an SEM back-scatter photograph like the one in Figure 11.

Figure 11. SEM Photograph of LAIS Sample ATC2-2 at 3640x Magnification



Sample ATC2-2
3640x

Conclusions and Recommendations

The fy-Gem process seemed to produce mixed results during these trials. It was desired to prove that fy-Gem could produce adequate grain refinement in wrought alloys at a commercially viable level of titanium and boron. While the boron level was within acceptable limits, the titanium level was approximately twice what is present commercial practice.

Prior to the trials, the theory was that the nuclei had to be sufficiently large enough to allow for grain growth and yet small enough to provide enough nuclei for adequate grain refinement. From some initial work conducted by JDC using a LAIS filter to study boride size and composition, a nuclei diameter of $1\mu\text{m}$ was thought to yield the best results. However, recent work conducted by A.L.Greer¹ suggests that the actual optimum nuclei size may be more in the range of 3-4 μm . During the course of this work, however, the fy-Gem process produced borides in the 0.5 to 0.7 μm range. It is believed that these may have been too small to provide adequate grain growth during the trials. Further tests in JDC's laboratory will focus on the effect of boride sizes on grain size.

Bibliography

1. A.L. Greer and A. Tronche, “Design of Grain Refineries for Aluminum Alloys”, TMS Annual Meeting, March 2000.

Fy-Gem Scale Up Trials in A356Alloy at Reynolds Tech Center

C.R. Durst
April 26, 2000

Jamegy Development Corporation, Inc.
South Chester Street
New Cumberland, WV 26047

Introduction

During the week of April 3, 2000, JDC, Inc. ran a series of eight tests using the fy-Gem process in a 400-lb furnace at Reynolds Research Facility in Richmond, Va. Fy-Gem v4.0, shown in Figure 1 below, utilized a system in which Argon pressurized a bottle of liquid Boron Trichloride, BCl_3 , pushing the liquid out of the bottle and into a vaporizer unit. Upon vaporization of the liquid, the gas moved into a rotometer where it was monitored and mixed with Argon before being sent to the agitator unit.

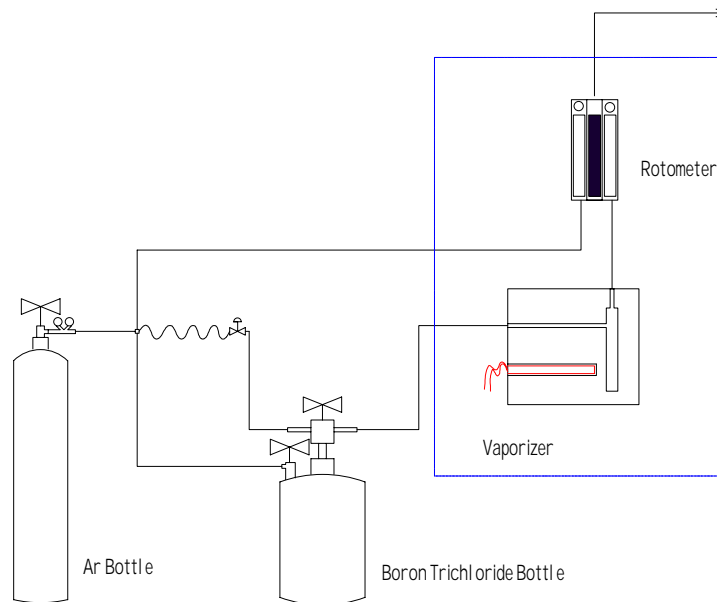


Figure 1. P&ID for fy-Gem v4.0

The main variable in these experiments was the amount of Boron introduced into the aluminum. However, there were several side-variables involving the agitator unit. One such variable was the geometry of the head on the agitator. The two heads that were implemented in this work were referred to as the

“Megy Head” and the “Mazurek Head.” It was believed that the Megy Head, shown in Figure 2, would produce finer and more uniform bubbles as it utilized a series of nipples with $\frac{1}{16}$ ” holes to distribute the gas to the melt. The theory on these nipples was that they would provide more turbulence at the point of exit for the gas. This in turn would shear the bubbles faster and produce a smaller bubble diameter. The Mazurek Head, however, is a scaled-down version of what is currently used in the wheel plants, so it was deemed necessary to determine the efficiency with which fy-Gem could operate if it were to be put into operation with minimal modification to existing plant equipment. The Mazurek Head, shown in Figure 3, was theorized to produce larger bubble sizes as it had no nipples to produce extra metal phase turbulence at the point of exit for the gas and the holes were twice as large at $\frac{1}{8}$ ”. It was believed that the larger blades on the head might have been able to produce enough overall turbulence to keep the bubbles small enough to produce sufficiently large nuclei for effective grain refinement. However, when nuclei become too large, there is an insufficient number to effectively grain refine at a given boron addition level.

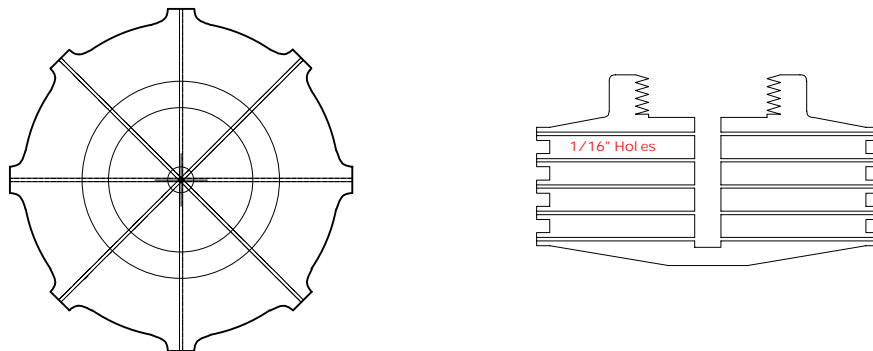


Figure 2. The “Megy Head” used in the Reynolds Trials
Outside Diameter (including nipples) = 6.5”

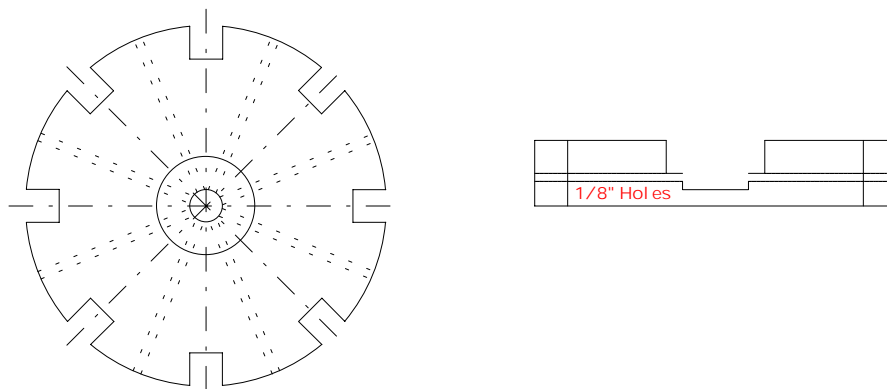


Figure 3. The “Mazurek Head” used in the Reynolds Trials
Outside Diameter = 5.5”

Another variable dependent on agitation was the speed at which the rotor operated. It was believed that faster rotation rates would result in finer bubbles and, therefore, coarser nuclei. Prior to the trials, the theory was that the nuclei had to be sufficiently large enough to allow for grain growth and yet small enough to provide enough nuclei for adequate grain refinement. From some initial work conducted by JDC using a LAIS filter to study boride size and composition, a nuclei diameter of 1 μ m was thought to yield the best results. However, recent work conducted by A.L.Greer¹ suggests that the actual optimum nuclei size may be more in the range of 3-4 μ m. Although this information became available just prior to the trials, it was determined that at this point, a scaled-up simulation of what was being conducted in JDC's laboratory would be more informative. Unfortunately, the drive could only spin the 5 1/2" scaled-down rotor at up to 480 RPM which did not provide the tip speed equivalent to what is used at JDC or in Reynolds's wheel plants. To simulate the rotation rate used in the wheel plant, approximately 900 RPM would be required for the scaled-down agitator head to yield the equivalent tip speed achieved by the 9 1/2" wheel plant agitator head.

Procedures

Prior to the start of each experiment, 400 lbs of A356 Aluminum were cut, weighed, and melted in a 400 lb capacity induction furnace. At the same time, the fy-Gem unit was turned on to warm up and ensure that the lines were purged from the previous experiment. When the appropriate metal temperature was reached, an Alu-Delta reading was taken. Upon the report of a large grain size from the Alu-Delta, a series of "blank" samples were taken. These included one PodFa, one Golf-Tee, one TP, and one Spectrographic Sample. At this point, the agitation unit was repositioned such that the agitator head was within an inch of the top of the melt and allowed to preheat. This was done for two reasons. First, preheating reduced the temperature drop associated with the introduction of a cold agitator into a pot of molten aluminum. Second, and more importantly, preheating helped remove any moisture which may have collected on the agitator overnight. During preheating, the Boron Trichloride valve was opened on the fy-Gem unit and a puff of smoke was emitted to ensure that the unit was functioning properly. After several minutes, the agitator was lowered into the melt with only Argon blowing out of the head. The rotor was set to the

desired RPM and the agitator fluxed with only Argon for 30 seconds. Then, the Boron Trichloride was turned on to the appropriate setting and allowed to react for 3 minutes. Finally, the Boron Trichloride was turned back off and the agitator fluxed with only Argon for a final 30 seconds. At this point, the rotor was turned off and the agitator was removed from the melt. Typically, Strontium is added to A356 as a modifier. However, it was believed that the chloride that disassociates from boron trichloride would react with the Strontium and remove it from the melt in the form of a dross. Therefore, Strontium additions were made subsequent to the Boron addition. Following this, a series of samples was taken. This series represented “Time 0” and consisted of the same samples that would be taken for the remainder of the experiment. They were one Alu Delta, one Golf Tee, one TP, and one Spectrographic Sample. The sampling was repeated at the 10, 20, 30, 60, 90, and 120-minute points. Additionally, a PodFa was taken at the 120-minute mark and on the second half of the experiments, an additional PodFa was taken after approximately 20 minutes. Upon taking the final set of samples, the molten Aluminum was poured into pig moulds and the crucible was prepared for the next run.

Results

The main variables throughout the course of this work were: Boron concentration, head design, rotor speed, and stirring/no stirring prior to sampling. Table 1 illustrates the parameters as defined prior to each run.

Table 1. Experimental Parameters

Series	Boron (ppm)	Head	Rotor RPM	Stirring¹
CK	20	Megy	460	No
CL	20	(TiBor)	-	No
CM	10	Megy	250	No (Stirred 8)
CN	20	Megy	475	Yes
CO	20	Mazurek	425	Yes
CP	20	Mazurek	480	No (Stirred 8)
CQ	10	Mazurek	425	No
CR	3	Mazurek	425	No

In the first series, CK, the target Boron concentration was 20 ppm. However, the spectrographic sample showed that only 12 ppm had gotten into the melt and this dropped off with time. During the course of the

¹Stirring refers to agitation by hand rod prior to taking aging samples after nuclei addition. No (Stirred 8) means only stirred prior to last aging sample.

experiment, the Alu-Delta reading dropped beginning with the 30-minute sample. It was determined after the experiment, though, that the grain size got increasingly finer according to the TP sample and stayed relatively the same in the Golf Tee (Table 2).

Table 2. Results of the CK Series

ID	Sample Time	HEAD	RPM	CONV	STIR	B AIM	PPM B	PPM Sr	Alu Delta	Golf T (μm)	TP-1 (μm)
CK1	0	MEGY	460	777	NO	20	12	53	11	530	320
CK2	10	MEGY	460	556	NO	20	8	73	13	450	380
CK3	20	MEGY	460	556	NO	20	7	67	13	430	410
CK4	30	MEGY	460	889	NO	20	7	62	10	470	420
CK5	60	MEGY	460	1027	NO	20	5	54	9	450	400
CK6	90	MEGY	460	556	NO	20	4	51	13	450	400
CK7	120	MEGY	460	1417	NO	20	1	42	6	490	380

Due to the fall of the Alu-Delta reading, it was determined that an equivalent TiBor run should be conducted next to define a baseline. This experiment, CL, showed that not only did the Alu-Delta remain high, but so did the Boron content. However, this experiment does seem to suggest that grain size may gradually worsen. with time when using TiBor (Table 3).

Table 3. Results of the CL Series

ID	Sample Time	HEAD	RPM	CONV	STIR	B AIM	PPM B	PPM Sr	Alu Delta	Golf T (μm)	TP-1 (μm)
CL1	0	MEGY	0	1417	NO	20	12	31	6	370	290
CL2	10	MEGY	0	416	NO	20	9		14	380	290
CL3	20	MEGY	0	889	NO	20	6	96	10	360	280
CL4	30	MEGY	0	416	NO	20	4	95	14	400	350
CL5	60	MEGY	0	416	NO	20	2	88	14	450	360
CL6	90	MEGY	0	638	NO	20	1	84	12	420	390
CL7	120	MEGY	0	777	NO	20	1	78	11	420	430

Following the results of the TiBor run, it was thought that the Borides produced via the Fy-Gem process were uniform in size and therefore settled out uniformly while the Borides from TiBor were of various sizes and therefore settled out at various times. So, in the next experiment, CM, it was determined that at the end of the run, a second sample would be taken at the 120-minute mark. However, prior to taking this sample, the aluminum would be stirred to allow the Boron to redistribute throughout the melt. Table 4 shows that the stirring did redistribute the Boron and improve the Alu Delta reading. In addition, it seemed to improve the Grain Size on both the TP and the Golf Tee.

Table 4. Results of the CM Series

ID	Sample Time	HEAD	RPM	CONV	STIR	B AIM	PPM B	PPM Sr	Alu Delta	Golf T (μm)	TP-1 (μm)
CM1	0	MEGY	250	1417	NO	10	3	23	6	470	340
CM2	10	MEGY	250	1417	NO	10	2	69	6	410	250
CM3	20	MEGY	250	1417	NO	10	0	77	6	440	260
CM4	30	MEGY	250	1027	NO	10	0	78	9	400	290
CM5	60	MEGY	250	889	NO	10	0	75	10	640	350
CM6	90	MEGY	250	1417	NO	10	0	68	6	1180	550
CM7	120	MEGY	250	1417	NO	10	0	62	6	540	870
CM8	121	MEGY	250	638	YES	10	3	61	12	490	260

Sample CM8 seemed to show that stirring may be necessary for the success of fy-Gem and it was determined that there would be some level of stirring in the wheel plants due to the backflow of Aluminum following the release of the vacuum used in the wheel cast. So, for the next series, CN, the melt was stirred prior to sampling. The results were as expected. The Boron level was on par with the TiBor experiment and the Alu Delta, Golf Tee, and TP all showed good results as shown in Table 5.

Table 5. Results of CN Series

ID	Sample Time	HEAD	RPM	CONV	STIR	B AIM	PPM B	PPM Sr	Alu Delta	Golf T (μm)	TP-1 (μm)
CN1	0	MEGY	475	1417	YES	20	11	78	6	490	260
CN2	10	MEGY	475	638	YES	20	6	57	12	450	270
CN3	20	MEGY	475	638	YES	20	9	50	12	400	260
CN4	30	MEGY	475	416	YES	20	7	44	14	380	230
CN5	60	MEGY	475	556	YES	20	4	35	13	360	250
CN6	90	MEGY	475	889	YES	20	3	30	10	380	240
CN7	120	MEGY	475	777	YES	20	10	30	11	330	240

At this point, the study shifted to determine how well the fy-Gem process would work with the minimum modifications necessary to wheel plant equipment prior to installation. So, the Megy Head was removed and the Mazurek head was attached. Series CO looked at how effective the Mazurek head would operate in direct comparison to series CN which utilized the Megy Head under similar operating conditions. The Mazurek Head proved to be nearly as effective as the Megy Head in producing grain refinement. Table 6 shows that the Boron concentration remained high throughout the 120-minute experiment and the Alu-Delta and grain size samples returned good results.

Table 6. Results of CO Series

ID	Sample Time	HEAD	RPM	CONV	STIR	B AIM	PPM B	PPM Sr	Alu Delta	Golf T (μm)	TP-1 (μm)
CO1	0	MAZUREK	425	1417	YES	20	13	83	6	520	280
CO2	10	MAZUREK	425	777	YES	20	13	59	11	530	280
CO3	20	MAZUREK	425	1111	YES	20	13	53	8	440	270
CO4	30	MAZUREK	425	777	YES	20	13	48	11	420	250
CO5	60	MAZUREK	425	1111	YES	20	14	40	8	420	250
CO6	90	MAZUREK	425	638	YES	20	12	39	12	410	250
CO7	120	MAZUREK	425	889	YES	20	11	24	10	390	270

At this point, the validity of stirring was questioned. It was determined that while there would be some effective stirring in the wheel plant, it was probably not being accurately modeled in these experiments. So, Series CP was run with no stirring until the end to determine how effective the Mazurek Head would be in producing Borides that would not settle. The results from this experiment, shown in Table 7, are somewhat mixed. The Boride concentration and Golf Tee grain size both decreased with time, then improved upon mixing. However, The TP sample remained consistent throughout and the Alu Delta, while initially dipping all the way down to a reading of 6, improved to a 13 and 6666 prior to mixing.

Table 7. Results of CP Series

ID	Sample Time	HEAD	RPM	CONV	STIR	B AIM	PPM B	PPM Sr	Alu Delta	Golf T (μm)	TP-1 (μm)
CP1	0	MAZUREK	480	1111	NO	20	2	4	8	600	320
CP2	10	MAZUREK	480	777	NO	20	16	37	11	520	330
CP3	20	MAZUREK	480	1417	NO	20	13	55	6	430	370
CP4	30	MAZUREK	480	1417	NO	20	10	58	6	440	290
CP5	60	MAZUREK	480	1417	NO	20	9	49	6	500	280
CP6	90	MAZUREK	480	556	NO	20	6	33	13	760	310
CP7	120	MAZUREK	480	222	NO	20	5	25	15	680	300
CP8	121	MAZUREK	480	638	YES	20	14	20	12	460	280

Following the return of the results from Series CP, it was determined that the next experiment, CQ, should not be stirred until the Alu Delta showed that it may be necessary in order to obtain adequate grain refinement. Additionally, the Boron target level was reduced to 10 ppm so that the effectiveness of the Mazurek Head could be determined at a lower Boron concentration. The results from this experiment (Table 8) show that the Alu Delta reading never fell long enough to justify mixing. As expected, the Boron

level did decrease with time, however, the Alu Delta, TP, and Golf Tee seemed to remain consistent throughout the length of this experiment.

Table 8. Results of CQ Series

ID	Sample Time	HEAD	RPM	CONV	STIR	B AIM	PPM B	PPM Sr	Alu Delta	Golf T (μm)	TP-1 (μm)
CQ1	0	MAZUREK	425	777	NO	20	14	31	11	570	290
CQ2	10	MAZUREK	425	777	NO	20	11	69	11	540	280
CQ3	20	MAZUREK	425	1250	NO	20	10	73	7	600	260
CQ4	30	MAZUREK	425	777	NO	20	9	67	11	720	330
CQ5	60	MAZUREK	425	777	NO	20	5	56	11	610	270
CQ6	90	MAZUREK	425	777	NO	20	5	50	11	520	270
CQ7	120	MAZUREK	425	222	NO	20	4	44	15	630	290

The general consensus by this point in the week was that fy-Gem could indeed produce adequate grain refinement. However, the fumes coming off the top of the melt became a major issue. Prior to the next experiment, an experiment was ran to determine if there may be a set of parameters at which the smoke could be eliminated. The most likely variables to affect fuming were the amount of Boron Trichloride introduced and the rotor speed. It was determined that lower rates of flow for both Argon and Boron Trichloride produced less fumes. This was later verified in a set of experiments run in JDC's laboratory. Additionally, it appeared that higher rotor speeds yielded a reduced amount of fumes. During the experiments at JDC following the Reynolds trials, however, it was observed that higher rotation rates actually caused more fuming. This may be due to the fact that the rotor can spin much faster at JDC (up to 800 RPM), so vortexing may have allowed more gas to evolve.

So, for the final series, CR, the Boron Trichloride flow rate was reduced to a target Boron level of 3 ppm. By running at the lower Boron Trichloride level, the fumes were reduced, however they were not eliminated. The results (Table 9) show that while the Alu Delta returned adequate ASTM grain sizes and the Boron level did not drop off too sharply, the grain size determined from the TP samples rapidly decreased. The initial grain sizes were excellent, but by the end, the grain size reached 700-900 μm. However, the Golf Tees showed that initially, the grain sizes were relatively large, but improved with time.

Table 9. Results of CR Series

ID	Sample Time	HEAD	RPM	CONV	STIR	B AIM	PPM B	PPM Sr	Alu Delta	Golf T (μm)	TP-1 (μm)
CR1	0	MAZUREK	425	1027	NO	20	6	86	9	680	290
CR2	10	MAZUREK	425	777	NO	20	5	84	11	780	390
CR3	20	MAZUREK	425	556	NO	20	4	79	13	760	440
CR4	30	MAZUREK	425	1417	NO	20	4	77	6	790	520
CR5	60	MAZUREK	425	889	NO	20	3	68	10	520	430
CR6	90	MAZUREK	425	1027	NO	20	2	61	9	450	930
CR7	120	MAZUREK	425	1027	NO	20	2	55	9	580	700

Additionally, Joe Megy sampled the fumes coming off the top of the melt during this series, as well as Series CN and CQ, for analysis. Using a cowl surrounding the agitator and furnace to reduce dilution of the off-gas, a 3-minute sample was pulled via a vacuum into a caustic solution through a Smith-Greenberg impinger. The solution was then analyzed for Chloride, Boron, and Aluminum. Megy shows that the off-gas consists of Boron Trichloride, not Aluminum Chloride, and that approximately 99% or more of the boron and chloride reacts or is absorbed by the molten aluminum.² The Boron reacts to produce the borides which act as a grain refiner, while the chloride presumably reacts to form Magnesium Chloride which forms a dry dross on the surface of the melt. The unreacted Boron Trichloride passes through the melt and is still concentrated enough at 500 ppm to be clearly visible as white fumes. This off-gas then reacts with water vapor to produce boron oxide fine smoke and hydrogen chloride as a very visible cloud. According to Megy, though, the chlorine off-gas is well below the new 0.04 lbs/ton standard.

Discussion

While it is not feasible to determine any optimum operating conditions from these results due to the fact that more than one variable was altered in nearly every experiment, it may be possible to make some generalizations of effectiveness based on the results from the Reynolds trials as compared to what has been observed in JDC's lab work.

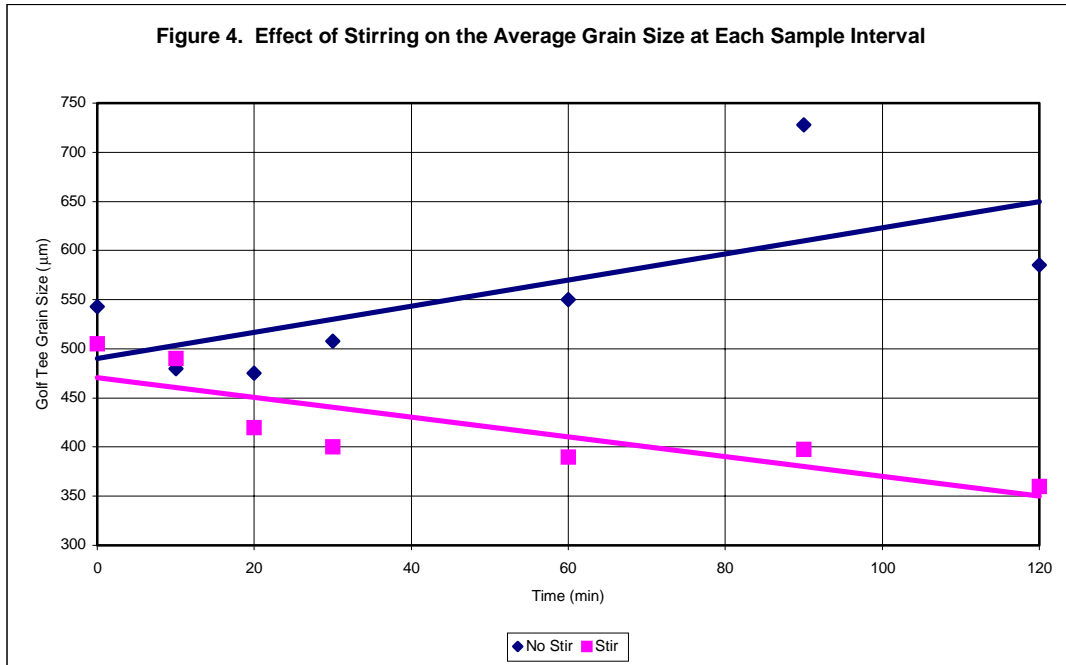
Table 10 illustrates the average Alu Delta, Golf Tee, and TP values. Numbers in RED indicate the best value achieved during the week of experimentation while numbers in BLUE indicate the worst results.

Table 10. Average Values for Experiments

ID	Number Samples	HEAD	RPM	STIR	B AIM	Alu Delta	Golf T (μm)	TP-1 (μm)
CK	7	Megy	460	No	20	10.7	467.1	387.1
CL	7	TiBor	-	No	20	11.6	400.0	341.4
CM	8	Megy	250	No	10	7.6	571.2	396.3
CN	7	Megy	475	Yes	20	11.1	398.6	250.0
CO	7	Mazurek	425	Yes	20	9.4	447.1	264.3
CP	8	Mazurek	480	No	20	9.6	548.8	310.0
CQ	7	Mazurek	425	No	10	11.0	598.6	284.3
CR	7	Mazurek	425	No	3	9.6	651.4	528.6

While the Alu Delta is the most convenient method of analysis for grain refinement, it is important to note that the Alu Delta cools at a very slow rate, in the order of 0.25°F/sec. This is much slower than the cooling rate associated with wheel casting. In a study by Sandy Levi, it was determined that Wheels could be expected to cool at a rate anywhere from 0.74°F/sec to 1.61°F/sec.³ The Golf Tee, which cools at 2.05°F/sec, would seem a more appropriate comparison. Finally, the TP sample cools at a rate of 8.47°F/sec. Although this would be appropriate for DC cast comparisons, the cooling rate is too fast for wheel cast comparisons. Therefore, for the Golf Tee grain sizes will be used for the analysis of the results from these trials.

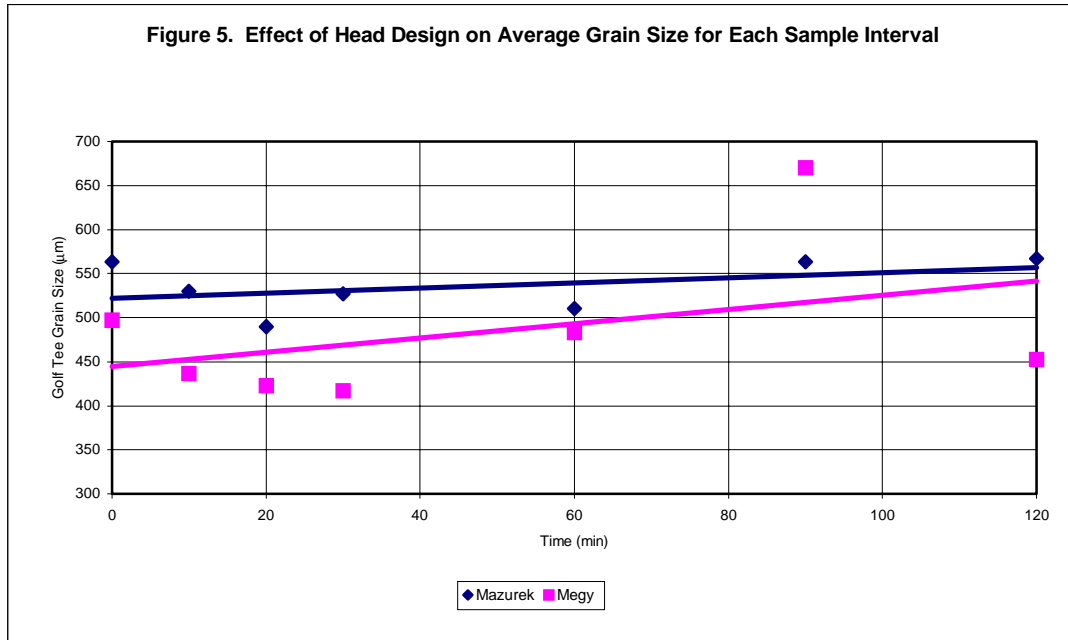
From Table 10, the variable that seems to most affect the results is stirring. When compared to TiBor, the results from Series CN are slightly better according to the Golf Tee grain size and significantly better when comparing the TP samples. However, no non-stirring experiment was within 15% of the Golf Tee grain size achieved using TiBor rod. When comparing the effect of stirring over time, it becomes obvious that the grain size continues to improve with stirring, while in the absence of stirring, it worsens (Figure 4).



This would seem to suggest that over a 2-hour hold-up time, which is what has been conveyed as the typical period between gas treatment and casting, some sort of mixing would be necessary. It has been suggested that metal backwash inherent with wheel casting may provide enough mixing as it dumps excess aluminum back into the crucible following a cast. In this case, the pink trendline in Figure 4 would be representative of what could be expected in the wheel plants.

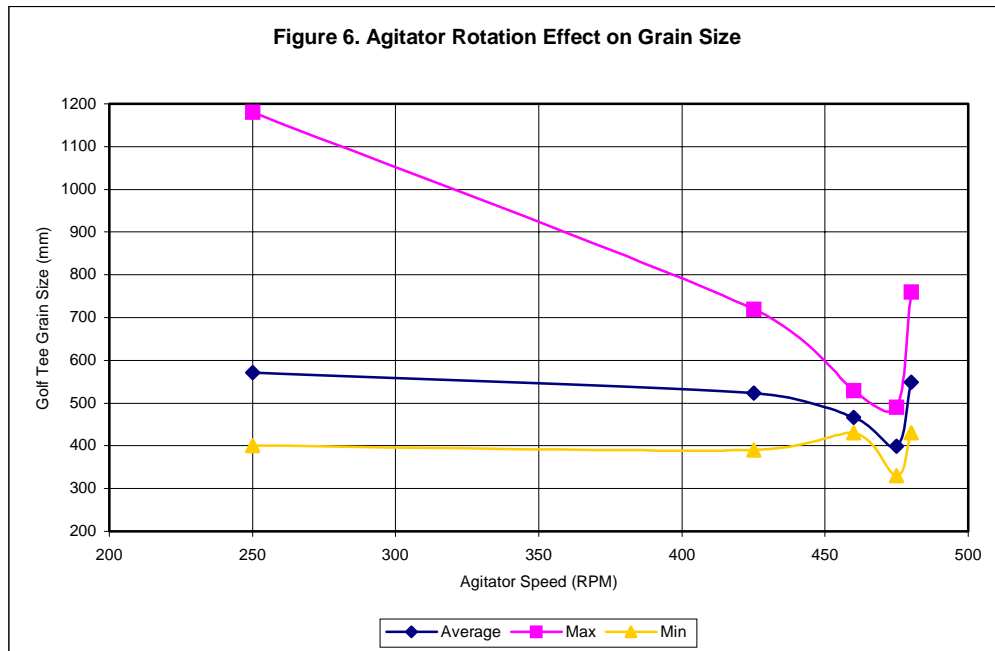
Head design was a major concern over the course of this work as well. It was determined that if the Mazurek Head could prove to be as effective as the Megy Head, there would be less resistance to the implementation of the fy-Gem process in the wheel plants since all existing equipment could be used and the fy-Gem would simply need to hook into the Argon fluxing line. The major problem with comparing the effectiveness of each head is that no two runs were the same. The closest two runs were CN and CO, which utilized the Megy and Mazurek Heads, respectively. While the comparison between these two would appear to show that the Megy Head is slightly better, it is also important to note that rotor speed was different between the two and tests at JDC's facility has shown that rotor speed does affect the grain size. However, excluding runs CL and CR which used TiBor and very low Boron levels, respectively, the average of all of the runs could be used to show an effective comparison between the two head designs. Figure 5 seems to show that while the Megy Head produces a finer initial grain size, the grain size

produced by the Mazurek Head is more stable. However, the results may be marred by the average grain size achieved at the 90-minute interval, Sample Number 7, using the Megy Head. By excluding this number, the trendlines become very similar.



From these results, it can be theorized that the Megy Head produces a slightly better grain size. However, it would have to be determined whether the better grain size would be worth the change in the head design and the effect that would have in the wheel plants.

The final variable that seemed to play a significant role in determining the final grain size was the speed at which the rotor spun. Figure 6 seems to show that a local optimum can be found at 475 RPM. However, this is somewhat of a false impression as this particular number comes from a single experiment, the CN Series, in which the melt was stirred prior to sampling and the Megy Head was implemented. What can be seen is that the grain size did seem to improve as rotor speed was increased. More focused experiments would need to be conducted, though, before any conclusions could be made.



During the course of these experiments, there were concerns that the fy-Gem process was not producing adequate grain refinement according to the Alu Delta reading. This was because the readings from the thermal analysis did not correlate accurately with the degree of refinement found in the Golf Tee samples. While there have been reports of good correlation between the thermal analysis and grain size when using TiBor, as seen in Series CL, two possible explanations for these results with the fy-Gem process should be considered.

First, it may be possible that something inherent in the fy-Gem process causes the thermal analysis to respond differently than what has come to be expected from conventional grain refiners. This may be due to the lack of inclusions or the uniformity in nuclei size associated with fy-Gem. This possibility should be considered although there is no technical or theoretical method of discerning if this is the cause at this time.

Another explanation for the results is that the Alu Delta method of thermal analysis for grain refinement is not sufficiently accurate to distinguish between levels of grain refinement. Discussions with Geoffrey Sigworth, who has conducted research with the Alu Delta, have led to the understanding that the use of undercooling measurements is more of a “go/no go” test than an accurate measurement of grain refinement. D. Gloria and J.E. Gruzleski at McGill University in Montreal have also shown that the conventional “Delta T” parameter is not very reliable.⁴ They suggest the use of a time parameter, which is the time elapsed

between the minimum undercooling temperature and the maximum recalescence temperature. While Gloria and Gruzleski's work was conducted in 319 Al-Si-Cu alloy, their conclusions may apply to A356 alloy as well.

One of the advantages of the fy-Gem process is that it produces uniform borides of a somewhat controllable size. While the actual data has not returned yet on the borides, previous experiments in the JDC lab have shown that the borides produced via the fy-Gem process were smaller than those in the TiBor experiments. A paper written by A.L. Greer shows that slightly larger borides, in the range of 2-3 μm , would be superior to the finer boride sizes typically produced via the fy-Gem process.¹ This would seem to indicate that it may be possible to improve the process merely by controlling the boride size.

Conclusions and Recommendations

From a grain-refining standpoint, fy-Gem appeared to be a success. fy-Gem yielded superior grain sizes according to the TP and equivalent grain sizes in the Golf Tee. With further optimization, it is feasible that the fy-Gem process could produce a consistently superior Golf Tee grain size as compared to the current practice.

Additionally, inherent in the fy-Gem process is a method to dry out the dross on top of the melt. This is caused by the chloride that is released when the boron reacts to form borides. The chloride then reacts to ultimately form a dry, gray dross that significantly reduces aluminum dross and may aid in inclusion removal during gas fluxing.

The failure of the Alu Delta to show an accurate portrayal of the level of grain refinement when using the fy-Gem process represents a problem in that conventional thermal analysis tests may not be reliable for this process. As many foundry plants use the Alu Delta as a convenient way to ensure quality control in their molten metal processing facilities, it may be necessary to perform further studies to determine if there is a solution to this problem.

At this point, there are only two hurdles that fy-Gem will need to overcome prior to commercialization: Boron control and fuming. Controlling the level of Boron addition is the lesser of the problems, as this only requires further calibrations and determining the pick-up efficiency for any given rotor speed and dilution rate. Additionally, a mass flowmeter can replace the rotometers that are equipped in the current fy-

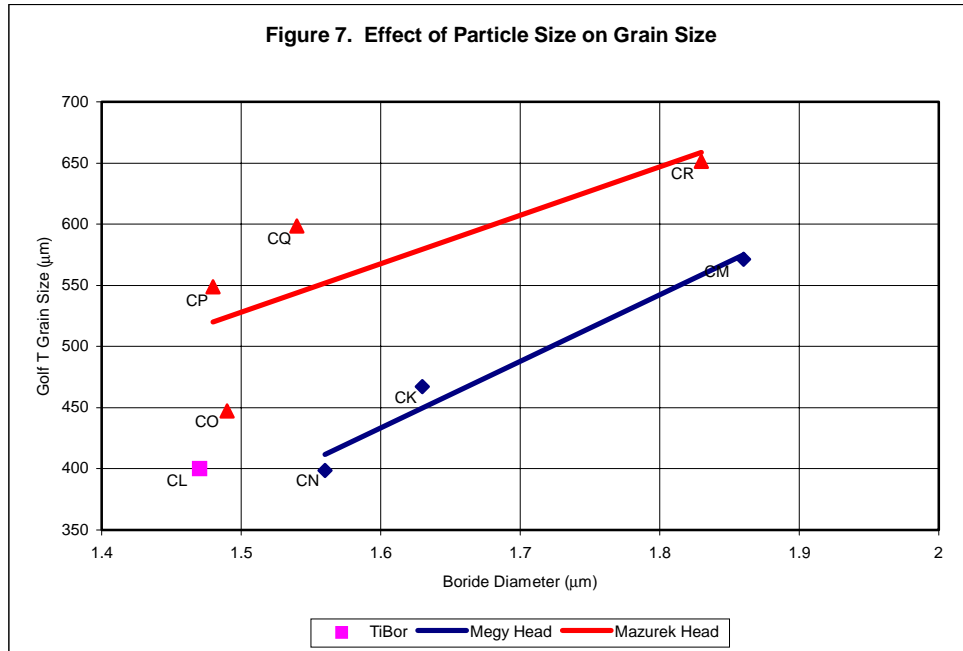
Gem cart. The mass flowmeter, manufactured by Thermal Instrument Co., has an accuracy of $\pm 1\%$ and a response time of 1 to 2 seconds.⁵ The fy-Gem unit will then consist of all Swagelok fittings and open tube runs which will ensure that there are no blockage or leakage problems. This method of control and enclosure is what is currently used by integrated circuit manufacturers when dealing with Boron Trichloride. The fuming, however, is troublesome. While administering the gas into the melt, white fumes have been found coming off the top of the melt. As reported previously in this report, Megy found that greater than 99% of the Boron Trichloride had reacted in the melt, and the remaining off-gas consisted of Boron Trichloride which reacted with water vapor to form boron oxide and hydrogen chloride. In an earlier experiment conducted at Littlestown, it was found that the fumes could be eliminated by dilution of Boron Trichloride with Argon and high agitator rates. Further experiments will be conducted to determine a solution for the elimination or removal of the fumes.

Addendum

Additional information on particle sizes has been provided by Touchstone Laboratory. The data has been summarized in Table 11. From this information it is not evident that the diameter of the boride directly affects the grain size. However, several interesting correlations can be drawn from the data. At low stirring speeds and low boron feed rates, the average boride diameter was significantly larger than for the rest of the experiments. In addition, as can be seen from Figure 7, the experiments run with Megy Head generally produced improved grain refinement at a given boride diameter.

Table 11. Average Values for Experiments

ID	Number Samples	HEAD	RPM	STIR	B AIM	Alu Delta	Golf T (μm)	TP-1 (μm)	Avg Boride Dia (μm)	Percent Boride Diameter Range (μm)					
										0.80-1.13	1.13-1.38	1.38-1.60	1.60-1.78	1.78-1.95	1.95-2.11
CK	7	Megy	460	No	20	10.7	467.1	387.1	1.63		3%	41%	54%	2%	
CL	7	TiBor	-	No	20	11.6	400.0	341.4	1.47	1%	18%	66%	15%		
CM	8	Megy	250	No	10	7.6	571.2	396.3	1.86				12%	86%	2%
CN	7	Megy	475	Yes	20	11.1	398.6	250.0	1.56		6%	72%	22%		
CO	7	Mazurek	425	Yes	20	9.4	447.1	264.3	1.49		22%	66%	12%		
CP	8	Mazurek	480	No	20	9.6	548.8	310.0	1.48		9%	88%	3%		
CQ	7	Mazurek	425	No	10	11.0	598.6	284.3	1.54		22%	68%	10%		
CR	7	Mazurek	425	No	3	9.6	651.4	528.6	1.83			1%	46%	48%	5%



One important conclusion from this recent data is that Touchstone reported that the borides appeared to be clean and free from agglomeration. However, any further conclusions will require additional analysis of the data.

Bibliography

1. A.L. Greer and A. Tronche, "Design of Grain Refineres for Aluminum Alloys", TMS Annual Meeting, March 2000.
2. J.A. Megy, "Analysis of Boron and Chlorine in Off Gas of Reynolds 356 fy-Gem Tests", April 10, 2000.
3. S.A. Levi, Presentation at Closing Meeting of Reynolds-JDC fy-Gem Trials, April 2000.
4. D. Gloria and J.E. Gruzleski, "Time as a Control Parameter in the Determination of Grain Size of a 319 Al-Si-Cu Foundry Alloy", 1999 AFS Transactions Paper.
5. Thermal Instrument Co., Product Information Packet, 1996.

Appendix E.

ENVIRONMENT, CAPITAL, AND LABOR COST OF PRODUCTION OF FY-GEM AND CONVENTIONAL GRAIN REFINERS

1. Raw Material for the fy-Gem Process

The only reagent used for the fy-Gem process is Boron Trichloride gas. Argon is already present in the metal treatment furnace to remove hydrogen and inclusions from molten aluminum just prior to casting. The chlorine in the boron trichloride reacts with aluminum to form aluminum chloride, which serves the same function, as the chlorine now used in the metal treatment machines. In current use the chlorine also forms aluminum chloride which then further reacts to remove sodium, calcium and magnesium impurities from the molten aluminum. It is fortuitous that the quantity of argon and chlorine presently used in the gas treatment of molten aluminum are nearly the same as that optimally used in the fy-Gem process.

In fact, it turns out that it is safer to add chlorine in the form of BCl_3 than in the form of chlorine. This is because of two factors. First the vapor pressure of BCl_3 (bp 12.4°C) is considerably below the vapor pressure of Cl_2 (bp -35.6°C). Thus, sturdier tanks are necessary to contain and ship liquid chlorine, and a rupture of the tank or attached piping results in a much greater release of chlorine before the heat of vaporization cools the remaining liquid to below its boiling point.

The second reason that the boron trichloride is safer is that it reacts with moist air to form a boron oxide/hydroxide, which is readily visible as a smoke at the 1 ppm level. Thus, any leaks that do occur are visible and traceable to their source.

The relative safety of boron trichloride is observed in both the OSHA and EPA regulations as can be noted in table YY, which compares chlorine and boron trichloride with several other commonly used inorganic halides.

Therefore, boron trichloride can be substituted for chlorine in the metal treatment unit and grain refine aluminum and supply the chlorine to remove sodium, calcium and magnesium impurities, help remove solid impurities, and make the dross drier in a safer fashion.

1 Supply of Boron Trichloride

Boron Trichloride is one of the best Lewis acids known and is used in manufacturing several organic products. It is also used in very high purity applications in electronic applications. It has been a routine commercial chemical used in the United States for over fifty years. At present Kerr-McGee Corporation is the only domestic commercial manufacturer of BCl_3 in a plant in

Henderson Nevada. They are manufacturing approximately 600,000 pounds per year of boron trichloride (~55,000 pounds contained boron), and have a plant capacity of roughly 1,000,000 pounds boron trichloride per year. The manufacture involves the chlorination of boron carbide at about 1000 °C in five chlorinators. The size of the chlorinators is kept small so that the heat released during the reaction results in adiabatic operation of the chlorinator. Expansion of capacity is obtained simply by adding more of the relatively simple chlorinators in series.

The boron carbide as raw material is manufactured in an electric arc furnace from borax and petroleum coke. Roughly four pounds of borax is needed to make a pound of boron contained in boron trichloride. Roughly 6×10^9 pounds of borax (B_2O_3 contained) is mined in the world, which is used mostly for glass manufacture and soap formulation at a value of about \$0.40/lb. Thus, the present consumption of boron used in aluminum consumes less than one twentieth of one percent of the borax mined. On the order of 30 million pounds of B_4C are produced worldwide principally for abrasives and as a reductant in refractory bricks. Thus, if the boron used in aluminum used this raw material it would consume about half of one percent of current production. The price of B_4C is currently about \$8 per pound or about \$9 per pound contained boron.

The current price of boron trichloride is \$9.25 per pound or \$100 per pound contained boron. Although this is approaching the cost of boron in conventional Al-Ti-B grain refiner, it reflects to a significant degree the cost of high purity customers and small production volumes. Large standard grade customers enjoy a significant discount and if the manufacturing scale were significantly increased an economy of scale would kick in particularly if another competitor entered the business.

A. The Current Al-Ti-B Master Alloy Grain Refiners

Commercial grain refining with titanium diboride master alloys involves three manufacturing processes, which are used almost exclusively to make aluminum grain refiner, as follows:

1. Manufacture of KBF_4
2. Manufacture of K_2TiF_6
3. Manufacture of Al-Ti-B master alloy from KBF_4 , K_2TiF_6 , and aluminum.

The aluminum industry has about fifteen manufacturing plants worldwide that carry out these processes. Each of these processes use manufactured raw materials as described below.

The manufacture of KBF_4 involves the mining of acid spar (CaF_2), borax, potassium chloride, sulfur, and the manufacture of sulfuric acid, hydrofluoric acid, and potassium hydroxide to make the major raw materials.

The manufacture of K_2TiF_6 involves the mining of rutile, salt, sulfur, KCl, acid spar, a source of coke, and the manufacture of sulfuric acid, chlorine, titanium tetrachloride, titanium hydroxide, sulfuric acid, hydrofluoric acid, and potassium hydroxide as raw materials.

In addition to the environmental costs of mining, all of the intermediates that do not end up in the aluminum end up as waste products. For example when making hydrofluoric acid from acid spar (CaF_2) the calcium ends up as calcium sulfate, and the iron and other impurities in the rutile usually end up as waste products. The potassium and fluoride end up as potassium aluminum fluoride, which has been a waste historically, but now has some recycle uses.

The Al-Ti-C Process: Although TiC nuclei have been known to be effective for grain refining since 1949, a practical method for their manufacture was not forthcoming until the work of Sigworth in 1978. He found you could form effective TiC nuclei by heating small amounts of carbon (i.e. 0.15% by weight) at high temperatures (e.g. $>1400^0$ C) where the solubility of carbon in aluminum becomes sufficient in the presence of titanium (i.e. about 3% by weight), and then quenching the molten solution. This process has been commercialized by Shieldalloy Metallurgical Corporation (SMC) over the last several years and now enjoys a couple of percent market penetration which is growing. It is now generally accepted this process gives higher quality aluminum due to lack of clusters and KAlF inclusions. At 0.15% carbon, however, there are less nuclei by weight in the master alloy than with standard Al-3Ti-1B. Note that in TiB_2 master alloys two boron atoms are associated with a titanium, where as in the carbon system TiC has one carbon atom per titanium atom. Also the molecular weight of carbon is 12 and boron is 10.8. In practice people find that nearly twice as much Al-3Ti-0.15C rod is required to give grain refining equal to Al-3Ti-1B rod. This means nearly twice as much rod needs to be prepared. At today's cost Al-3Ti-0.15C is perhaps 50% higher than the cost of Al-3Ti-1B for equivalent grain refining.

The fy-Gem Process The titanium source for the fy-Gem process (~10 ppm used to form the grain refiner in situ) comes as an impurity from the alumina and carbon anode used in the production of aluminum in the pot room. Aluminum from pot room cells typically contain 30-60 ppm titanium. Further titanium additions are usually added to facilitate grain refinement regardless of what grain refining process is used. This is added as a titanium metal or master alloy addition in the casthouse furnace with the other alloying materials. Additions of titanium used in the U.S. are mainly from co-product titanium metal fines which, because of their fineness, are pyrophoric and because of certain impurities otherwise become a waste product.

The source of boron in the fy-Gem process is B_4C , which is made on the large scale in electric furnaces for abrasive and refractory applications from borax ore and coke. Boron trichloride is manufactured by reacting B_4C with chlorine in a

carbon walled chlorinator at about 1000⁰ C. The reaction is exothermic and is self-heating.

When considered broadly the number of manufacturing steps is reduced substantially with the fy-Gem process with resulting capital, energy, environmental, and labor benefits.

The conventional master alloy process uses electrical energy in making aluminum used to reduce K₂TiF₆ and KBF₄, and to make KOH from KCl, and to make chlorine from NaCl, mining the raw materials, manufacturing the various intermediates, and melting the aluminum metal twice. The biggest single energy component is the electrolytic formation of potassium hydroxide, chlorine, and aluminum. There is also an energy cost associated with transporting and packaging all of the intermediate materials. An estimate of the quantities of raw materials to make two pounds of grain refiner master alloy for one ton of aluminum is as follows:

<u>Item</u>	<u>Use</u>	<u>lbs.</u>	<u>KWH/lb.</u>	<u>KWH/ton Al</u>
K(OH)	To make KBF ₄ & K ₂ TiF ₆		0.64*	1.6
Cl ₂	To make TiO ₂		0.46*	1.6
Al	To reduce salts		0.16**	15
	Sub total			<u>3.00</u>
				4.76

- @ 60% overall yield Electrical Power requirement to make one pound of Chlorine is 1.6 KWH/lb. – Kirk & Othmer, Encyclopedia of Chemical Technology.

** @ 80% overall yield

If we use grain refiner on 16 million tons of aluminum per year processed in the US, the amount of electricity used to reduce the required aluminum, potassium hydroxide and chlorine is about 76 million KWH/year. Additional electrical energy is required for the other mining, manufacturing and transport operations, and considerable thermal energy is also consumed. The electrical energy to produce 350,000 lbs of B₄C in the electric furnace to grain refine 16 million tons of aluminum per year is about 7 million KWH. The manufacture of BCl₃ from B₄C and chlorine is exothermic (self-heating).

The fy-Gem manufacturing process as outlined above is considerably simpler than the master alloy processes, but a detailed comparison of the advantage involves comparing the many mining and manufacturing processes of each of the raw material streams. A listing of the mining, processing and major waste streams are shown in the table below

Comparison of Manufacturing steps to produce grain refining by conventional process and the fy-Gem process

A. Conventional Process for Al-Ti-B Master Alloys

<u>Mining</u>	<u>Manufacturing</u>	<u>Final Products</u>
Sulfur (S)	Sulfuric Acid (H_2SO_4)	$CaSO_4$ gypsum
Acid Spar (CaF_2)	Hydrofluoric Acid (HF)	$KAlF_4$
Potassium chloride (KCl)	Potassium Hydroxide (KOH)	$KAlF_4$
Borax (B_2O_3)		Aluminum Nuclei
Salt (NaCl)	Chlorine (Cl_2)	$FeCl_3$
Rutile (TiO_2)	Titanium Tetrachloride ($TiCl_4$)	Aluminum Nuclei
Coke (C)		CO, CO_2
Alumina (Al_2O_3)	Aluminum (Al)	$KAlF_4$, Al

B. Conventional Process for Al-Ti-C Master Alloys

Salt (NaCl)	Chlorine (Cl_2)	$FeCl_3$, $MbCl_2$
Rutile (TiO_2 , FeO)	Titanium Tetrachloride ($TiCl_4$)	$MgCl_2$, Nuclei
Coke		CO_2 , Nuclei
$MgCl_2$	Magnesium	($MgCl_2$ Recycle)

C. fy-Gem*

Borax (B_2O_3)	Boron Carbide (B_4C)	Aluminum Nuclei
Carbon (C)	Boron Trichloride (BCl_3)	Carbon

* NOTE: Titanium to make nuclei is an impurity in the aluminum, and Cl_2 is already added in these amounts in the metal treatment system and $AlCl_3$ is already formed as a waste product in the metal treatment process.

Appendix F

Boron Trichloride Production Furnace

Introduction

Boron trichloride is the critical raw material required by the fy-Gem product. It is produced by one domestic plant owned by Kerr McGee in Henderson, Nevada at a rate that would require expansion to meet the needs of a developed fy-Gem requirement.

Alternatively it can be produced in a straightforward manner from chlorination of boron carbide at about 1000 °C. chlorine and an argon carrier are currently used in the gas treatment equipment at the casthouse. Boron carbide is a safe, concentrated, cheap, stable raw material that could be the raw material feed for the fy-Gem process. A large primary aluminum plant (200,000 tons/yr) would require less than 5000 pounds of boron carbide for one year of operation.

These considerations led us to a development program to demonstrate a suitable chlorinator early in the fy-Gem program. A small chlorinator was adapted from an induction furnace and initial shakedown tests were run as discussed below.

As the fy-Gem program progressed the effective level of BCl₃ was approximated and it became apparent that the chloride in the BCl₃ may in most cases be able to supply all of the chlorine required in the casthouse and that it was safer to ship and handle than chlorine as discussed in the raw material section. The chlorinator program was then put on hold and use of liquid boron trichloride as a raw material was favored.

Construction

The carbon furnace was donated to JDC, Inc. by Carnegie-Mellon University. Originally, the furnace was designed and operated by Geoffrey Sigworth during his time with the University. 20 years later, the furnace was brought to JDC, Inc where it was used to produce boron trichloride by passing chlorine gas across a boron carbide bed. Placed on each end of the carbon tube as a clamp which was connected to a transformer via a 400MCM cable. To limit the incoming power, a variac was installed between the transformer and the 240 Volt power source. A high temperature (~1000 °C) was required for reaction, so the carbon tube was encased in Thermax Powder (N-991), manufactured by Cancarb, which insulated the tube very well. The remaining heat passed through the mild steel shell of the chlorinator and was absorbed by a 50:50 mixture of ethylene glycol and water. The heat transfer took place at 3 levels. The first level was the shell of the chlorinator. A copper tube wrapped around the body absorbed a small amount of the total heat produced. The second level was the “raceway” which was effectively a multi-pass heat exchanger that sat on top of the chlorinator body. It absorbed a large portion of the heat from the Thermax as it had a substantial contact area with the insulating powder. The third level of heat transfer occurred in the end caps. These caps secured the carbon tube to the rest of the chlorinator. These caps absorbed a significant amount of the total heat transferred to the

water-cooling system. The coolant was then passed down to a radiator. An attached fan pushed a constant flow of air across the radiator to pull out the heat. The coolant was then pumped back into the chlorinator. The resulting boron trichloride gas which formed as a result of this reaction was mixed with Argon and blown into a scrubber until such time as a sample was to be taken.

Results of Operation

The findings of this study were mixed. First, the chlorinator did indeed prove to produce boron trichloride at the level necessary for grain refinement in an aluminum production facility. Also, the cooling-system worked extremely well with very few problems. However, the purity of the boron trichloride gas was never determined and the system was not run long enough to determine stability, and yield over long periods. There were leaks of boron trichloride from the top and bottom flanges of the furnace shell which would have required improvement prior to long time operation.

In all, the chlorinator seems like a viable solution to the need for a system which will produce boron trichloride over a long period of time in some of the larger aluminum plants. However, the results from the first set of experimental work were very inconclusive as the only definite finding was that the chlorinator does indeed produce boron trichloride. The quantity and quality of the gas has yet to be determined, and more importantly, the dependability of the system needs to be determined. These questions should be answered in additional experiments which will utilize a new chlorinator designed with vacuum technology.

Appendix G. Supporting Experimental Data

Heat Logs

Following is a copy of the Heat Log tables. The accumulation of this data began in October of 1998 with Heat Number 98-68. Prior to this heat, the focus of the program was more investigative. A number of experiments were run using carbonaceous gases and mixed boron gases. In addition, inoculation times reached up to 90 minutes. With Heat 98-68, the fy-Gem delivery process was adjusted to model the hold-up time and gas flow rates that would be encountered in a typical commercial degassing unit. To accomplish this, the delivery time was reduced to anywhere from 30 seconds to 5 minutes and the BCl_3 gas flow rates were increased to compensate. This shift in the program marked a great leap in the effectiveness of the fy-Gem process to achieve a high level of grain refinement.

Since that time, 116 heats have been made. The main variables for these tests included: alloy compositions, titanium level, boron level, head design, agitator rotation speed, gas composition, gas delivery time, and others. For 110 of these experiments, spectrographic coupons were sent to Alcoa Technical Center for quantometer analysis. Typically, this analysis returned the percent composition of typical aluminum alloying agents, such as boron, titanium, vanadium, magnesium, manganese, etc. This information is available in the Heat Log titled "Compositions". In addition to chemical analysis, the blank and 5-minute TP and Alcoa samples were polished, etched, and the grain size was recorded for 110 of these experiments. These 110 do not necessarily correspond to the 110 heats with chemical analysis results. Out of the 110 grain sizes, 42 include either 1-minute grain sizes, 20-minute grain sizes, or both. The time refers to how long after inoculation that sample was drawn from the melt. This data is available in the "Grain Size" Heat Log entry. Another source of information was provided by Touchstone Laboratory. From the LAIS samples that were pulled on nearly every run beginning with Heat Number 98-69, 40 were sent to Touchstone for SEM and EDAX analysis. From this, the diameter of the borides could be determined. The typical report consisted of the average boride size, standard deviation, minimum and maximum boride sizes, and a distribution. This data is reprinted in the "Borides" section of the Heat Log. In addition to the average sizes, Touchstone sent the individual boride sizes for each experiment. This data is available in "Individual Boride Diameters."